PERMANENT MAGNET SYNCHRONOUS GENERATOR (PMSG) TO USE ON BOARD OF YACHTS

THESIS

submitted for the degree of

Master of Science (MSc)

in

Electrical Power Engineering

by

Nada Al Fartusi

Supervised by

Dr. ir. Henk Polinder

Examination committee: -**Prof. Dr. Eng. J.A. Ferreira**

-**Dr. ir. M. Gibescu**

-Ir. **J.M. Gutierrez Alcaraz**

Electrical Power Processing Group (EPP)
Department of Electrical Power Engineering
Faculty EEMCS,
Delft University of Technology
Delft, the Netherlands
www.ewi.tudelft.nl

Mastervolt
Amsterdam, the Netherlands
www.mastervolt.com

Whisper Power
Drachten, the Netherlands
www.whisperpower.nl

August 2010

ACKNOWLEDGMENT

I express my deep gratitude to God Almighty, for giving me the needed energy to do this work and the courage to overcome all difficulties and accomplishing it.

I would like to convey my gratefulness to my supervisor Mr. Henk Polinder, for offering me a lot of his precious time and for his availability at any moment. I want to thank him above all for his human qualities, his constant encouragement and moral support throughout this project, and for his valuable guidance.

I thank my daily supervisor Mr. J. Marcelo Gutierrez Alcaraz, for his contributions in this work.

I thank Ms. Madeleine Gibescu for the encouragements she sent me to finish this work.

I am very sensitive to the honour that Prof. J.A. Ferreira grants me, by chairing my jury, I thank him very much.

I also extend my thanks to all professors and instructors who have contributed in our curriculum: Mr. S.W.H. de Haan, Mr. P. Bauer, Mr. M.J. Hoeijmakers, Mr. L. Van der Sluis, Mr. W.L. Kling, Mr. G.C. Paap, Mr. M. Popov, Mr. E Gulski, Mr. P.H.F. Morshuis, Mr. S. Meijer, Mr. J.J. Smit, Mr. P. Schavermaker, Mr. F.M. Mulder and Mr. J. de Vries. Not to forget the technical staff, particularly Mr. Rob Schoevaars for his assistance during this project.

I thank Mr. J. Ritskes and Mr. A. van Zwam from Whisper Power and Mastervolt for their cooperation.

My sincere appreciation goes to Clarisa for her concern and Mr Hans Schenkel for his efforts, during tough periods.

I am grateful to my family, my friends and my colleagues at ABB Rotterdam, especially Mr Godfried Kockelkorn, for their support, inspiration and encouragements. Without forgetting Mr. Mark te Lindert from TRIUS.

My recognition goes also to Ms. Paula Suarez, Mr.J.H. Molema, Mrs. Annelies Bongers, Mr. and Mrs W. & A. de Jong, for their involvement, help and guidance in order to realize my dream to enter Delft University of Technology "TU Delft".

Abstract

This project is part of the project "GenPowerBox"; this is a project of the company Mastervolt, realized by Whisper Power. The objective of this project is to develop a compact and noiseless energy management system for use on board of yachts. The "GenPowerBox" system is composed of a battery and a generator set; consisting of a diesel engine and a Permanent Magnet Synchronous Generator (PMSG). This MSc project is focused on the Permanent Magnet generator. The generator is integrated in the flywheel of the diesel engine. The main objective of this project is to determinate the most suitable generator for the application on yachts. Another goal is to validate the models of different generators designs. These models represent the induced voltage, different losses and the efficiency of the generator. This is done by performing several tests on different prototypes of both 3kW and 9kW generators. The measurements results are then compared with the simulated results. The distinctions between the designs consist of:

- The type of the permanent magnets (ferrite or NdFeB),

- The combination of number of poles and slots (2/3 or 8/9), and

- The type of the slots (Open or semi-closed slots).

TABLE OF CONTENTS

TABLE OF FIGURES

Chapter I

I. INTRODUCTION

This work is part of the project entitled "GenPowerBox" of the company Mastervolt; a worldwide company active in the field of electrical power systems. The purpose of Mastervolt is to guarantee an independent electric power for different applications; therefore it develops, manufactures and distributes high quality electrotechnical systems for independent energy supply. Mastervolt works on three main sectors: Maritime energy, mobile energy and solar energy. In the maritime energy sector, different 'on-board' electrical systems are provided by Mastervolt like; storage batteries, charging units, transformers, display panels, invertors and generators sets.

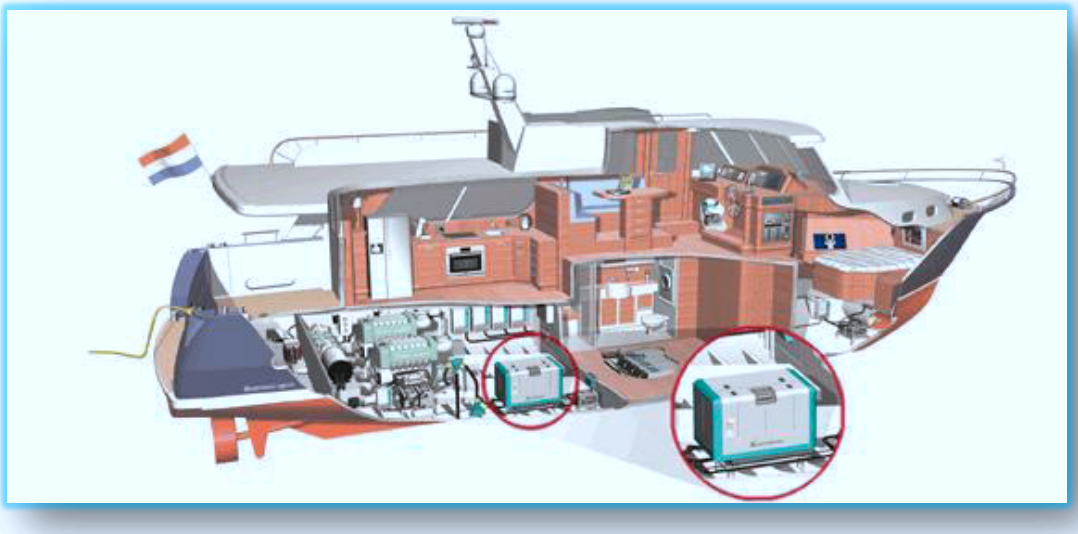

Figure I-1 The GenPowerBox® on board of a yacht (1)

The intention of the GenPowerBox® project is to provide electrical power for different loads on board of the yacht. These loads can be from a basic to an extended range, we can mention lighting, kitchen appliances (such as refrigerator, microwave oven, oven and coffee machine), laptop and entertainment equipment (TV for instance).

The GenPowerBox is a system that can have different sources of energy; such as shore connexion, batteries, and/or the generator set, consisting of a diesel engine and a permanent magnet synchronous generator. The connection between the different sources and loads is guaranteed by the power electronics system (*Figure I-2*)

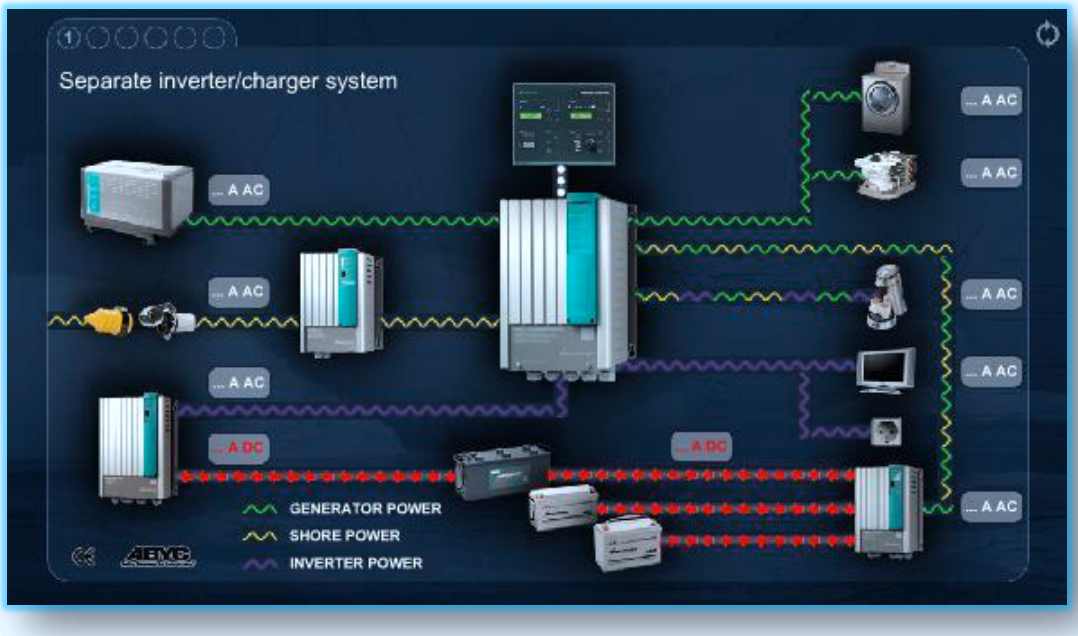

Figure I-2 **Different sources and loads of the "GenPowerBox" system** (1)

The focus of this MSc project is on the Permanent Magnet (PM) generator, which is integrated in the flywheel of the combustion engine, the objective is to develop a compact and efficient generator. Two levels of power have been considered; 3kW and 9kW generator.

To fulfil the requirement of having a compact generator, the basic construction of the permanent magnet generator has been selected to be with a high number of poles, concentrated windings and with an outer rotor design.

By making the generator small and compact we are confronted to problems like dissipation of the heat, which is one of the major problems, therefore an analysis of the losses has to be done. Thus in this MSc project the losses have been modelled and analysed by comparing them with the experimental results.

Different generators have been studied; with different magnets materials (ferrite and NdFeB), different combinations of number of poles and slots (3/2, 9/8), and different types of slots (Open and Semi-Closed slots).

The following pictures show the present generator set that is constructed by Whisper Power and used in the Mastervolt installations; this system is consisting of a diesel engine and a conventional synchronous generator.

Figure I-3 Conventional generator set of Whisper Power

Figure I-3 shows an assembled 3kW generator set and the rotor of the synchronous generator mounted on the flywheel of the combustion engine (right up) and the stator of the conventional synchronous generator with its cooling system (right down).

Figure I-4 The 9kW generator set

Figure 1-4 shows one of the 9kW generator sets of Mastervolt manufactured by Whisper Power where the generator take a considerable space of the whole set.

As the generator system is designated to be used on board of yachts, space represents an important issue as well as the quietness of the system, especially that mostly this system is involved in leisure yachts. Consequently the size, compactness and noiselessness of the system are essential concern.

By replacing the conventional generator by a permanent magnet synchronous generator the generator set will be 40% compacter and smaller.

This thesis has been divided into five chapters. It opens with this introductory chapter where a brief background is given with the motivation behind this project. Also the objective and problems have been stated. This is followed by a second chapter where the theory of PM machines is brought in with an overview of the design choice and the motivation behind it. Chapter three present the modelling of the generator, with derivation of equations presenting the magnetic flux density, the induced voltage and the losses in the studied generators. To validate the models chapter four is introduced where an analysis of the simulation and experimental results is given. Finally conclusions have been drawn in the fifth chapter which contains some prospective and recommendations for future work as well.

Chapter II

II. PERMANENT MAGNET MACHINES

II.1 INTRODUCTION

As mentioned in the foregoing chapter, this work is focussed on the Permanent Magnet (PM) generator of the GenPowerBox ®.

PM machines have been used in different applications during the last years, due to the improvement of magnetic materials (better characteristics and lower prices), in addition to the advanced technology of power electronics that provides practical ways and possibilities to control these machines. The PM machines are used as motors and as generators. They can be linear or rotating machines. The PM machines can be classified according to different parameters, among these parameters, we can cite: the materials of the permanent magnets and their mounting, the air-gap (or the flux lines), the rotor position with regard to the stator, and the stator winding.

In the coming sections, a brief overview is given about the main possible constructions of permanent magnet machines, and the motivation behind the selection of the generator design, that have been used in our application.

II.2 PERMANENT MAGNET MATERIALS

Permanent magnets used in rotating electric machines are of two general classes: ferromagnetic materials and ferrimagnetic materials. Ferrimagnetic permanent magnets, often called hard ferromagnetic materials are formed from metallic alloys, usually containing one of the three natural magnetic metals, iron (Fe), nickel (Ni) or cobalt (Co). Ferromagnetic materials, often called hard ferrites, are oxides of iron and one other metal, usually barium (Ba) or strontium (Sr). (2)

In general, all magnetic materials exhibit varying degrees of permanent magnetism, often called remanence.

PM materials are characterized by what is called a hysteresis loop, ***B(H)***, where ***B*** is the magnetic flux density measured in Tesla [T], and ***H*** is the magnetic field strength measured in Amps per meter [A/m]. For ***H*** is equal to zero a residual flux density remains. This is the remanent flux density B_{rm} which characterizes the permanent magnet. H_c is the coercive field strength for which the flux density becomes null.

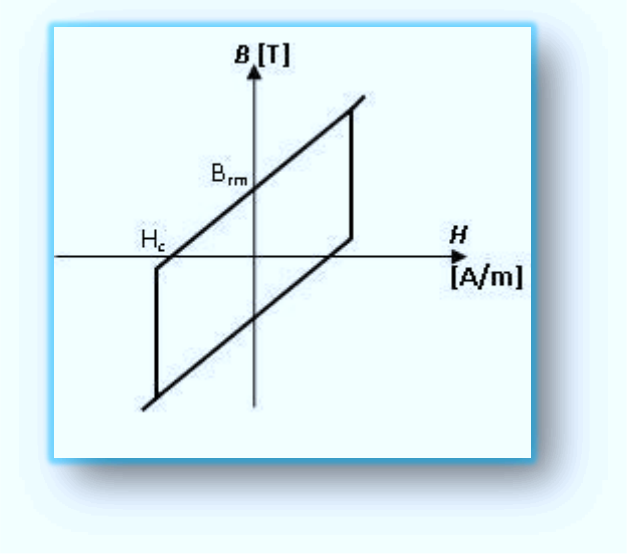

Figure II-1 Hysteresis cycle of a Permanent magnet

The second quadrant of the Hysteresis loop represents the demagnetization curve which characterizes the parameters of a permanent magnet. *Figure II-2* illustrates the demagnetization curve for some permanent magnets that are usually used in machines construction (3).

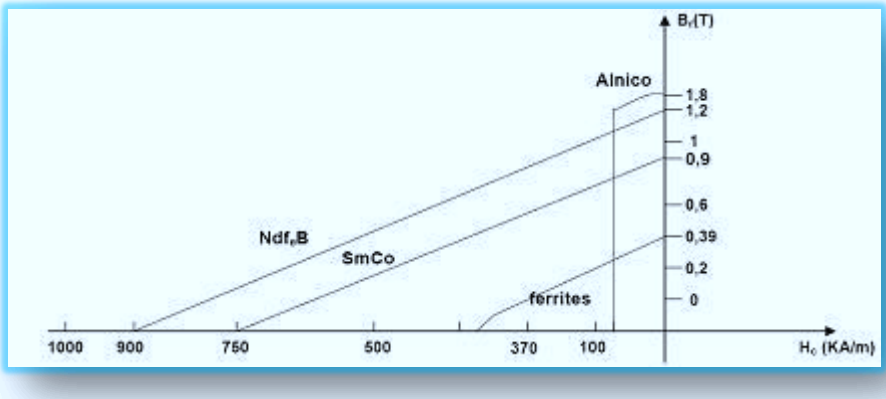

Figure II-2 Demagnetization curve of permanent magnets

Besides the magnetic properties that are essential in the choice of permanent magnets, there are other features, which are also determinant for this choice. Among these features, we distinguish the temperature properties, since the magnetization is influenced by the temperature; this dependence is described by the Langevin-Brillouin function (*Figure II-3*) (3). When the temperature is above the Curie temperature ***Tc***, the magnets lose their magnetization. For instance, for NdFeB magnets, the maximum allowed temperature is usually 120 °C. (In some new magnets this value can even reach 150°C)

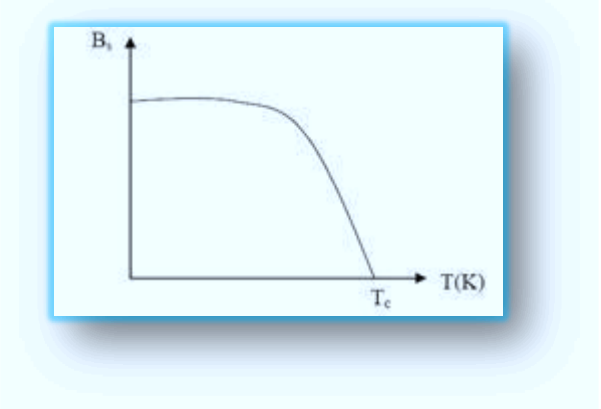

Figure II-3 Flux density versus temperature

- In our design we adopted the NdFeB PM material for the reason that it possesses a higher remanent flux density compared to the Ferrite magnets. It means that for the same magnetic flux production, we would need thicker Ferrite PM than when using NdFeB PM. This choice leads to have a more compact machine, which is the major requirement for our application.

II.3 Permanent Magnet Machines Design

Different topologies of the PM machine can be found in practice, and they can be classified according to different aspects as follows:

II.3.1 Air-Gap

Based on the air-gap or on the flux direction three types can be distinguished axial flux machines, radial flux machines and linear machines

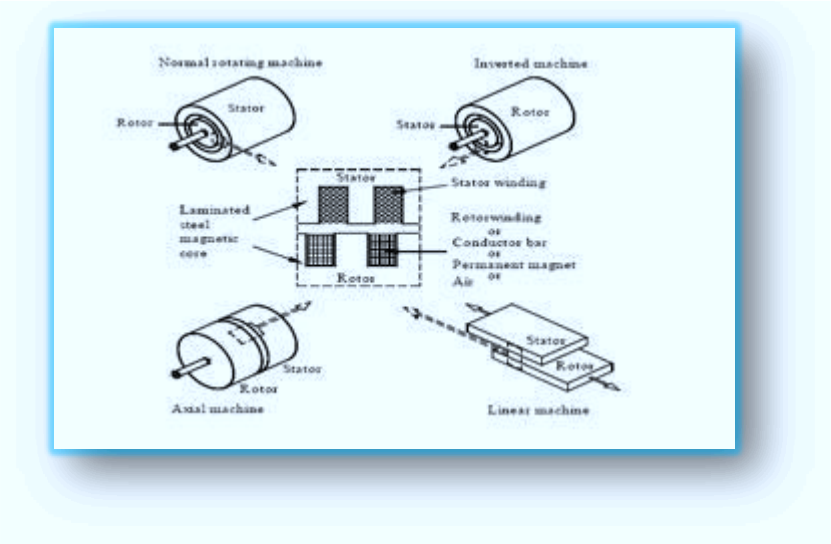

Figure II-4 Different machine constructions based on flux direction (4)

II.3.1.1 **Axial air-gap (Disc rotor):** There are many forms of axial flux air gap permanent magnet machines, they can be classified based on air-gap (single or double air-gap), on the position of the stator with respect to the rotor, and on the slots (slotless or with slots).
The use of slotless construction would reduce cogging torque and result in a small winding inductance. The advantage of a dual air-gap topology is the cancellation of the axial attractive forces between the rotor and the stator resulting from the attraction between the magnets and the stator iron. Usually an axial field permanent magnet machine is used when high torque and very high power density is required, hence it is mostly used in very specific applications. (5) (6) (7)

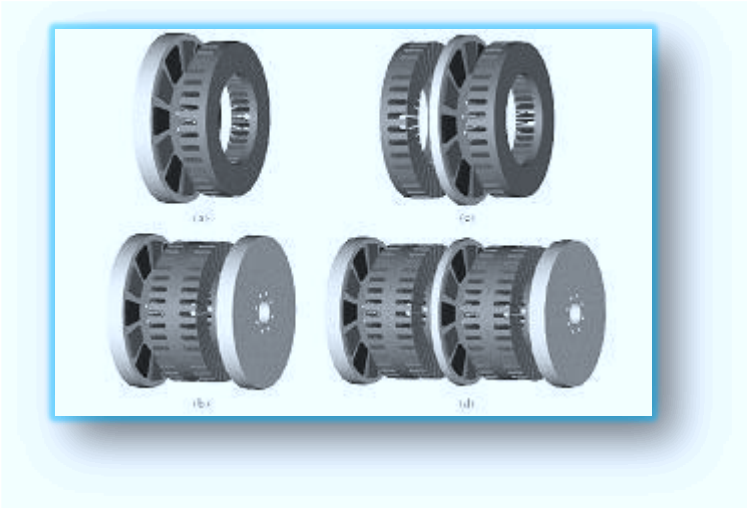

Figure II-5 **Axial flux machines configurations** (a) Single rotor- single stator structure. (b) Two rotors-single stator structure. (c) Single rotor-two stators structure. (d) Multistage structure including two stator blocks and three rotor blocks. **(5)**

II.3.1.2 **Radial air-gap (Cylindrical rotor):** This type of machines is the most common variant of electrical machines, and is very flexible in terms of scaling in production. The power capability and torque of these machines can be increased simply by expanding the stack length. Generally the rotor is mounted inside the stator, but an opposite placement is sometimes done to fulfil certain requirements as it will be presented in the next section. In (6) and (7) a comparative study is presented of a radial flux machines with axial flux machines that have different topologies.

II.3.1.3 **Linear flux (Linear machines):** The use of linear permanent magnet actuator is relevant for certain specific applications where high force density and high torque are required (8). In some applications the use of linear machines is the most suitable due to the nature of the system itself, a typical example of that is the AWS (Archimedes Wave Swing) system, where the linear machine topology fits the linear movement of the waves (9).

- For our application, as the generator will be mounted on the flywheel of the engine, a rotational machine has been adopted with a cylindrical rotor (radial flux) configuration.

II.3.2 ROTOR

According to the rotor position with respect to the stator, two types are distinguished:

II.3.2.1 **Inner rotor;** Generally the rotor is placed inside the stator; this is usually the adopted design for machines construction, unless some specific requirements are necessary. In (10) it has been shown that the outer rotor design is slightly lighter than the inner rotor. On the other hand the mechanical design of the outer rotor motor might, however, be tricky in comparison to the inner rotor and the advantage would then be reduced.

II.3.2.2 **Outer rotor;** This construction can have some advantages compared with the inner rotor topology. In this case there is lower chance of magnets detachment because of centrifugal forces. Another advantage is that outer rotor geometry allows a larger bore diameter which makes it possible to have larger number of poles. Thus a lower current loading is needed to obtain the same torque.

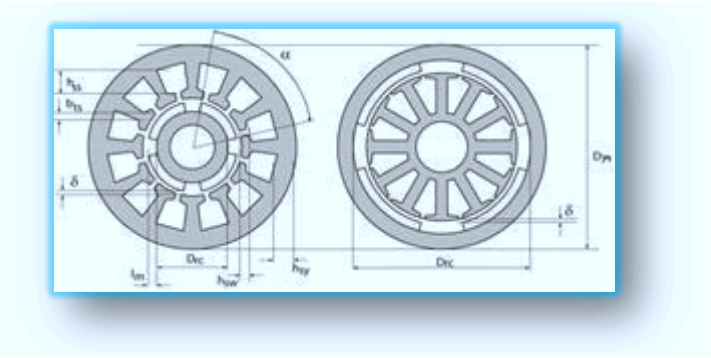

Figure II-6 **Cross section of an inner rotor and an outer rotor** (10)

- As it has been pointed out earlier, the main requirement of our generator is to be as small and compact as possible, that leads us to take on the outer rotor configuration. It permits us to have a larger number of poles in comparison with a machine of the same size but with an inner rotor.

II.3.3 PERMANENT MAGNETS MOUNTING

Based on the arrangement of magnets in the rotor, the Permanent Magnet machines can be classified into three types, which are:

II.3.3.1 **Surface-mounted PM rotor;** Compared to interior magnet type, the surface –mounted PM rotors have simple structure, and are more suitable to produce the sine wave form back electromotive force. In this topology the magnets are usually glued on the iron rotor surface.

II.3.3.2 **Inset PM rotor;** The same advantages of simplicity and more suitable emf form can be listed for this type of magnets arrangement. Moreover, inset type has the advantage of compact structure to protect against large centrifugal force at high speed operation. In addition this structure presents a shorter air gap. Inset permanent magnet machines produce a reluctance torque in addition to the torque created by the magnets that could improve the performances compared to the surface-mounted permanent magnets (10)

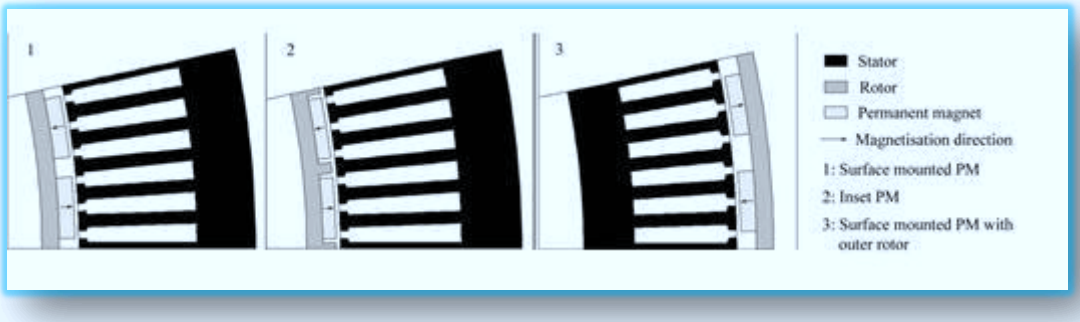

Figure II-7 Cross-section of surface-mounted and inset Permanent Magnets (2poles represented) (10)

II.3.3.3 Interior (buried) PM rotor; Buried magnets generate flux concentration in the rotor that could allow thinner or cheaper magnets, the protection of the magnet against demagnetization and it provides mechanical strength. The figure below (*Figure II-8*) illustrates two topologies; (V-shape and tangentially magnetized PM). The drawbacks of the rotors with V-shape magnets are the iron bridges that cause a high leakage flux. Furthermore the V-shape rotor is not very adapted for high pole numbers. It can easily get saturated between the magnets if the angle is too small. Another drawback of the V-shape configuration is the high number of magnets that increases the production cost. The tangentially magnetized PM rotor presents the drawback of many iron and magnet pieces to be manipulated if the number of poles is high. Therefore some production difficulties can arise. However it does not present any bridges and the flux leakage is then very low (10). It has to be mentioned that as precaution to be taken in this case, is that the shaft should be non- ferromagnetic, because with a ferromagnetic shaft, a large portion of flux from the magnets would leak through the shaft.

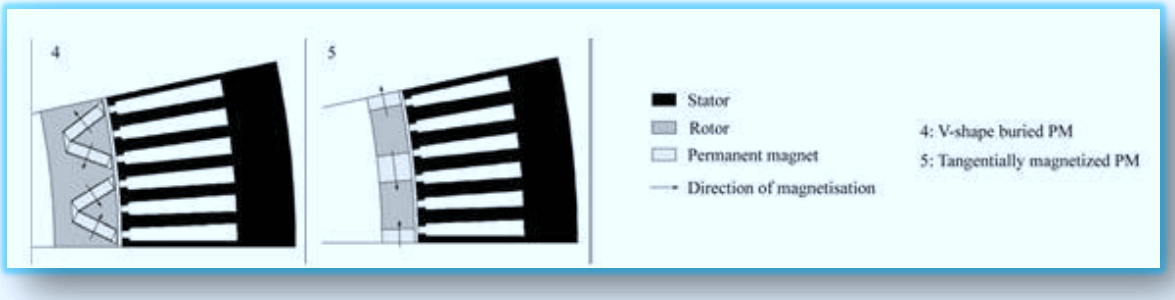

Figure II-8 Cross-section of interior Permanent Magnets (10)

- The surface mounted PM rotor structure has been adopted, in the design of our generator, for its simple construction. There is no need for a more complicated configuration (inset or interior PM), since it is an outer rotor model, which makes it less probable do have magnets detachment, besides we would not reach extremely high speeds in our application.

II.3.4 WINDINGS

The stator windings can be either distributed or concentrated winding.

II.3.4.1 Distributed winding: Is the most common winding type for rotating machines. It provides an almost sinusoidal magneto motive force, which makes it to be preferred rather than the concentrated winding. But the distributed winding has also drawbacks because of the coils overlapping that leads to longer ends, which means more copper hence more losses and more costs due to that. Another disadvantage is that the construction of such a winding is more expensive than the concentrated one.

II.3.4.2 Concentrated winding: This type of winding can be divided into two types; single layer; which means one coil each second tooth, and double layer; by having one coil on each tooth, i.e. each slot has conductors from different coils. The concentrated winding is easier to realise and less costly. Furthermore another advantage of this construction is that it has shorter end-windings compared to the distributed winding. This results in a more compact machine (shorter axial length), and the volume of copper used in the end-windings is significantly reduced, consequently lower copper losses and lower costs are achieved. (11)

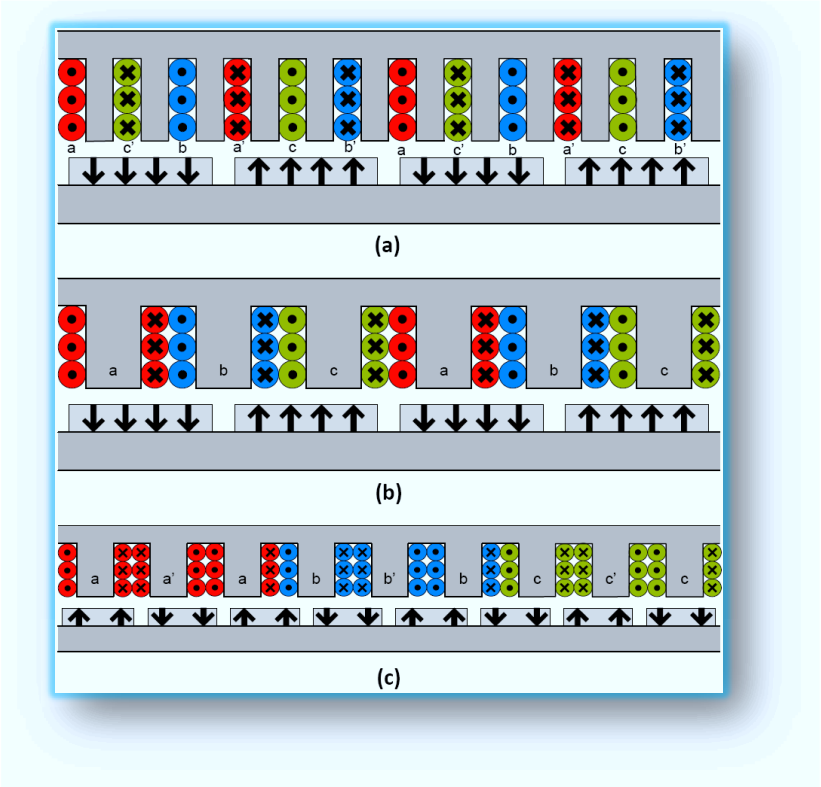

Figure II-9 Distributed and concentrated winding

(a) Distributed winding
(b) Concentrated winding (2/3)
(c) Concentrated winding (8/9)

- As stated here above, the concentrated winding is more suitable for a compact machine. And to overcome the problem of harmonics, resulting from the concentrated winding, we make use of different combinations of number of teeth and slots, as it will be shown in a later section.

II.3.5 SLOTS

Three different slots types can be cited: totally open, semi-closed or totally closed slots. There are also different slots shapes that can be found; it may be for instance rectangular, trapezoidal, oval or round. Here bellow are mentioned some of the features of different slots types:

II.3.5.1 **Open slots;** The advantage of the open slots is that it is easier wound; the winding process can also be automated, hence cheaper construction. In addition it has lower leakage reactance. On the other hand the slotting causes a higher cogging torque and eddy current losses, compared to the closed and semi-closed slots.

II.3.5.2 **Semi-closed slots;** By adopting this type of slots, lower slot harmonics are produced, thus a reduction in the reluctance variation around the stator and hence the torque ripples can be notably reduced. For this topology the leakage inductance is higher than in the precedent case, which means that lower power can be produced than that of open slots construction.

II.3.5.3 **Closed slots;** this structure presents more robustness than the two precedents, however it is more difficult to put the winding in the closed slots. Another drawback of such slots is the saturation that is higher in this case.

- Basically the semi-closed slots design have been implemented in our generator, as it provides an adequate robustness, and a lower slotting factor compared to the open slots. However, in the 9kW generator, both options have been tested the semi-closed and the open slots.

II.3.6 POLES TEETH COMBINATION

As it has been stated in an earlier section, the use of concentrated winding leads to harmonics appearance. To overcome this problem, different combinations of number of poles and number of slots can be applied, in order to get an appropriate performance of the machine. Parameters that depend on winding configuration are cogging torque and the study in (12) shows the influences that have the different poles-teeth combinations on eddy-current losses in the back iron. Among these combinations we mention:

3/2 combination; (3 teeth per 2 poles). This combination presents lower losses than the next one, but on the other hand it has a poor winding factor.

9/8 combination; (9 teeth per 8 poles). This combination presents higher losses, which might be acceptable regarding the benefit of having higher winding factor.

On reference (12), more combinations are presented and studied. Based on the provided results, we adopted the two combinations mentioned here above.

II.4 The Chosen Design

The main requirement for our generator is to have a compact generator with high power density and lower losses, hence high efficiency. Therefore the approved design was, a radial flux, surface mounted permanent magnet generator with an outer rotor, thus a larger rotor diameter, which allows us to have a higher number of poles, and moreover the permanent magnets detachment that can be caused by centrifugal forces is less probable.

The magnet material that has been used is NdFeB, which has a high remanent flux density (1.2T) compared to the ferrite magnets, which need to be thicker to get a flux density comparable to rare-earth magnets. That means larger diameter of the generator. Nevertheless we also tested a machine with Ferrite magnets in order to compare its performances with the NdFeB one.

For the windings we selected the double layer concentrated winding topology with the purpose of having more compactness and lower losses caused by copper, which would increase the efficiency. The concentrated winding will produce a lot of voltage harmonic content compared to the distributed winding. For improving the induced voltage we have chosen certain combinations of number of poles and number of slots; (2/3 and 8/9). For the 3kW generator prototypes, both topologies have been built. This would give us the opportunity to compare the performances of both, and to have a deeper insight on the out coming of this choice. And finally make a decision about which combination should be approved.

For the stator slotting we chose a semi-closed slot structure, which presents less cogging torque. Moreover it will produce less eddy current losses in the permanent magnets, which is very important, especially that we are using NdFeB magnets that are more sensitive to temperature increase. For the 9kW generator we have two prototypes as well, one with open slots and the other with semi-closed slots, for comparison purpose, and for analysing the extra losses caused by the open slots, and to decide if a good cooling method can improve it in order to preserve the extra power produced in the case of open slots.

Chapter III

III. MODELLING

III.1 INTRODUCTION

After choosing the generator design, as has been presented in the previous chapter, models should be derived for prediction and calculation of the generator performance. As the objective of this work is to determine and compare the efficiency of the different designs, we derived equations that model the no-load voltage, the different losses, (copper losses and iron losses), and the efficiency of the generator.

III.2 MAGNETIC FLUX DENSITY

Based on Ampere's law, the air gap flux density can be calculated as follows:

Ampere's law; *The line integral of the magnetic field intensity H around a closed path is equal to the total current linked by the contour.*

$$\oint \vec{H} \cdot \overrightarrow{dl} = \iint \vec{J} \cdot \overrightarrow{dA}$$

Equation III-1

With: J the current density

For Permanent Magnet machines we have:

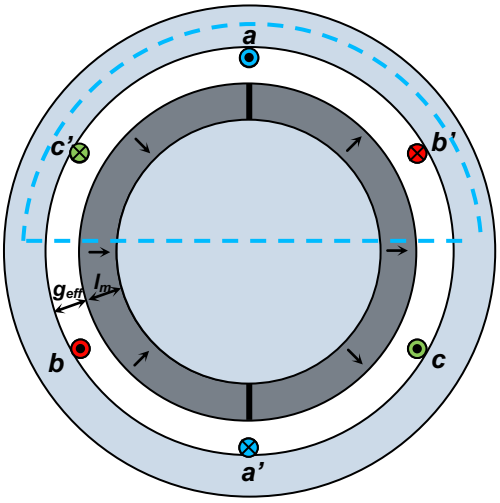

$$\oint \vec{H} \cdot \overrightarrow{dl} = 0$$

Equation III-2

$$2\left(H_g \cdot g_{eff} + H_m \cdot l_m\right) = 0$$

Equation III-3

$$2\left(\frac{B_g}{\mu_0} \cdot g_{eff} + \frac{B_{rm}}{\mu_0 \cdot \mu_{rm}} \cdot l_m\right) = 0$$

Equation III-4

$$\left|B_g\right| = \frac{l_m}{g_{eff} \cdot \mu_{rm}} \cdot B_{rm}$$

Equation III-5

The maximum flux of the permanent magnets is calculated based on the fundamental flux density by:

$$\hat{\Phi}_{PM} = B_{gl} \cdot \frac{2}{\pi} \tau_p \cdot l_s \cdot k_w \cdot k_{fring}$$

Equation III-6

With:

$$B_{gl} = \frac{4}{\pi} \cdot B_g \cdot \sin\left(\frac{\pi \cdot b_m}{2 \cdot \tau_p}\right)$$

Equation III-7

With: τ_p the pole pitch

$$\tau_p = \frac{\pi \cdot r_s}{p}$$

Equation III-8

g_{eff} the effective air-gap, calculated as follows:

$$g_{eff} = \left(l_g + \frac{l_m}{\mu_{rm}}\right) k_{Carter}$$

Equation III-9

III.2.1 CARTER'S FACTOR

Due to slotting the effective magnetic air gap is different from the mechanical air gap in machines.

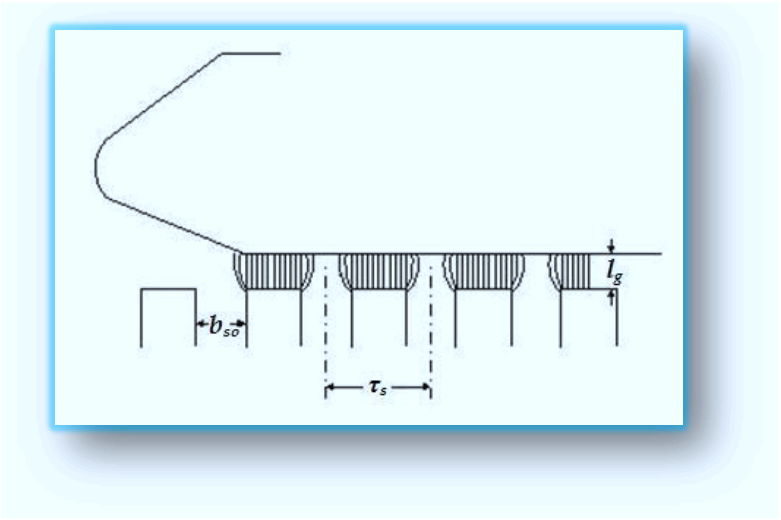

Figure III-1 Distribution of flux in the air-gap

The effective magnetic air gap is calculated by introducing the Carter factor, which is given in (13) as follows:

$$k_{Carter} = \frac{\tau_s}{\tau_s - \gamma\left(l_g + \frac{l_m}{\mu_{rm}}\right)}$$

Equation III-10

Where:

$$\gamma = \frac{4}{\pi}\left[\frac{b_{so}}{2\cdot\left(l_g+\frac{l_m}{\mu_{rm}}\right)} \cdot \tan^{-1}\left(\frac{b_{so}}{2\cdot\left(l_g+\frac{l_m}{\mu_{rm}}\right)}\right) - \ln\sqrt{1+\left(\frac{b_{so}}{2\cdot\left(l_g+\frac{l_m}{\mu_{rm}}\right)}\right)^2}\right]$$

Equation III-11

III.3 INDUCED VOLTAGE

The induced voltage is found by the change in flux i.e. is derived from Faraday's law;

Faraday's law; *The induced e.m.f. in a coil equals the negative of the time rate of change of magnetic flux through the coil.*

From Faraday's law, the equation of the voltage induced in N_s-turns coil is:

$$e(t) = N_s \frac{d\Phi}{dt}$$

Equation III-12

Assuming a sinusoidal waveform, the root-mean-square (rms) value of the induced voltage is:

$$E_{rms} = \frac{\hat{E}}{\sqrt{2}}$$

Equation III-13

$$E_{rms} = \frac{N_s \omega_e \hat{\phi}_{PM}}{\sqrt{2}}$$

Equation III-14

Where: N_s The number of turns per phase

ω_e The electrical angular frequency; $\omega_e = \omega_m \cdot p$ with $\omega_m = \frac{2\pi \cdot N}{60}$

$$\omega_m = \frac{2\pi \cdot N}{60}$$

Equation III-15

$\hat{\phi}_{PM}$ The flux produced by the magnets

III.3.1 WINDING FACTOR

The winding factor is defined as the ratio of the resulting emf E_{cp} per current path (or phase) divided by the product of number of coils N_{cp} to their emfs E_c. (8)

$$k_w = \frac{E_{cp}}{N_{cp} \cdot E_c}$$

Equation III-16

Given that a concentrated winding is implemented in the studied generators, a winding factor is introduced in the calculation of the induced voltage. The winding factor k_w consists of pitch factor (also called chording factor or coil-span factor): k_p,and distribution factor: k_d.

In case of skewing (to improve performances), in some machine the skew factor: k_s is also a constituent of the winding factor. This is not applied to the generators designed for this project.

In (14) and (15), a theoretical method is presented for calculation of winding factor, which yield to winding factors tables, that give the winding factors values for different combinations of number of poles and slots .

III.4 LOSSES

The losses in electrical machines can be classified according to different bases; location, origin.

- Based on the location of the loss, there are:

- Winding losses, since the studied generator here is a permanent magnet generator; this loss is only present in the stator.

- Core losses; are found in both the stator core and the back iron of the rotor.

- Friction and windage losses; these losses are due to bearings and air friction.

- Based on the origin,

- Electromagnetic loss: these are winding and core losses

- Fundamental losses: - Fundamental winding losses (stator)
  - Fundamental core losses (stator & rotor)
- Space Harmonics losses: - Space harmonic core loss (stator & rotor)

These losses are related to, mmf space harmonics, air-gap permeance harmonics due to slotting, leakage and main path saturation.

In the coming sections we will derive the equations used in the program for calculation of the studied losses, which are Iron losses, including hysteresis and eddy currents losses in both the teeth and yoke, copper losses and back iron losses.

III.4.1 IRON LOSSES

The iron losses in the generator are caused by two phenomena; Eddy-currents and hysteresis that occur in the stator core. Both losses are proportional to the flux density and the rotational frequency.

$$p_{iron} = p_e + p_h$$

Equation III-17

- Eddy-current losses are given by the following equation:

$$p_e = k_e \cdot \hat{B}^2 \cdot \omega_s^2$$

Equation III-18

With: k_e The eddy-current loss constant (From manufacturer's data)

- Hysteresis losses are given by:

$$p_h = k_h \cdot \hat{B}^{\beta} \cdot \omega_s$$

Equation III-19

With: k_h The Hysteresis loss constant (From manufacturer's data)

β The Steinmetz constant $(1.5 < \beta < 2.3)$

For the calculation of the iron loss, the core has been split into two parts (yoke & teeth):

$$p_{iron} = p_y + p_t$$

Equation III-20

- p_y The iron loss in the stator yoke;

The nominal value of the iron loss in the stator yoke is given by the following equation;

$$p_{y\_nom} = M_{Fesy} \cdot \hat{B}_y^2 (k_e \omega_e^2 + k_h \omega_e)$$

Equation III-21

Where: M_{Fesy} the iron mass of the yoke, calculated as follows;

$$M_{Fesy} = \rho_{Fe} \cdot V_{Fesy}$$

Equation III-22

With: ρ_{Fe} the iron mass density

V_{Fesy} the yoke volume, given by;

$$V_{Fesy} = l_s \cdot \pi \cdot \left((r_s - h_s)^2 - \left(r_s - h_s - h_{sy} \right)^2 \right)$$

Equation III-23

And $\hat{B}_y$ the maximum flux density in the stator yoke, given by:

$$\hat{B}_y = \frac{\hat{B}_{gl} \cdot 2\tau_p}{2\pi \cdot h_{sy}}$$

Equation III-24

- p_t The iron loss in the stator teeth;

$$p_{t\_nom} = M_{Fest} \cdot \hat{B}_t^2 (k_e \omega_e^2 + k_h \omega_e)$$

Equation III-25

Where: M_{Fest} the iron mass of the teeth, calculated as follows;

$$M_{Fest} = \rho_{Fe} \cdot V_{Fest}$$

Equation III-26

With: V_{Fest} the teeth volume, given by;

$$V_{Fest} = N_t \cdot l_s \cdot \left(h_s \cdot b_t + h_{so}(b_{tt} - b_t)\right)$$

Equation III-27

And $\hat{B}_t$ the maximum flux density in the stator tooth. Since we have a concentrated winding, the flux through one tooth is given by:

$$\hat{B}_t = \frac{\hat{\Phi}_{PM}}{l_s \cdot b_t}$$

Equation III-28

Finally the stator core loss is:

$$p_{iron} = 1.6\left(p_y + p_t\right)$$

Equation III-29

As it can be remarked, a correcting factor (1.6) has been introduced to take into account the material deterioration due to punching.

III.4.2 Copper Losses

For the calculation of the copper losses, the stator resistance is calculated first, using the following basic equations:

$$R_s = \frac{\rho_{Cu} \cdot l_{Cu}}{A_{Cu}}$$

Equation III-30

With: ρ_{Cu} The copper resistivity ($= 2.4 \times 10^{-8} \Omega.m$) (for temperatures 100-120 °C)

l_{Cu} The length of the phase conductor, given by:

$$l_{Cu} = 2N_s\left(l_s + \frac{\pi \cdot \tau_s}{2}\right)$$

Equation III-31

Where N_s Number of turns per phase; $N_s = \left(\frac{N_t}{3}\right) \cdot N_c$

N_t Number of teeth

N_c Number of turns per tooth

τ_s The slot pitch, given by:

$$\tau_s = \frac{2\pi \cdot r_s}{N_t}$$

Equation III-32

A_{Cu} The conductor cross section, calculated as follows:

$$A_{Cu} = \frac{K_{fill} \cdot A_{slot}}{2N_c}$$

Equation III-33

With: K_{fill} The fill factor

A_{slot} The slot area, given for semi-closed-slots and open-slots by *Equation III-34* and *Equation III-35* respectively:

$$A_{slot\_scs} = \frac{(b_{si}+b_s)\cdot(h_s-h_{so})}{2}$$

Equation III-34

$$A_{slot\_os} = \frac{(b_{si}+b_s)\cdot h_s}{2}$$

Equation III-35

The bellow figure shows the different dimensions used in the foregoing equations.

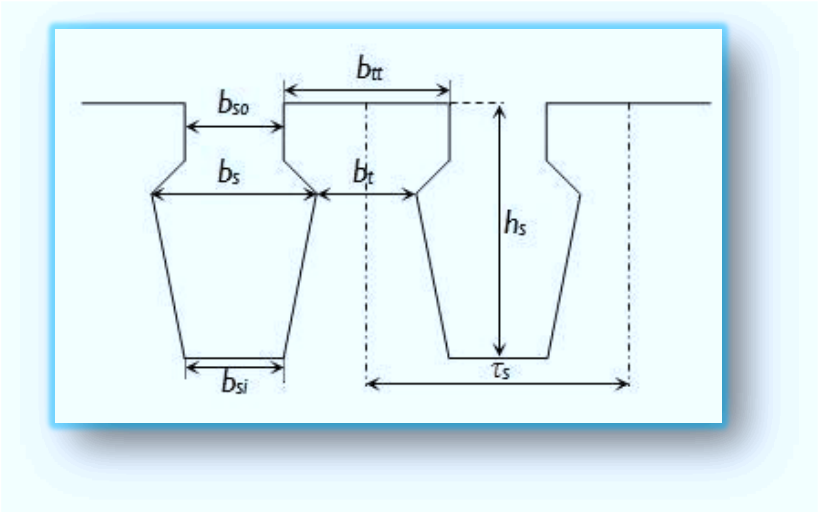

Figure III-2 Slots and teeth dimensions

In the 3kW NdFeB generators, parallel winding has been used (*Appendix_5*), as consequence of that the resistance is one third of the stator resistance calculated according to *Equation III-30*.

For parallel winding the stator resistance is then;

$$R_s = \frac{\rho_{Cu} \cdot l_{Cu}}{3 \times A_{Cu}}$$

Equation III-36

After calculation of the stator resistance, the copper loss is given by the following equation:

$$p_{Cu} = I_s^2 \cdot R_s$$

Equation III-37

Where I_s can be calculated from the induced emf as follows;

$$I_s = \frac{P}{3 \cdot E_{rms} \cdot \cos\varphi}$$

Equation III-38

With: P The generator power

$\cos\varphi$ The generator power factor

III.4.3 Back Iron Losses

The rotor eddy-current loss in conventional permanent magnet machines is usually considered to be negligible, since high order time harmonics in the stator currents and space harmonics in the winding distribution are generally small. However the stator magneto-motive force (mmf) distribution contains a richer set of space harmonics. Consequently the rotational speeds of both lower and higher order space harmonic mmfs, which differ from that of the rotor magnets, may induce significant eddy-current loss in the magnets, and results in excessive heating. Furthermore, slotting causes a variation of the magnetic field in the magnets, this component of rotor-eddy current loss is dependent of the slot opening and the pole/ slot number combination. (16)

In (12) a detailed study of eddy-current losses in the solid back-iron of PM machine has been done for different concentrated fractional pitch windings. It shows that these losses are considerable in fractional-pitch windings machines and depend strongly on the combination of number of teeth and number of poles. This study reveals that the eddy-current losses in machines with distributes full-pitch windings are negligible. In machines with fractional-pitch windings, these losses are significant and excessive for machines with a number of coils half the number of teeth.

Many papers present models of the eddy-current losses in the solid back-iron and the permanent magnets of the rotor, that are compared with experimental results and/ or finite elements methods (17; 18)

In the present work these losses are not considered. Nevertheless these can be included in future work to have a more accurate modelling of the generators.

III.5 Conclusion

After derivation of the machine models (induced emf and different losses), we are going to implement the derived equations in Matlab® in order to simulate the performances of the different designed machines. The results of the simulations are presented in the next chapter, where it will be compared with the experimental results of the different tested generators.

Chapter IV

IV. VALIDATION

IV.1 INTRODUCTION

To validate the models that have been derived in the prior chapter, the equations have been implemented in Matlab® programme, where they have been simulated (the Model program is presented in *Appendix_2*). The simulation results are then compared with the experiments results, from which conclusions are drawn.

This chapter is introduced by an overview of the tested generators, and then a summarising comparison of the simulated performances of the different generators is given. After that the different performed tests are shown. Finally the experiments results are presented and discussed.

IV.2 TESTED GENERATORS

For the validation of the derived models, different prototypes have been tested.

Table IV-1 gives an overview of the studied generators.

	Code	Power	Magnets Material	Number of poles	Number of slots/teeth	Slots/poles combination	Remarks
1-	G3k0	3kW	Ferrite	16p	24t	(3/2)	*Reference machine*
2-	G3k_3-2	3kW	NdFeB	18p	27t	(3/2)	
3-	G3k_9-8	3kW	NdFeB	24p	27t	(9/8)	*wrong magnets size (wider magnets)*
4-	G3k_9-8c	3kW	NdFeB	24p	27t	(9/8)	*corrected magnets size*
5-	G9k_scs	9kW	NdFeB	18p	27t	(3/2)	*Semi-Closed slots*
6-	G9k_os	9kW	NdFeB	18p	27t	(3/2)	*Open slots*

Table IV-1 Overview of the studied generators

The different machines parameters are given in *Appendix_1*

Table IV-1 gives an idea about the major differences between the tested generators. It has to be mentioned that the 1st generator (G3k0) is an off-the-shelf generator for which the stator winding has been adapted to our application. The structure of this generator has been the base of the other NdFeB generators (Generator 2~6) that have been designed and developed at TU Delft by the EPP group.

The 2nd generator to be tested is a 3kW generator with NdFeB magnets and (3/2) combination of number of poles and teeth (i.e. 18 poles, 27 teeth).

The 3rd generator to be tested is similar to the second one (it is a 3kW NdFeB magnets), the difference consists on the combination of number of poles and teeth. It is a (9/8) combination with 27 teeth and 24 poles this time (instead of 18poles).

The first prototype of this configuration was manufactured with a mistaken rotor, in which the permanent magnets of the 3/2 combination have been used. As this generator (9/8) contains 6 additional poles, it implies that the spacing between the poles is small, which may affect the generator performances. Nevertheless we kept this rotor before adjustment, to conduct the experiments on it, with the intention of observing the effect of this construction anomaly on the results.

That means we have two 3kW generators with the 9/8 combination to be tested; one with wrong magnets size, and the other where the permanent magnets are with the right width. We differentiate them by "_**c**" (for **c**orrected) extension on the generator code.

It has to be mentioned that by using a wrong permanent magnets size (wider magnets), we expected that, the fact that the spacing between the magnets is small would result in higher saturation, hence a lower performance of the generator. In order to validate our suspicion, we have run the experiments on the machine with the wrong PM, before sending it back for adjustment.

IV.3 SIMULATION

IV.3.1 SIMULATION RESULTS OF THE STUDIED GENERATORS

Table IV-2 summarize the simulated performances of different tested generators at rated speed (3150 rpm):

		G3k0	G3k_3-2	G3k_9-8	G3k_9-8c	G9k_os	G9k_scs
V_nl	[V]	178.23	113	135.98	123.53	120.45	127.77
P_Cu	[W]	266.59	90.31	50.73	61.67	385.86	347.27
P_Fe	[W]	53.38	67.79	94.19	77.72	238.44	483.83
P_tot	[W]	319.97	158.10	144.92	139.39	624.30	831.10
η	[%]	91.44	93.16	94.42	92.22	94.58	94.51

Table IV-2 Simulated performances of the different studied generators

The simulation results show that the efficiency of the NdFeB PM generators is higher than that of the Ferrite magnets machine. That is a consequence of the lower losses present at the NdFeB machines.

IV.3.1.1 3kW Generators

- *No-load voltage*

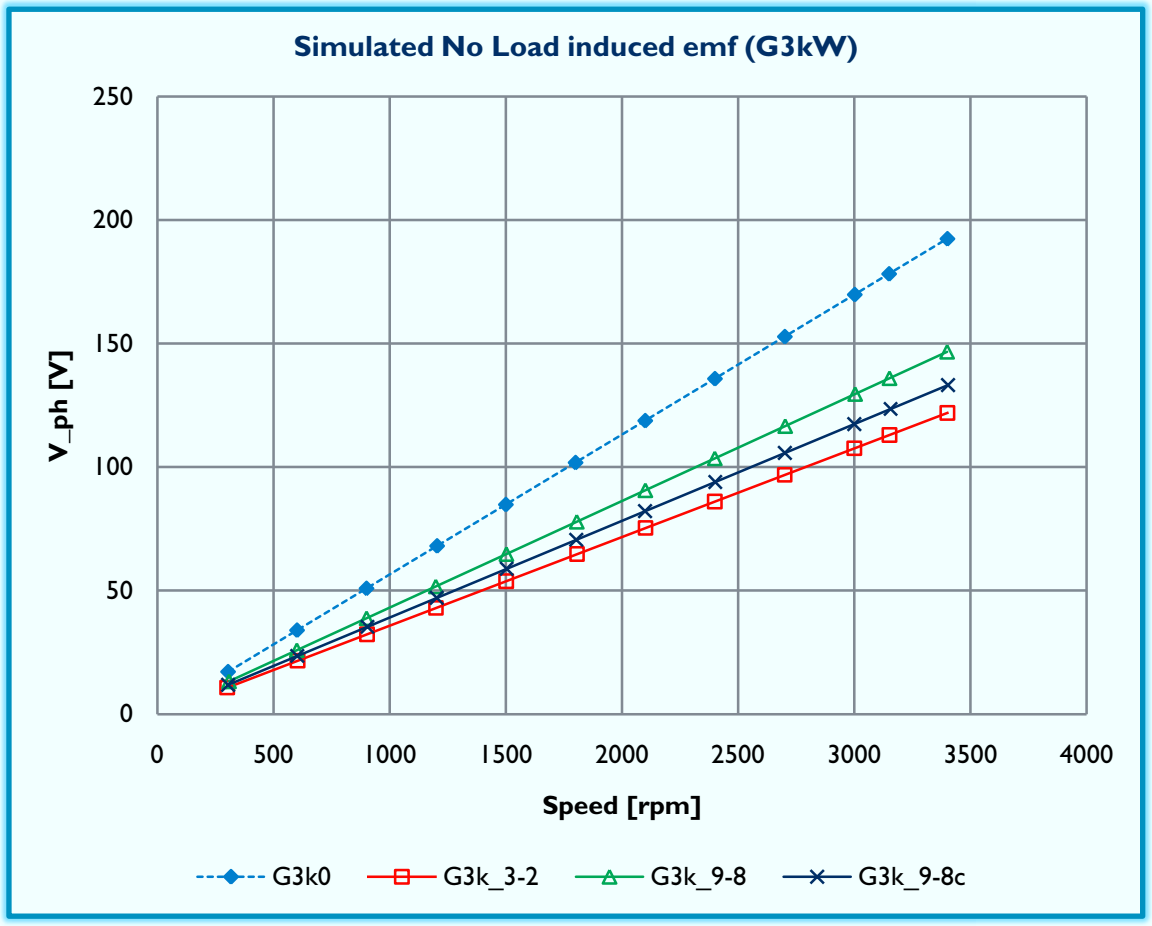

Figure IV-1 Simulated No-load voltage versus speed for the different 3kW generators

The simulation graphs show that the ferrite magnet machine produces more voltage than the NdFeB machines.

The NdFeB machine with 3-2 combination of number of slots and poles seems to be producing the lowest voltage.

By comparing the two 9-8 machines, it is obvious that the one with mistaken rotor generates more voltage, which is logical due to the wider magnets.

Iron losses

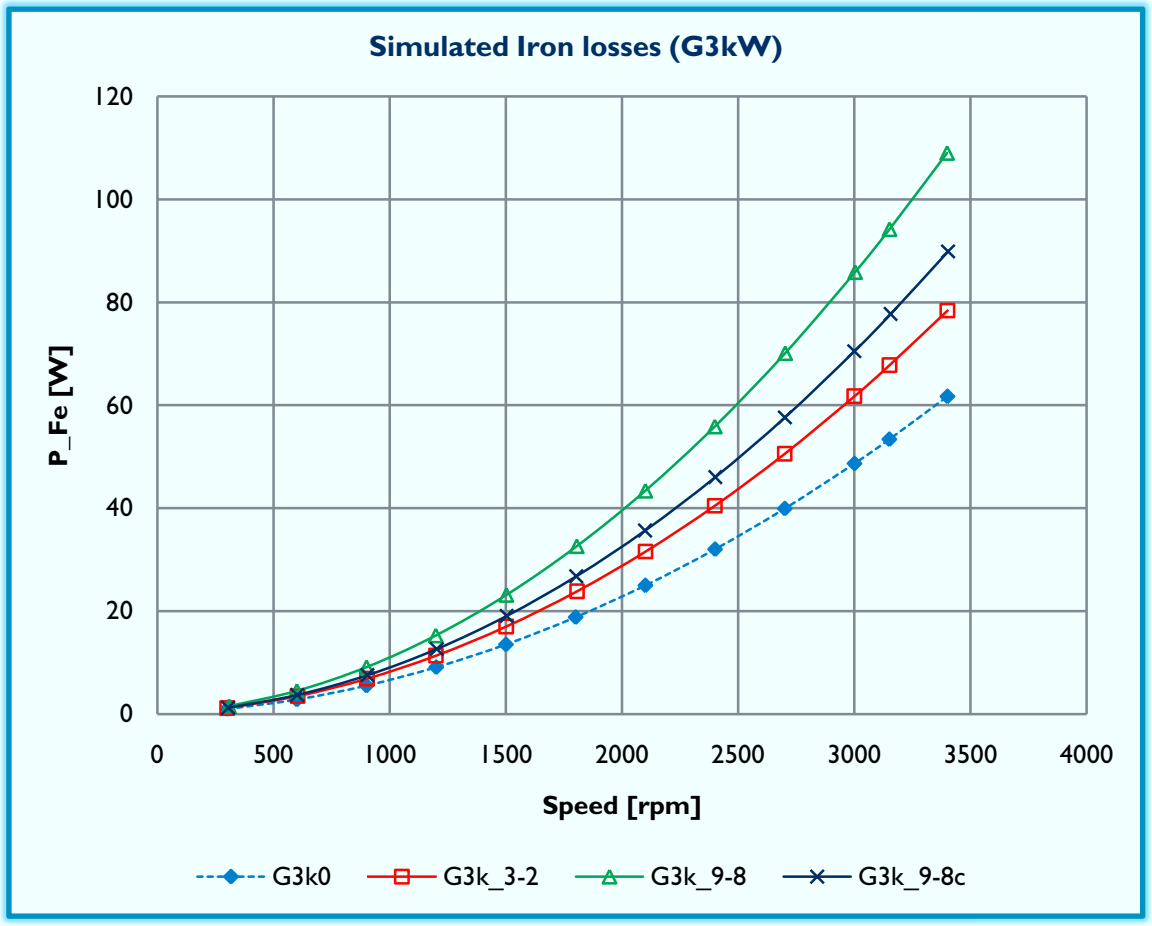

Figure IV-2 Simulated iron losses versus speed for the 3kW generators

From the graphs we can see that the ferrite magnet machine is predicted to provide lower iron losses in comparison with the NdFeB machines.

Within the NdFeB machines, the Generator with the 3-2 combination presents the lowest iron losses.

As expected the 9-8 generator before correction, thus with wider magnets would have higher iron losses.

Efficiency

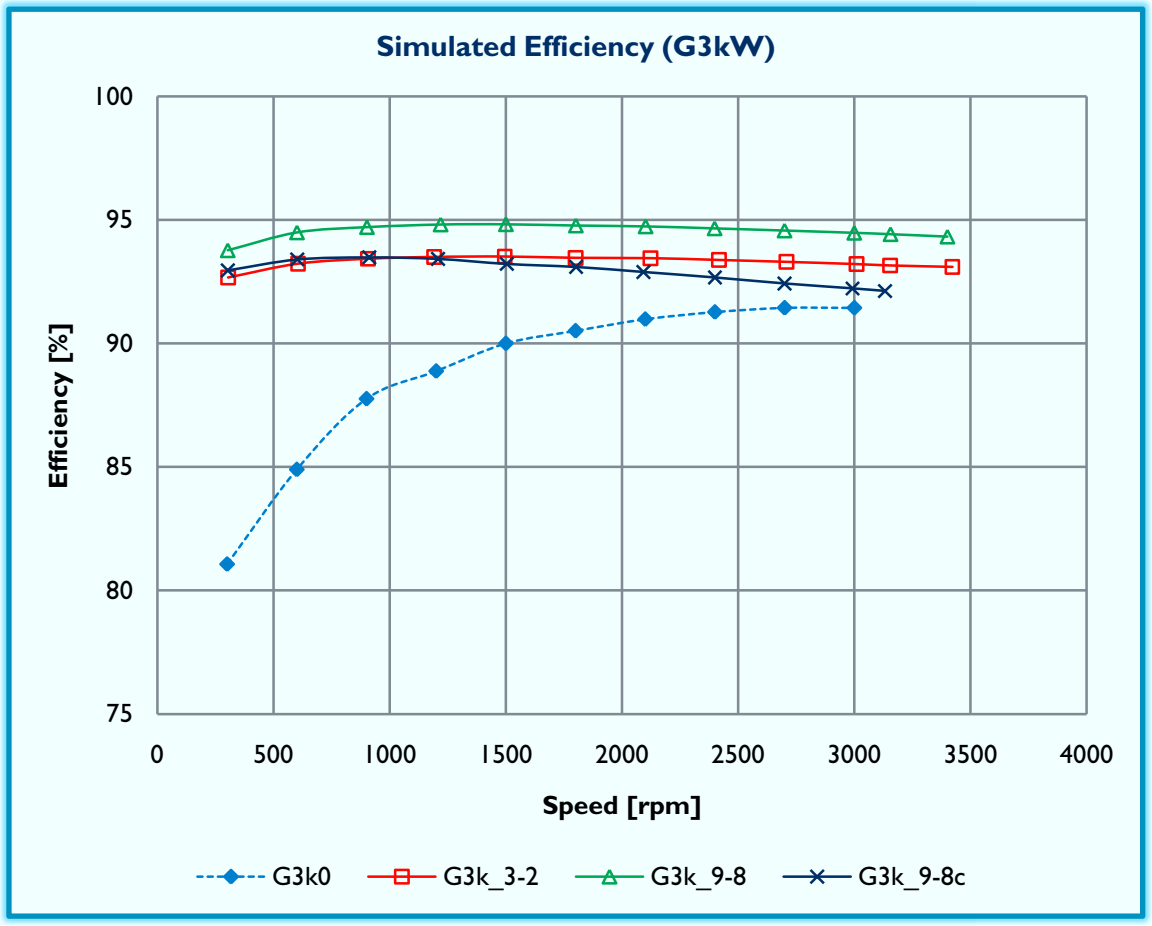

Figure IV-3 Simulated efficiency versus speed for 3kW generators

From simulation we notice that the ferrite magnet machine has lower efficiency in comparison with the NdFeB machines.

Contrary to what was expected, from the calculated efficiency, we perceive that the erroneous 9-8 generator presents higher efficiency than after correction, which is the result of the high produced voltage.

Based on simulation results, we can conclude that NdFeB generators perform better than the ferrite magnet machine, given that they present higher efficiency.

Among the NdFeB generators, the 9-8 combination is expected to be the best option.

IV.3.1.2 9kW Generators

For the 9kW generator version, two designs have been realized; one with Semi-Closed Slots (scs) stator, and the second with Open Slots (os). The aim behind the execution of both designs is to get a better understanding of the effect of the slots type on the performances of the machine. It has to be considered that the same rotor is used for both machines, the difference consist only on the stator. Thus we have one rotor, with 18 poles made of NdFeB permanent magnets, that is used for both stators.

- *No-load voltage*

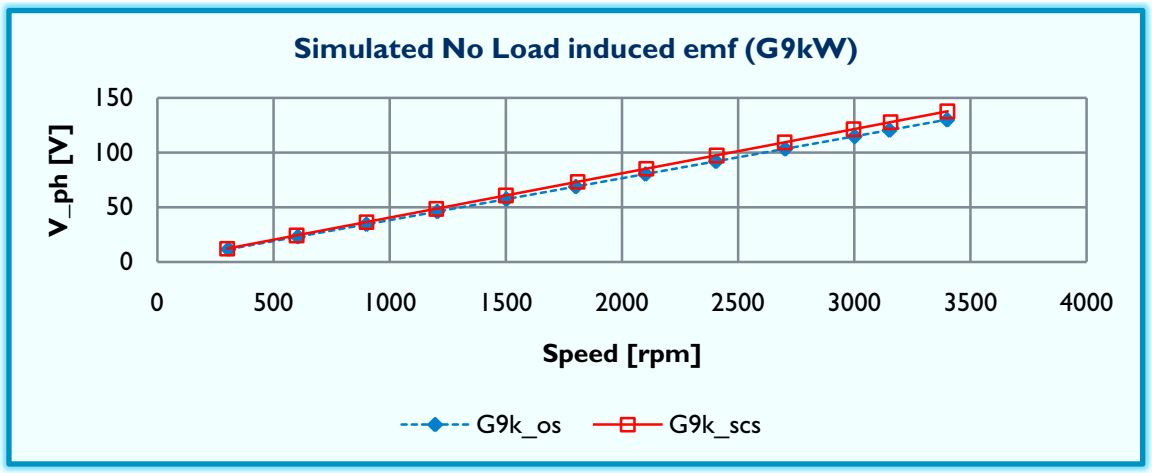

Figure IV-4 Simulated No-load voltage versus speed for the different 9kW generators

From simulations we expect to have more voltage with the semi-closed slots generator than with open slots.

- *Iron losses*

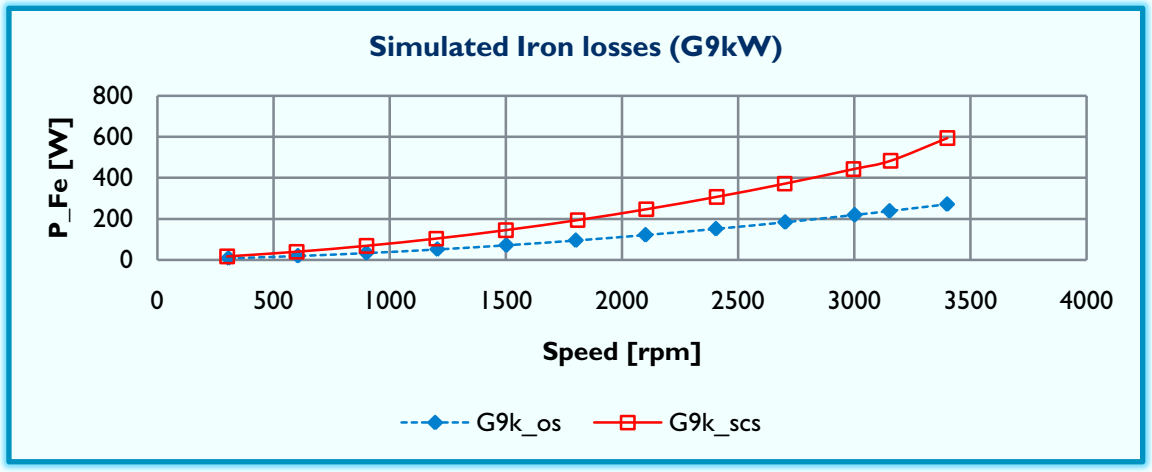

Figure IV-5 Simulated iron losses versus speed for the 9kW generators

Simulation results show higher iron losses in case of semi-closed slots generator in comparison with open slots.

Efficiency

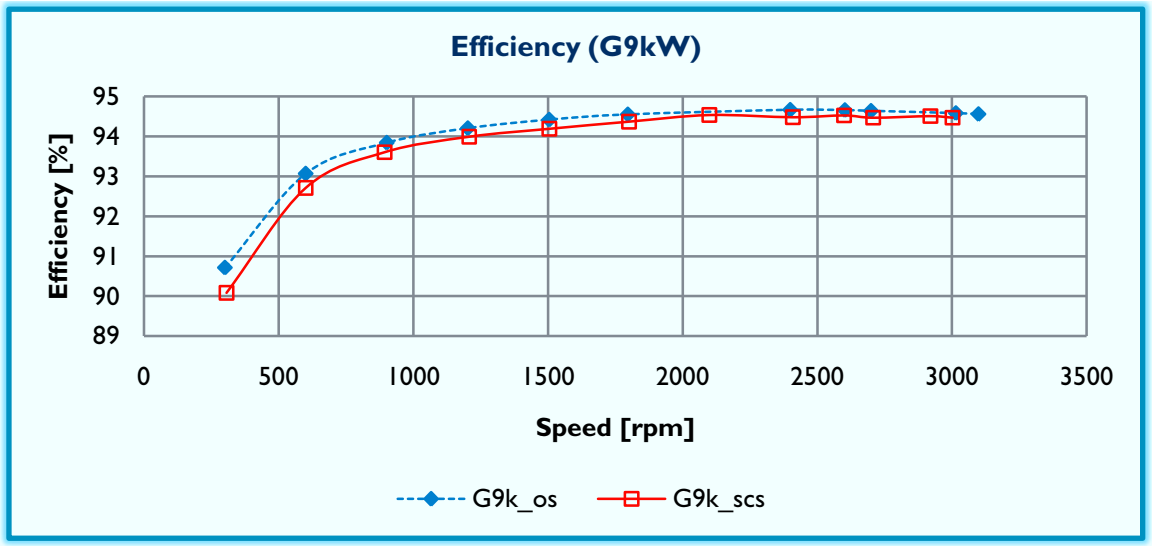

Figure IV-6 Simulated efficiency versus speed for 9kW generators

We predict a slightly higher efficiency with the open-slots generator in contrast with the semi-closed slots.

- After giving an overview of the simulation results, at this stage it is important to remember that the models on which the simulations are based, are simplified and many parameters are neglected; particularly the back iron losses as well as the eddy current losses in the magnets, which might have a huge affect on the machines performers, especially in the case of NdFeB magnets, as it will be noticed in the coming sections.

In order to validate these results, a number of experiments should be carried out on the provided prototypes. The experiments and their results are presented in the coming sections.

IV.4 EXPERIMENTS

In this section, first of all an overview of the performed tests is given, it is then followed by the experimental results.

IV.4.1 TESTS TO BE PERFORMED

IV.4.1.1 No-load test without stator

The purpose of this test is to measure the mechanical losses of the generator, i.e. the losses due to friction and windage.

In this test the speed and torque are measured, from which the mechanical losses are calculated as follow:

$$P_{mech\_loss} = T \cdot \omega_m$$

Equation IV-1

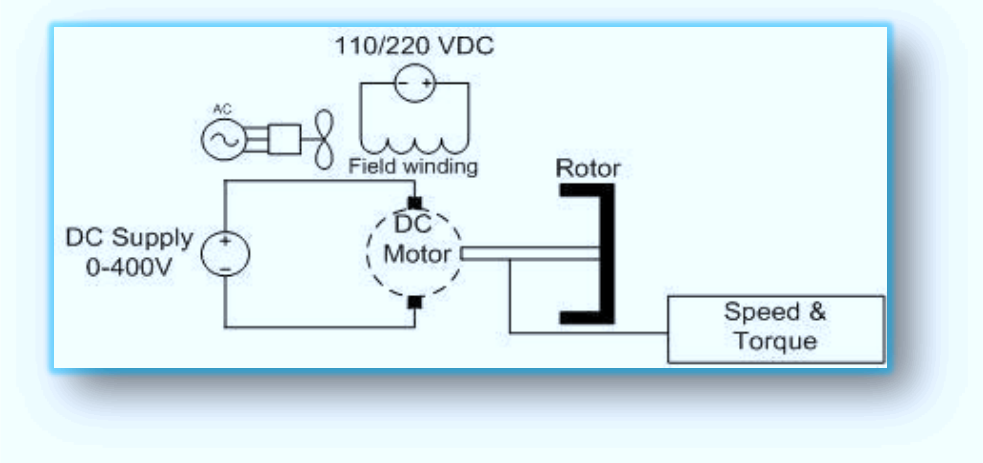

Figure IV-7 Schematic of the no-load test without stator

IV.4.1.2 No-load test with stator

This experiment is performed to determine the No-load voltage by measuring the line to line voltage across two phases (E_{LL}); the phase voltage is calculated by the formula:

$$E_{ph} = \frac{E_{LL}}{\sqrt{3}}$$

Equation IV-2

The second purpose of this test is to measure the No-load losses $P_{N.L\_Loss}$;

$$P_{N.L\_loss} = T \cdot \omega_m$$

Equation IV-3

The iron losses are determined by subtracting the mechanical losses, measured in the previous test (No-load test without stator), from the No-load losses.

$$P_{iron\_loss} = P_{N.L\_loss} - P_{mech\_loss}$$

Equation IV-4

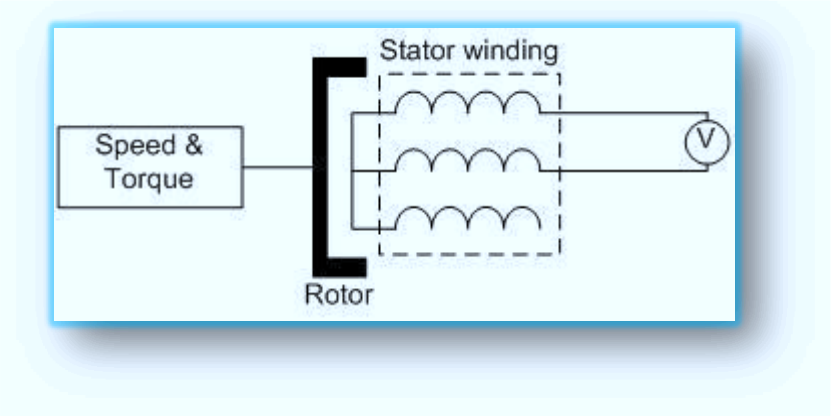

Figure IV-8 Schematic of the no-load test with stator

IV.4.1.3 Load test

The purpose of this experiment is to measure the efficiency of the generator by using the formula:

$$\eta = \frac{P_{out}}{P_{in}} \times 100$$

Equation IV-5

Where the output power P_{out} and the input power P_{in} are calculated as follows;

$$P_{out} = \sqrt{3} \cdot I_{rms} \cdot V_{rms(LL)}$$

Equation IV-6

$$P_{in} = T \cdot \omega_m$$

Equation IV-7

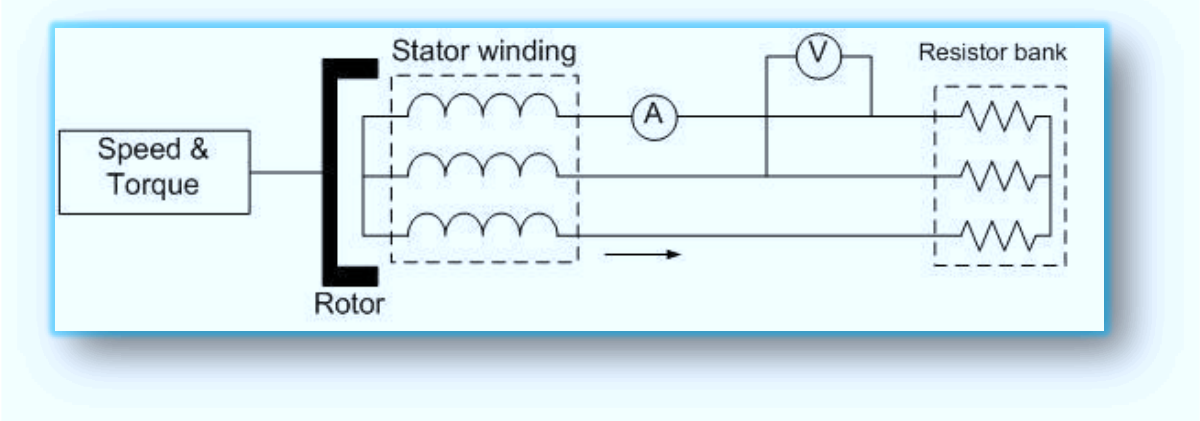

Figure IV-9 Schematic of the load test

IV.4.1.4 Short-circuit test

This experiment is performed to measure the generator inductance based on the formula;

$$I_{sc} = \frac{E}{\sqrt{{R_s}^2 + (\omega_e L)^2}}$$

Equation IV-8

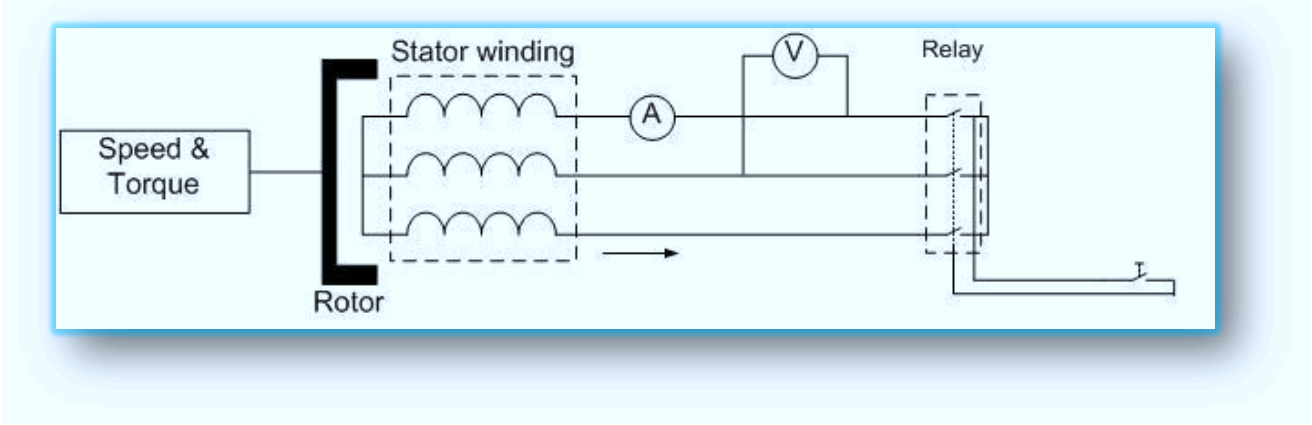

Figure IV-10 Schematic of the short-circuit test

From the foregoing sections, it is noticeable that there are lots of experiments and measurements to be carried out; therefore we opted for measurement automation. For the measurement automation we used a GPIB (General Purpose Interface Board), using Matlab® programming (*Appendix_4*).

IV.4.2 Experiments Problems

It has to be mentioned that during the testing phase, we faced many problems and challenges. Starting with the mechanical problems of the experimental setup; for instance (stators with different dimensions thus we had to make a new adaptor piece for fixing the stator on the mounting plate). Passing through the coupling of the generator with the DC Motor (the driving machine): in order to have a more stable set up we attempted to put a flexible coupling but it turned out to be inappropriate to our experiment bench. And the most struggling trouble was the torque sensor which was giving inconsistent measurements, therefore it had been sent to the manufacturer for recalibration, yet the readings were not always reliable.

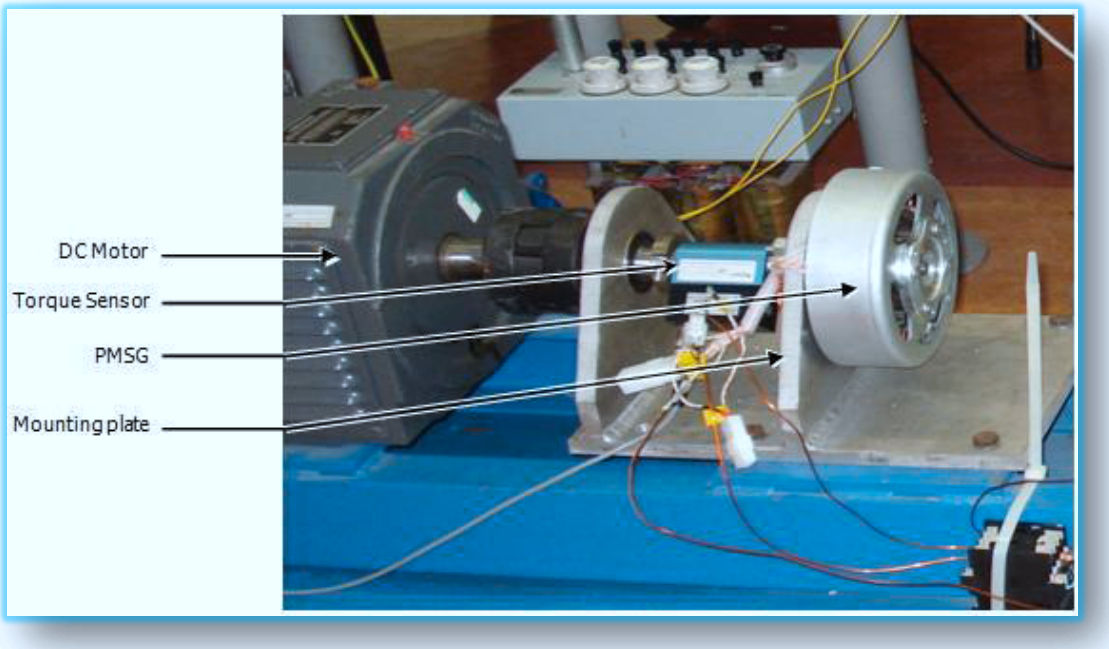

Figure IV-11 Initial experimental setup

As it can be seen in *Figure IV-11*, in the initial setup the torque sensor was coupled directly to the PM generator through ball bearings. After the malfunctioning of the torque sensor, we suspected that the magnets are having an erroneous influence on the sensor so we decided to rebuild the setup as shown in the schematic of *Figure IV-12*, where a stiff shaft has been introduced between the PM generator and the torque sensor and the coupling with the DC machine (prime mover) has been replaced to adapt to the new situation.

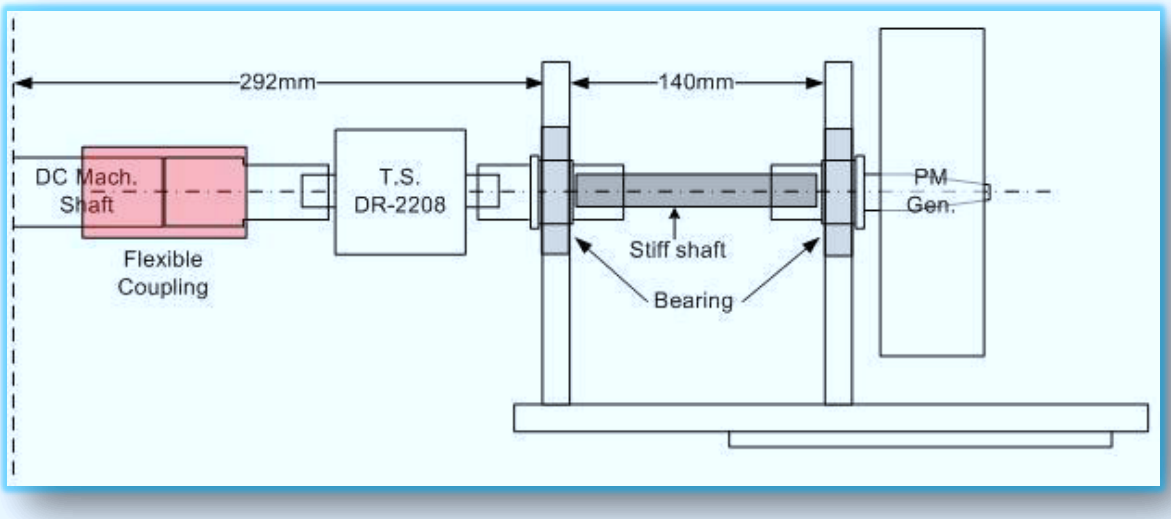

Figure IV-12 Sketch of the alternative experimental setup

Due to malfunctioning of the torque sensor, we adopted an alternative method to calculate the torque, based on the measurement of the DC machine current.

As there is a linear relation between the DC machine current and torque (*Equation IV-9*)

$$T = K_T \cdot I_{DC}$$

Equation IV-9

Where K_T The DC machine constant

K_T has been determined by measuring the voltage and the speed of the DC motor according to *Equation IV-10*

$$E = K_T \cdot \omega$$

Equation IV-10

With:

$$\omega = \frac{2\pi}{60} \cdot N$$

Equation IV-11

By measuring voltages for different speeds it appears that the Dc motor constant K_T is equal to ***1.3*** (average value); this value is adopted for the calculation of the torque for the following tests, except for the first tested generator (G3k0), for which we only applied the torque sensor measurements.

It should be taken into consideration that the motor constant value is not completely accurate, due to the fact that the motor constant depends on the machine construction parameter and the magnetic flux $K_T = K \cdot \Phi$. As the flux is not absolutely constant, because of the presence of hysteresis, this may explain the inaccuracy of the results obtained by calculating torque based on the DC current, in a number of experiments.

IV.4.3 EXPERIMENTAL RESULTS

The following sections contain discussion of the experimental results by comparing them with the simulation results. First the 3kW generators results are presented with different combinations, followed by a comparison. And then the two 9kW generators are presented as well as a comparison between the open and the semi-closed slots. For each tested generator we present the graphs comparing simulation with experiments results for: no-load voltage, iron losses and efficiency. The experiments data are also given as tables in *Appendix_3*, for all performed tests.

IV.4.3.1 3kW Generators

IV.4.3.1.1 G3k0 (3kW with Ferrite magnets)

- *No-load voltage*

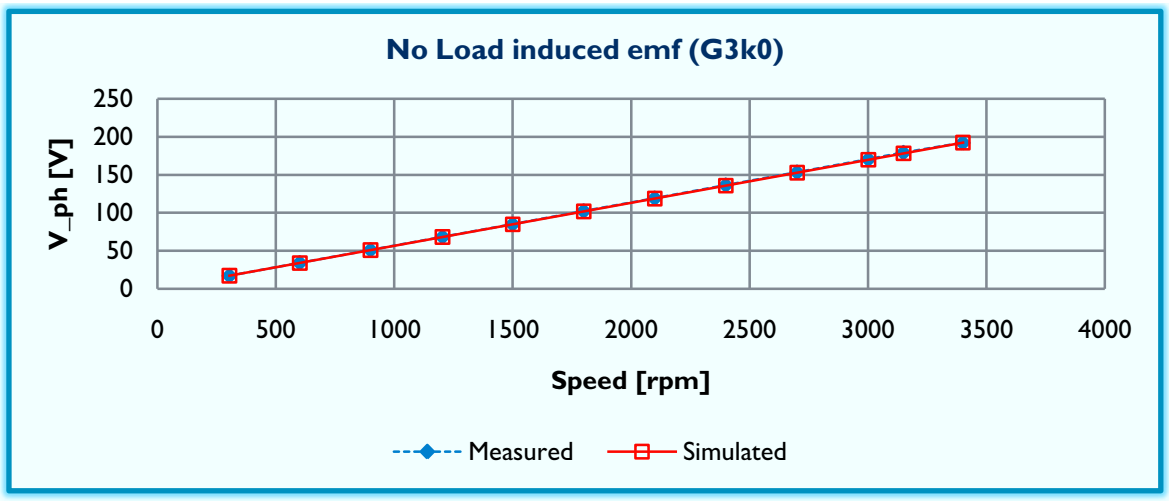

Figure IV-13 Measured and simulated induced voltage versus speed for G3k0

The results of the measured voltage compared with the calculations, show that the calculated voltage coincides perfectly with the measurements, which validate the model.

For a maximum speed of 3400 rpm the generator delivers 192 V.

- *Iron losses*

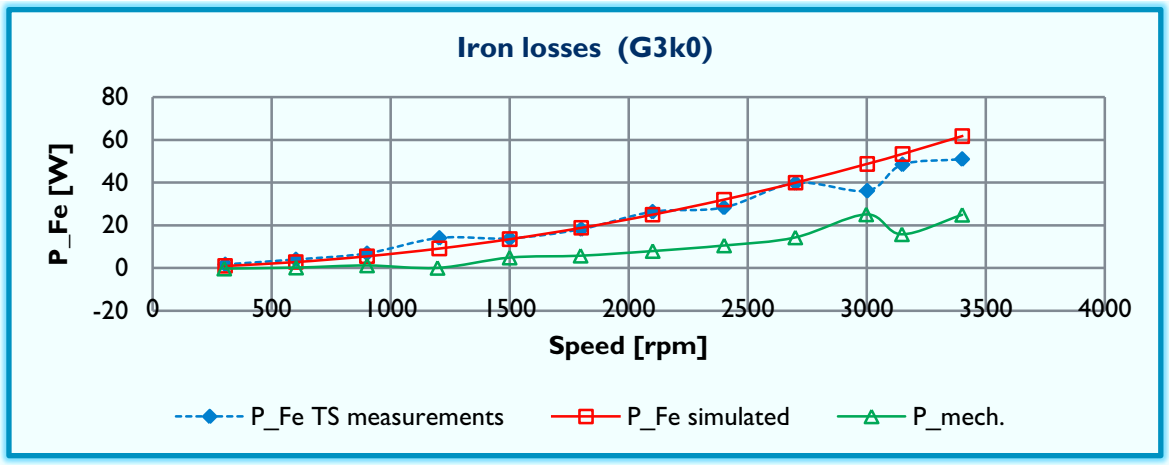

Figure IV-14 Measured and simulated iron losses versus speed for G3k0

Figure IV-14 shows the measured and predicted iron losses of the 3kW generator with ferrite magnets at different speeds. Although there is a slight difference between the measured and calculated values, the difference is not so much, which allows us to validate the model. In the figure we can also see the measured mechanical losses to give an idea of its link to iron losses.

Efficiency

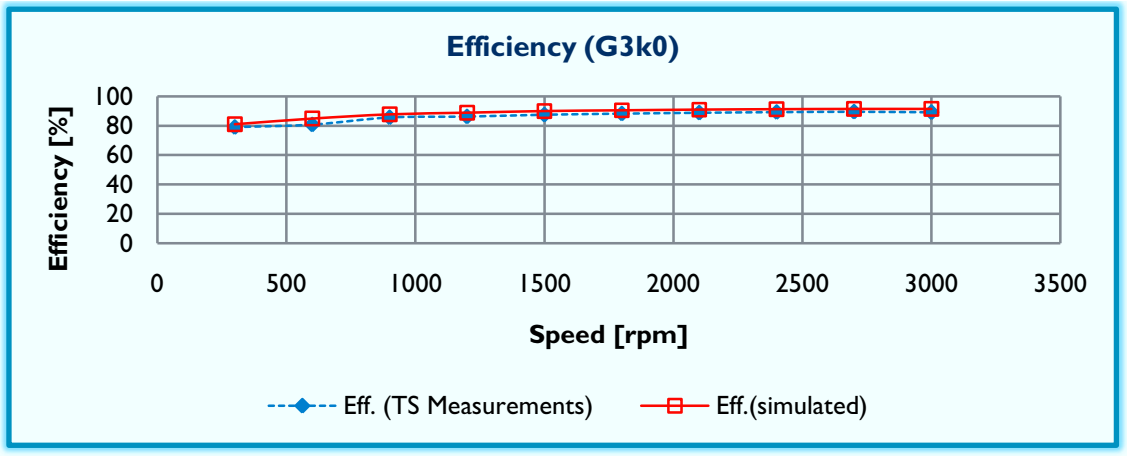

Figure IV-15 Measured and simulated efficiency versus speed for G3k0

It can be remarked that the measured efficiency is slightly lower than what was predicted from the simulation results, which shows that the model is accurate in this case.

IV.4.3.1.2 G3k_3-2 (3kW with NdFeB magnets_3/2)

No-load voltage

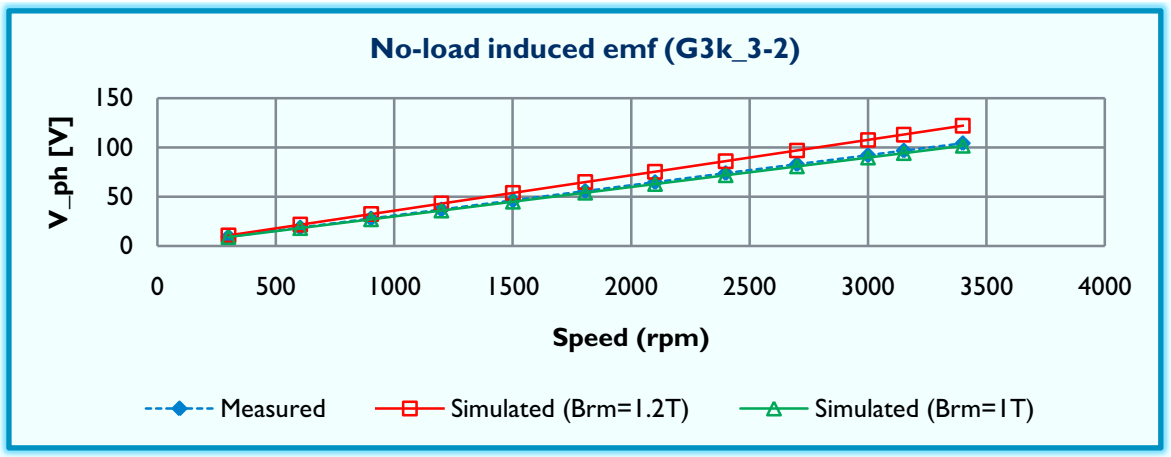

Figure IV-16 Measured and simulated induced voltage versus speed for G3k_3-2

The figure above shows that the predicted no-load voltage for the 3kW NdFeB generator is higher than the actual measurements.

By analysing this results, and based on the induced voltage equation (*Equation IV-12*) that can be derived from Chapter III equations, we have;

$$emf = \frac{1}{\sqrt{2}} N_s \cdot \omega_e \cdot \frac{l_m \cdot B_{rm}}{g_{eff} \cdot \mu_{rm}} \cdot \frac{4}{\pi} \cdot \sin\left(\frac{\pi}{2}\frac{b_m}{\tau_p}\right) \cdot \frac{2}{\pi} \cdot \tau_p \cdot l_s \cdot k_w \cdot k_{fring}$$

Equation IV-12

From the above equation we can have two hypotheses;

- The first one is that the remanent flux density of the magnets is lower than expected; (i.e. $B_{rm} = 1\,T$ instead of $1.2\,T$).
- Or the effective air gap formula (*Equation III-9*) that is based on simplifying assumptions, does not model precisely the actual value of the effective air gap (which is the most probable hypothesis).

By simulating the model by putting $B_{rm} = 1T$, we remark that the simulation results match perfectly the measured values (*Figure IV-16*)

The fact that the no-load voltage is actually20% lower than expected can also be due to the eddy current losses in the magnets.

Iron losses

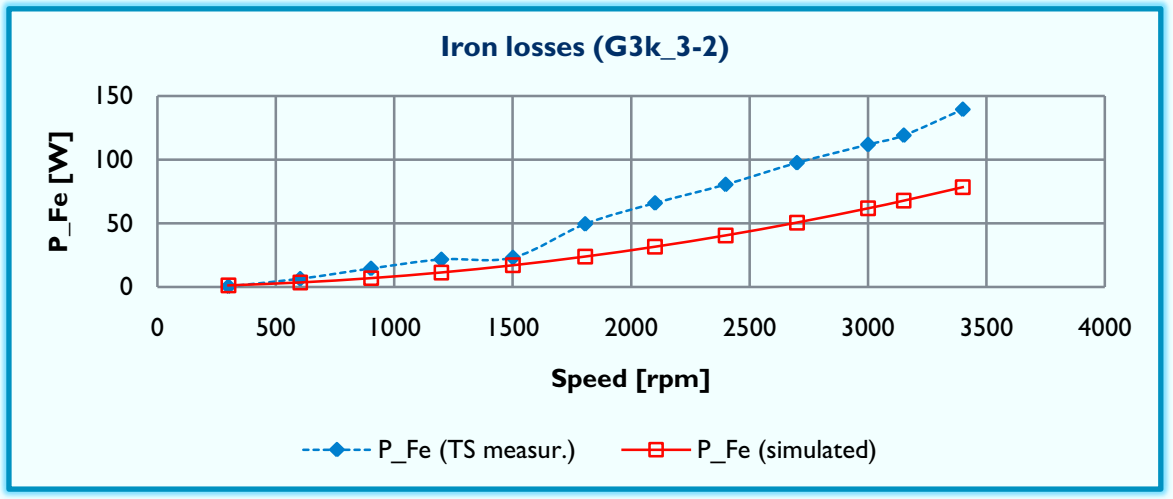

Figure IV-17 Measured and simulated iron losses versus speed for G3k_3-2

As it has been made known in section *IV.4.2*, this is one of the experiments where the results, which are obtained by using the torque, calculated from the DC current measurement, are totally inaccurate. That is why they have been omitted from the graph.

According to the torque sensor measurements, the actual iron losses are higher than what was predicted particularly for high speeds.

In our model we only considered iron losses, whilst the eddy current losses in the magnets are not taken into account. Nevertheless the actual measurements consist of eddy current losses in the magnets as well as iron losses. In comparison with the ferrite magnet machine we note that the eddy current losses in the NdFeB magnets have more influence, which makes that the experimental results are not matching with the simulation expectations.

Efficiency

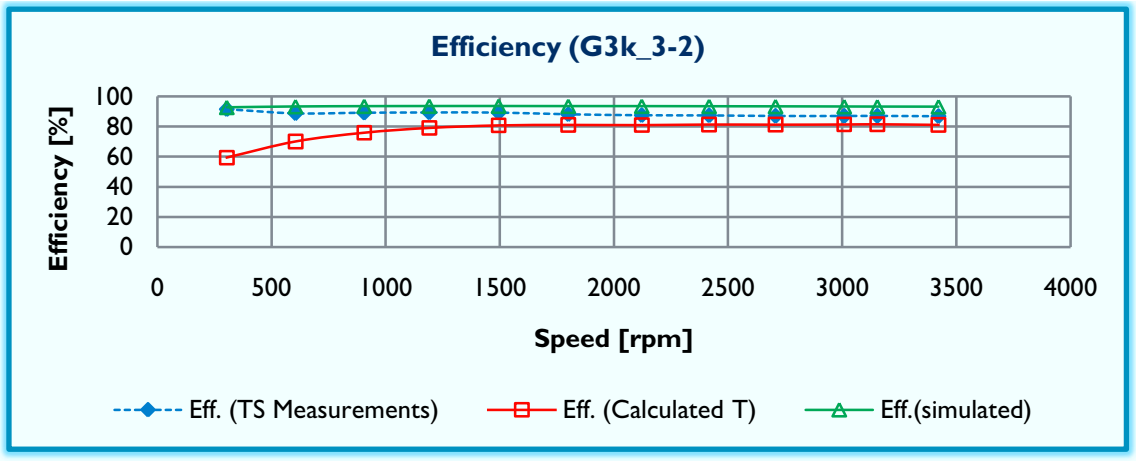

Figure IV-18 Measured and simulated efficiency versus speed for G3k_3-2

The actual efficiency based on the torque sensor measurements, is slightly lower than what was predicted from the simulation results. It is also remarkable that the measured efficiency based on the torque sensor readings is closer to the simulation results than the alternative measuring method which is based on DC current measurements, which leads us to ignore the efficiency results.

IV.4.3.1.3 G3k_9-8 (3kW with NdFeB_9/8 "wrong magnets size")

This section contains the experiment results of the machine with the "wrong" rotor. And the next one shows the experiments results, after replacement of the wrong size magnets by the ones according the designed machine.

No-load voltage

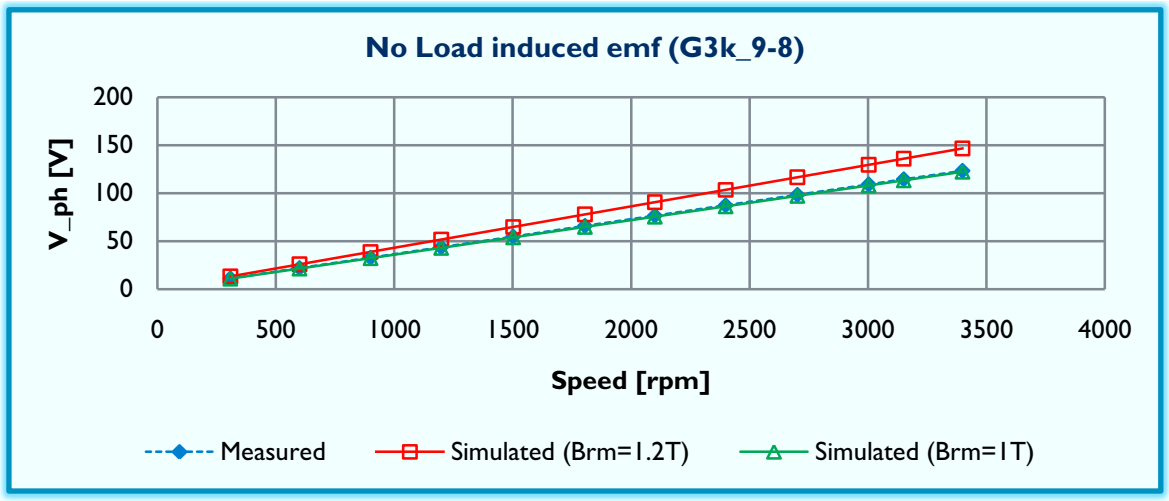

Figure IV-19 Measured and simulated induced voltage versus speed for G3k_9-8

Similarly to the previous generator (G3k_3-2), by simulating with taking $B_{rm} = 1T$ instead of $1.2T$, we get comparable results for both measured and predicted voltage. However it can also be that the applied assumptions for the modelling have a bigger effect, which results in a rougher estimation than expected. Same applies for the modelling of the Carter factor.

Iron losses

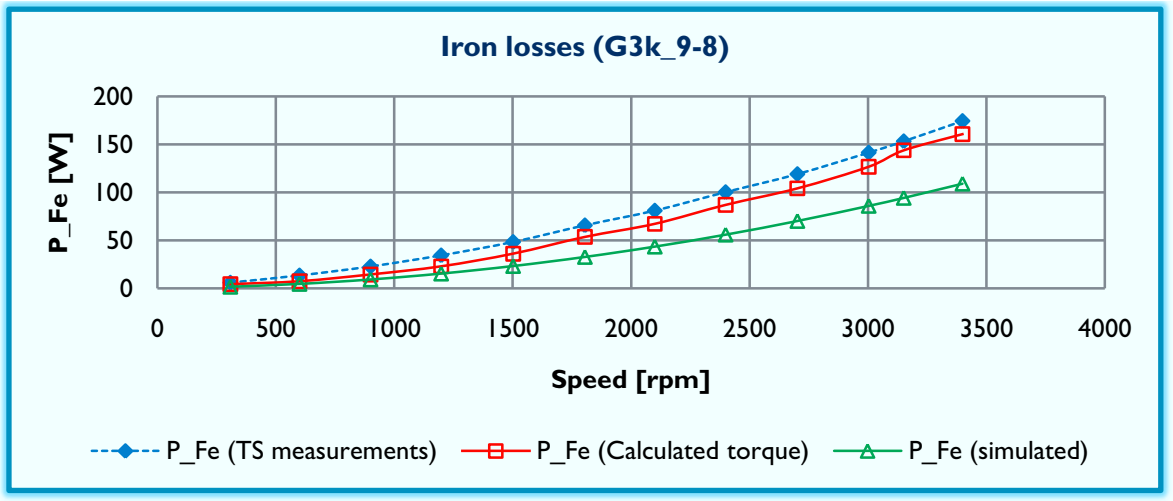

Figure IV-20 Measured and simulated iron losses versus speed for G3k_9-8

From the no-load test results, we can notice that the predicted iron losses are lower than what has been measured by using both measuring methods (torque sensor and calculated torque, based on DC current measurement).

Efficiency

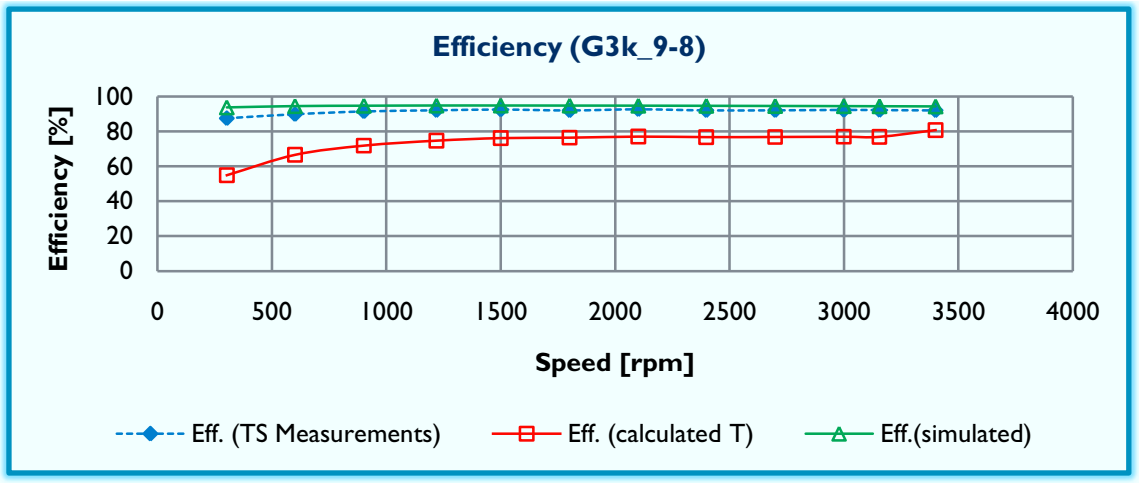

Figure IV-21 Measured and simulated efficiency versus speed for G3k_9-8

Likewise the previous generator the measured efficiency is slightly lower than the calculated one. In this case also we have got a better correlation between simulation and the measurements obtained by using the Torque sensor readings instead of the DC current measurements.

IV.4.3.1.4 G3k_9-8c (3kW with NdFeB_9/8 "corrected magnets size")

As pointed out in the preceding section, the present results are obtained after replacement of the PM on the Generator. (PM width is 15mm instead of 20 mm)

No-load voltage

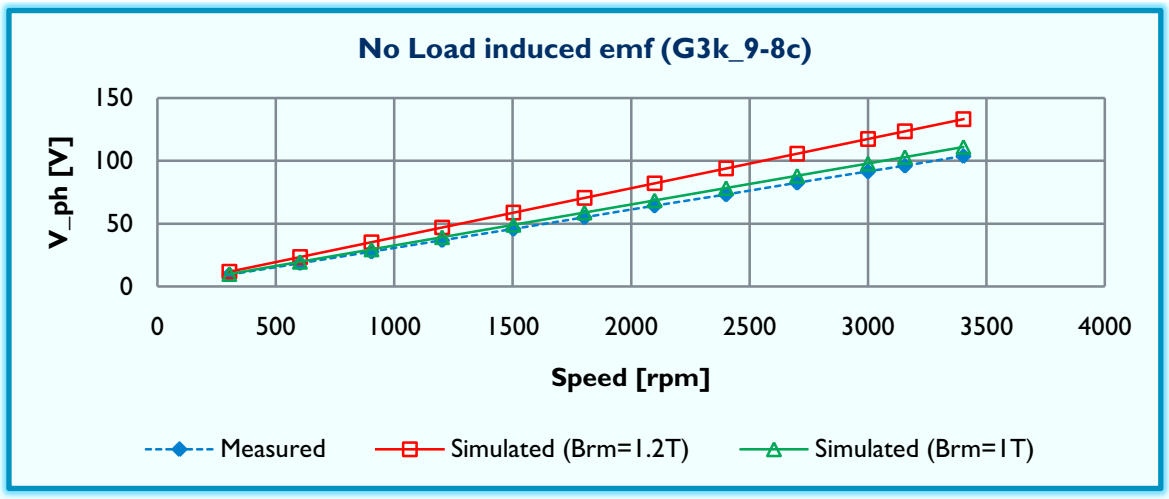

Figure IV-22 Measured and simulated induced voltage versus speed for G3k_9-8c

The induced voltage measurements show that by considering $B_{rm} = 1T$, the simulated voltage is closer to the actual voltage in comparison with $B_{rm} = 1.2T$. Nevertheless contrary to the previous generator, the simulated values do not fit perfectly with the measured ones. As we said previously this could be an indication that the inaccuracy may be caused by the model and is not due to the magnets' remanent flux density.

Iron losses

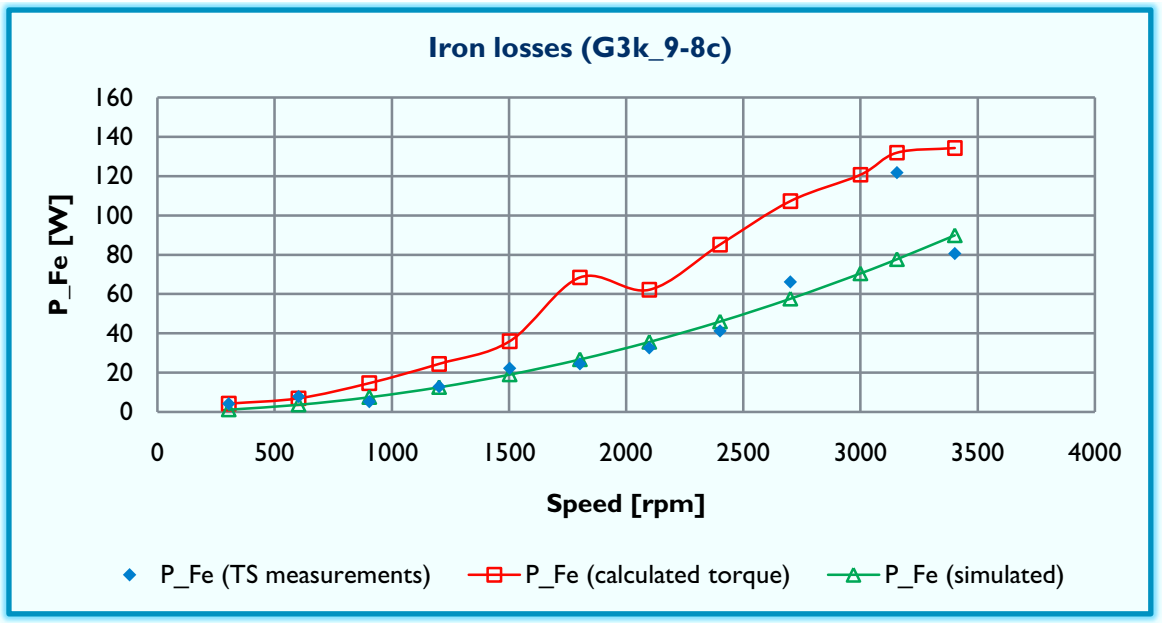

Figure IV-23 Measured and simulated iron losses versus speed for G3k_9-8c

Despite the previous experiments, in this case, it seems that the readings given by the torque sensor are more correlating. The measured losses are very close to the simulated values. The measurements based on the calculated DC current show higher iron losses.

Efficiency

Contrary to the preceding generators, the efficiency based on the Torque sensor measurements is very low, that is why the torque sensor measurements are not considered in this case. Therefore we omit the efficiency graph, yet it can be found in *Appendix_3*.

IV.4.3.2 9kW Generators

IV.4.3.2.1 G9k_scs (9kW with NdFeB "Semi-Closed Slots")

No-load voltage

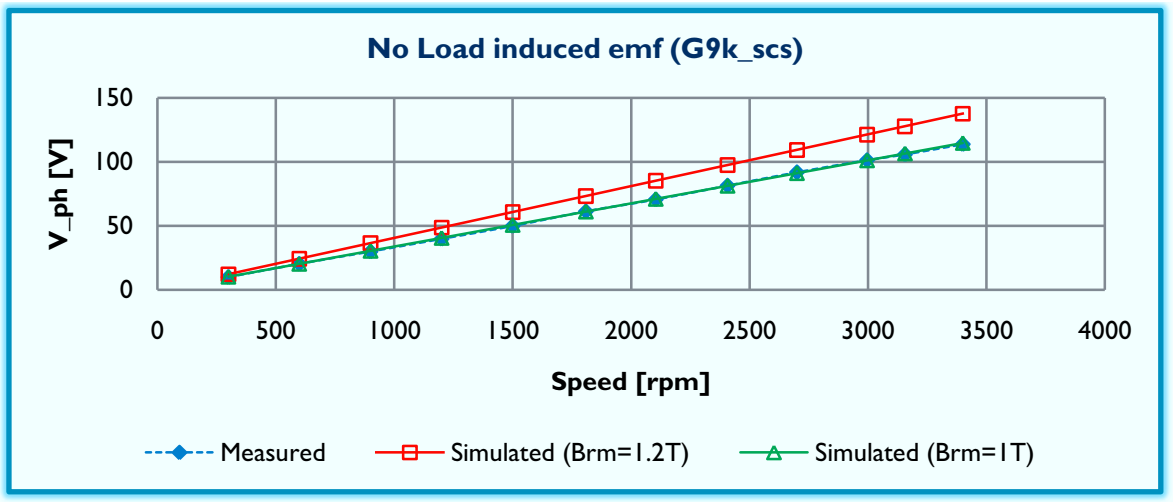

Figure IV-24 Measured and simulated induced voltage versus speed for G9k_scs

Similar to the 3kW generators (with NdFeB PM), the results shows that induced emf, calculated based on a remanent flux density value of $1T$, coincides perfectly with the measured emf. But as it will be shown in the next section (*IV.4.3.2.2*), this might not be a valid justification of the non correlated results.

Iron losses

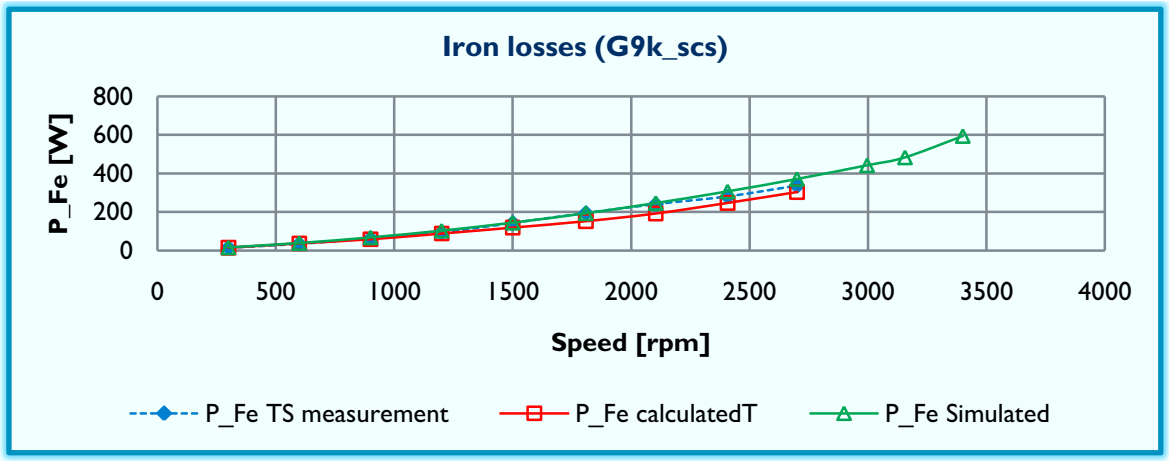

Figure IV-25 Measured and simulated iron losses versus speed for G9k_scs

The figure shows that the iron loses increase with speed. It is also remarkable that there is a slight difference between the measured and the predicted iron losses, especially the measurements based on the torque sensor readings, which seem to correlate almost perfectly with the simulation during this experiment.

As it can be seen, the experiments for the last three speed values were not executed, due to the fact that during testing the available prime move could not deliver the needed power at speeds higher than 2600rpm.

Efficiency

As it has been revealed earlier, the torque sensor readings were not completely trustworthy, due to its malfunctioning. The torque sensor gave very low values of efficiency especially for low speeds. But the alternative method measurements reveals lower efficiency than what was predicted, but once again this result is omitted and the graphs can be found in *Appendix_3*.

IV.4.3.2.2 G9k_os (9kW with NdFeB "Open Slots")

This section is about the Open Slot 9kW generator. Despite the stator slots, everything else is the same as for the G9k_scs.

No-load voltage

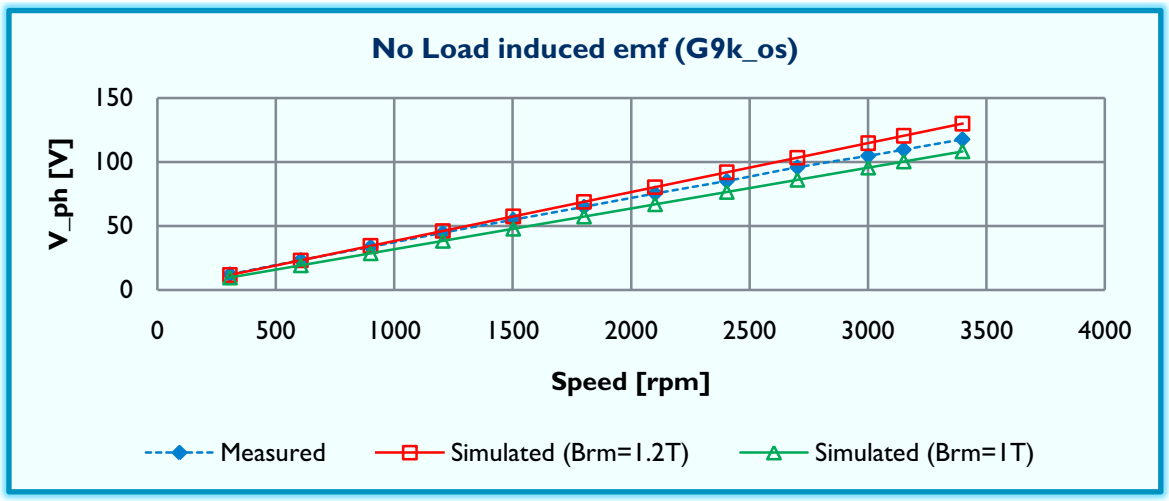

Figure IV-26 Measured and simulated induced voltage versus speed for G9k_os

The no-load voltage results revealed some remarks related to the induced voltage models. Keeping in mind that the rotor is the same, (for both OS- and SCS-slots generators), thus the same PM. Our hypothesis that the remanent flux density was $B_{rm} = 1T$, is not validated in this case, which lets us suspect that it is the effective air-gap models that need to be reviewed.

Iron losses

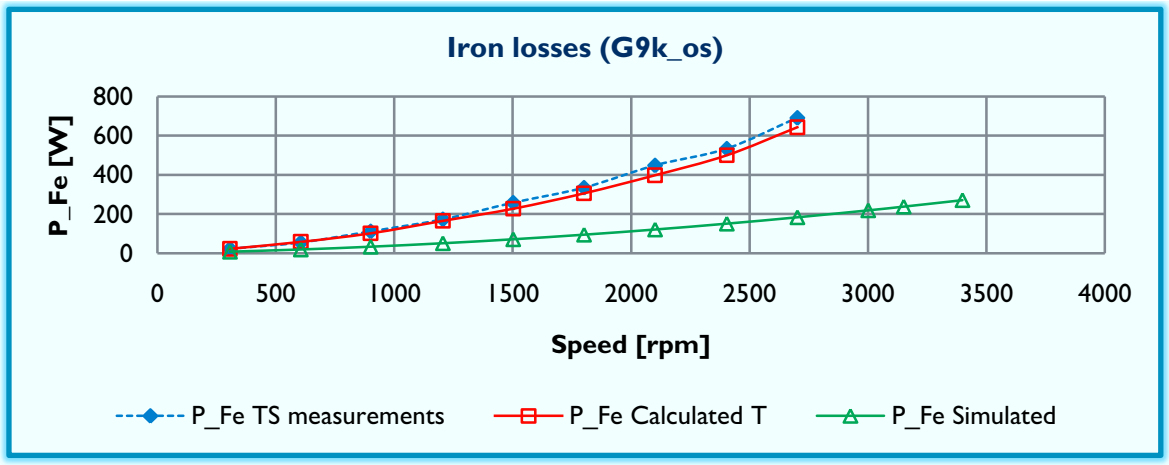

Figure IV-27 Measured and simulated iron losses versus speed for G9k_os

The experiment results reveal much higher iron losses than those expected from the simulation results. This observation implies that the used model is far from being representative of iron losses in the open slots stator contrary to the semi-closed slots stator where it gave correlating results. This can be explained by the fact that the eddy current losses in the magnets, which are not considered in the simulating model, are much higher because of the open slots.

Efficiency

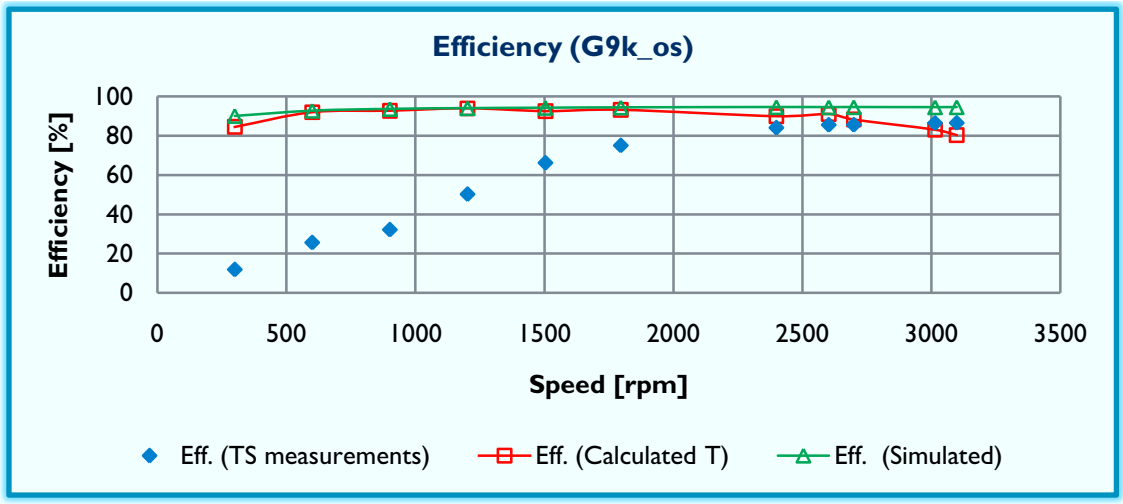

Figure IV-28 Measured and simulated efficiency versus speed for G9k_os

Here once more the torque sensor readings for low speeds measurements were very low. But around nominal speed, these were more acceptable and closer to the expected results as well to the measurements based on DC current measurements. Again this can be explained by the malfunctioning of the torque sensor and the inaccuracy of the dc current measurement method.

IV.4.3.3 Comparison of the different generators

IV.4.3.3.1 Comparison between 9/8 & 9/8_c

No-load voltage

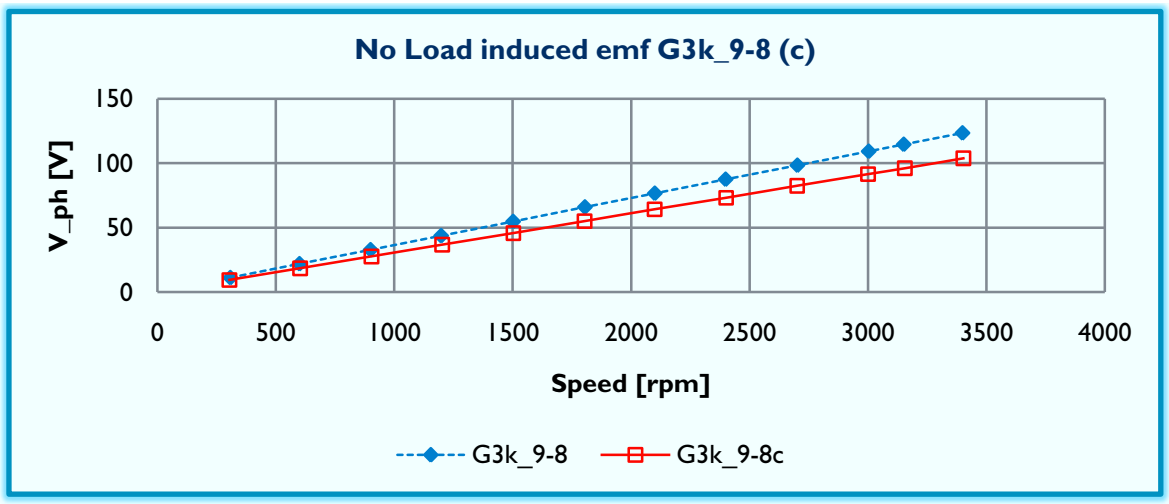

Figure IV-29 Measured induced voltage versus speed for G3k_9-8 & G3k_9-8c

As it can be seen the measured No-Load voltage in the 3kW generator with 9-8 combination was higher before correcting the permanent magnets size. That is due to the fact that the permanent magnets were wider, so they produce more flux. From this perspective the mistaken machine was performing better than after magnets correction.

Iron losses

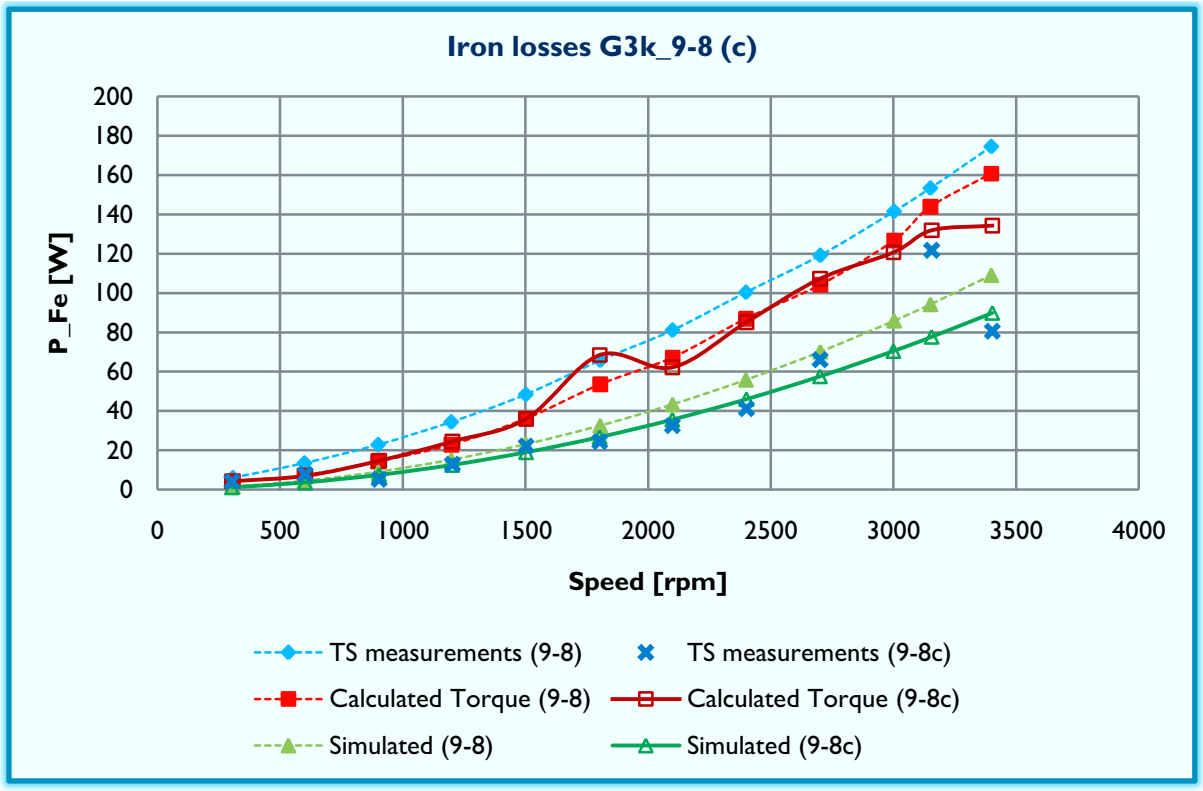

Figure IV-30 Iron losses versus speed for G3k_9-8 & G3k_9-8c

The figure above illustrates the iron losses results for the 3kW generator with 9-8 combination in both situations; before and after the correction of the permanent magnets size. The comparison between the two constructions is done for both measuring methods (Torque Sensor measurement and Calculated Torque based on the DC current measurement).

From the simulation results it is noticed that we expected lower iron losses after correction of the PM size. The experimental results based on the torque that was calculated from the DC current readings, shows almost no difference between the two generators for low speeds. For higher speeds we notice that iron losses are lower after correction of the magnets.

The measurements based on the Torque Sensor readings shows that the iron losses of the generator with correct permanent magnets size are noticeably lower (two times lower) than those of the rotor with wider magnets.

Efficiency

From simulated results, it can be seen that with the corrected generator, we expect lower efficiency. This is an effect of the wider magnets; in consequence more voltage is produced.

The experimental results based on the torque measured from DC current readings, show similar results but with lower values. The reason can be that our model is based on simplifying assumptions. Moreover as we already mentioned in *Chapter II*, our model does not include the back iron losses as well as the eddy current losses in the magnets, which are significant.

As stated in section *IV.4.3.1.4*, the torque sensor measurements are not considered in this test due to the fact that they are considerably low. And the alternative method results are also far from being representative. (see graphs in *Appendix_3*)

IV.4.3.3.2 Comparison between 3/2 & 9/8

No-load voltage

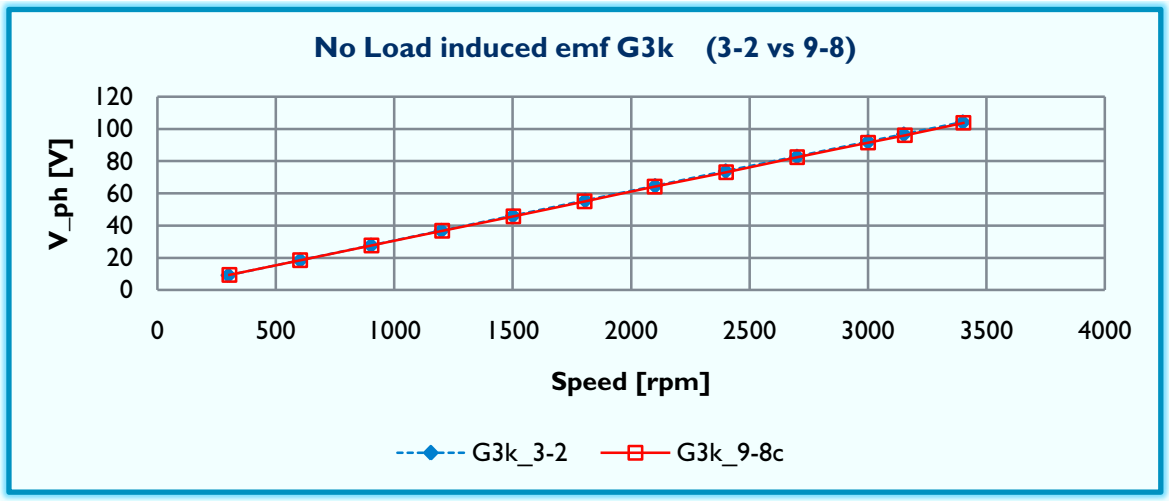

Figure IV-31 Measured induced voltage versus speed for G3k_3-2 & G3k_9-8c

It is obvious from *Figure IV-31* that the induced no-load voltage is almost the same for the 3kW NdFeB permanent magnet generator with both 3-2 and 9-8 poles/slots combinations.

Iron losses

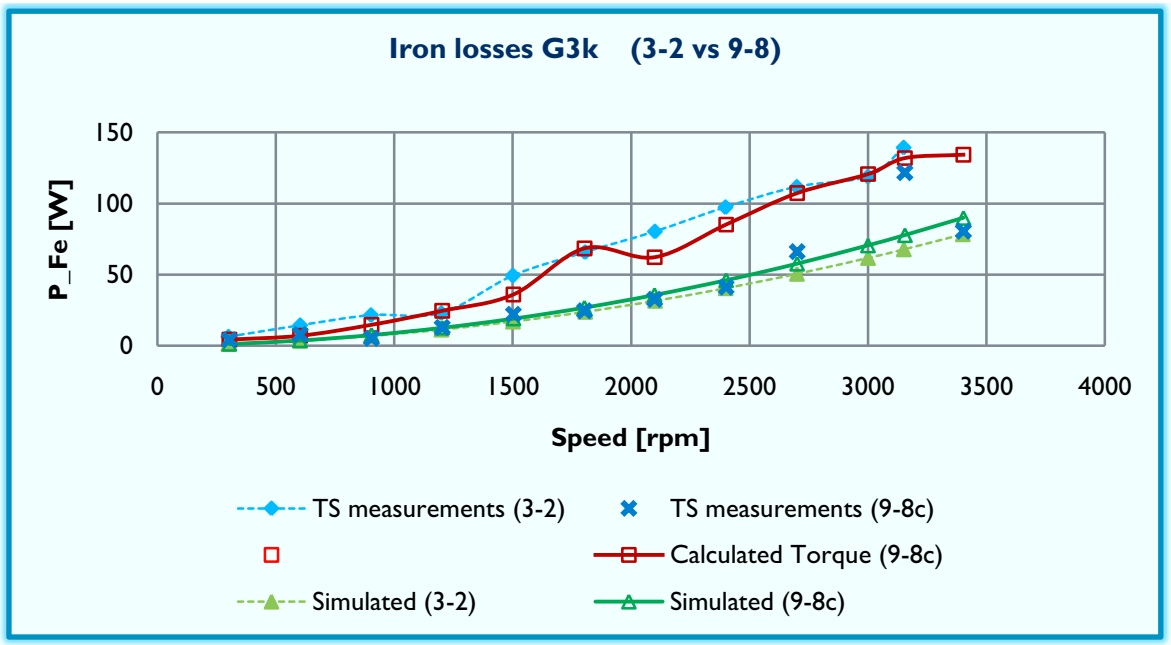

Figure IV-32 Iron losses versus speed for G3k_3-2 & G3k_9-8c

Based on simulations we expected higher iron losses with the 9-8 combination than those produced in the generator with3-2 combination. The experiments results revealed different results, but as the torque sensor measurements are not reliable, we didn't consider these results.

Efficiency

The results show that the predicted efficiency is slightly higher for the 3-2 combination. We see this difference back in the experiments based on DC current measurements, but in this case the difference is higher than expected. Since the torque sensor readings, when running the experiment on the 9-8 generator, gave very low values, these results were discarded.(see graphs in *Appendix_3*)

IV.4.3.3.3 Comparison between OS & SCS

No-load voltage

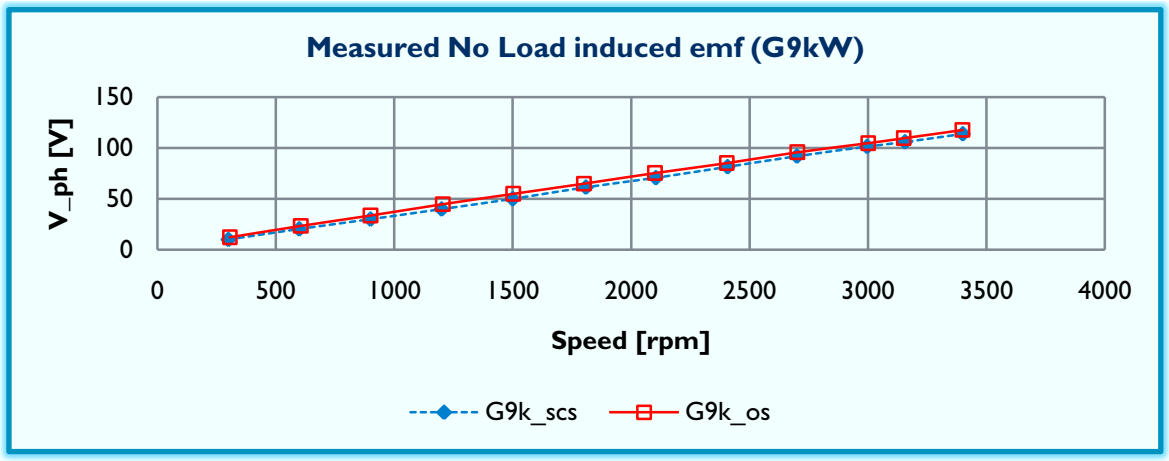

Figure IV-33 Measured induced voltage versus speed for G9k_scs & G9k_os

The above figure shows that the no-load voltage produced by the open slots machine is slightly higher than what is supplied from the semi-closed slots generator. The reason is that the number of turns per tooth in the open slots stator is 10 turns whereas in the semi closed slots stator is 9 turns per tooth *(Appendix_5)* .

Iron losses

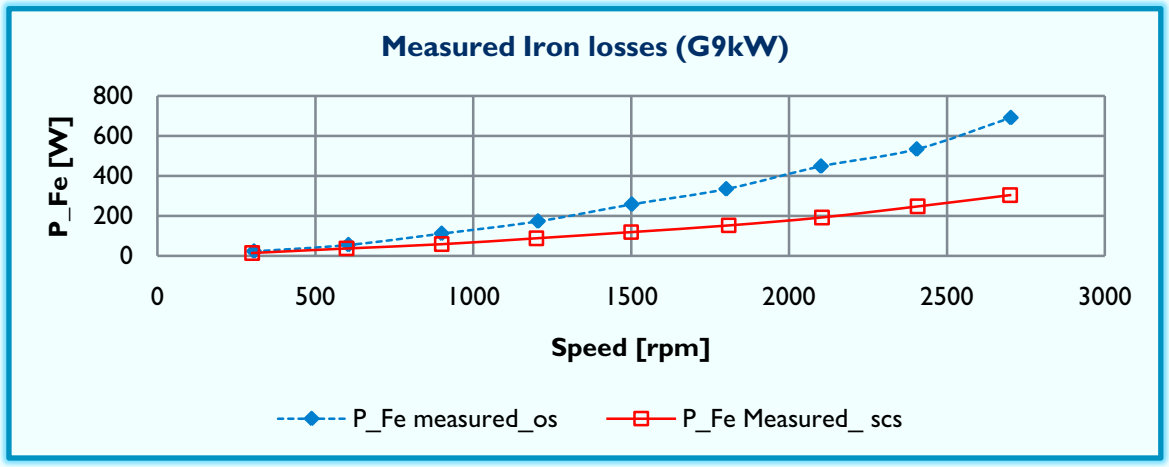

Figure IV-34 Measured iron loses versus speed for G9k_scs & G9k_os

By analysing the above figure, the relatively high iron losses in the open slots machine, compared with the semi-closed slots generator, may be explained by the fact that the eddy current losses on the Permanent magnets are higher, because of the reluctance variation due to the higher slotting factor in the open slots stator.

Efficiency

The generators efficiency based on the calculated torque from DC current measurements of the generator with open slots stator is higher than that of the semi closed slots stator, despite that we have more iron losses in the open slots generator. This result is again not valid.

IV.5 CONCLUSION

A survey of the simulations and experiments results of the different studied generators was presented in this chapter.

From the experimental results, we noted that the models are validated for the ferrite magnets machine, but are less representative in the case of NdFeB magnets.

For the no-load voltage we noticed that the experimental results in the NdFeB magnet machines were 20% lower than expected. Except for the open slots 9kW generator where the deviation was less than 20%. This result may be a motivation for further research over the influence of the magnets type on the no-load voltage.

For the losses, the models could not be completely validated (for the NdFeB machines), this is due to neglecting eddy current losses in the magnets which has a bigger effect on the non correlation of the experimental results with simulation expectations. As the ferrite magnets are non conductive the eddy current losses have less effect and therefore they could be neglected. Consequently the model should be improved by considering eddy current losses in the magnets, and the back iron.

Comparing the two 3kW generators with different number of poles and number of slots combinations, we noticed that the 3-2 combination shows higher iron losses in comparison with the 9-8 combination.

Against expectations, we realised that the original 9-8 generator, (with "wrong" magnets size) was performing better than after correction. The extra losses produced by the wider magnets were well compensated with the higher induced voltage.

By comparing both variants of the 9kW generator, we could conclude that open slots leads to a huge increase in the iron losses as expected, and this is a result of the eddy current losses increase in the magnets due to slotting. However the efficiency results show that these losses have been compensated. But efficiency results are far from being trustworthy. Therefore more investment has to be made to acquire a better and reliable setup.

Chapter V

V. General Conclusion

In this MSc project based on simulation and experimental work, the objective was on one hand to determine the most suitable generator construction for our application, which is about generators that will be used on board of yachts, on the other hand to validate the models by applying experiments on different prototypes.

First of all we had to make a choice of generator topologies and construction that would meet the requirement of the customer, which is to obtain a generator that is as compact and efficient as possible. Based on literature research we found out that the most suitable design for our application is basically a permanent magnet machine with concentrated windings. In order to be able to come up with the best generator for the application, we considered different designs. The differences consist in; magnet materials, combinations of number of poles and slots, slots type (open- or semi-closed slots).

After making our choices, models have been derived representing; produced no-load voltage, iron and copper losses and efficiency of the constructed machines.

After derivation of the machine models (induced emf and different losses), the equations have been implemented in simulating program (Matlab®) to replicate the behaviour of the different machines.

Simulations show that that the ferrite magnet generator produce more voltage than the NdFeB ones, on the other hand it presents low efficiency compared to NdFeB generators.

Further the simulation results have been compared with the experimental results of the different tested generators.

As a consequence of the problems faced during the experimentation phase, the results were way far from our expectation. Nevertheless we could draw some conclusions.

First of all we concluded that the model is validated for the ferrite magnet machines, but because of neglecting assumption, these models do not give an accurate representation of the NdFeB magnets machines. This result is mostly for the reason that we did not consider the eddy current losses in the back iron and the magnets, which appears to be huge in the case of NdFeB machines.

For the 9kW generator variants, as has been expected, the use of open slots hugely increases the losses. However it appeared that it does not have that much influence on the efficiency, but the efficiency measurement are not considered because of unreliability of the setup.

The work on this topic is far from being finished, which makes it open for future studies and improvements regarding the models, by including the eddy current losses in the back iron and the magnets. Also the experimental setup has to be enhanced in order to get more accurate and trustful results.

Due to the generator's complex construction, the models used in this work are based on different assumptions, simplifications and neglected parameters, which are for a first design acceptable but for a more accurate imitation of the generator behaviour, a finite element study may be a good option especially for the electromagnetical behaviour of the generator.

Another aspect of this project is the thermal study; Thermal analysis was first included in the work planning. Some experiments were performed using thermocouples placed on different locations in the PMSG, (on the windings and the stator tooth and yoke), and a thermal camera was used to record the thermal behaviour of the rotor, these experiments were not finished because of time limitation resulting in the several setup problems. But this study can be carried out in future work on the generators including possible cooling solutions.

Appendix_2

MODELLING PROGRAM

MATLAB® SCRIPT FOR ONE OF THE STUDIED GENERATORS

```
%############ Generator : G3k2 ################
%###    3kW NdFeB 24 Poles 27 Teeth  9/8    ###
clear
%% _________CONSTANTS____________________

mu_0=4e-7*pi;    % magnetic permeability in vacuum  [T.m/A]
mu_rm=1.05;      % recoil permeability of magnets      =
mu_rFe=200;      % relative permeability of Iron Fe    =
rho_mCu=8900;    % Mass density of Copper Cu [kg/m^3]   {{8960}}
rho_mFe=7700;    %   =     =    =  Iron Fe      =
rho_mm=7500;     %   =     =    =  Magnets      =
rho_Cu=1.72e-8;  % resistivity of Cu      [Ohm.m]   {{ 1.72e-8} @20oC}
rho_Fe=10e-8;    % resistivity of Fe         =      {{ 10e-8} @20oC}
rho_m=1.30e-6;   % resistivity of magnets    =

P_Fe0h=.65;      % hysteresis loss coefficient
P_Fe0e=.65;      % eddy_current loss coefficient

%________Factors_______________
%k_sfil=0.25;     % fill factor
k_fring=1.11;    % fringing factor
%k_w=sin(2/3*pi);% winding factor
k_w=.945;   %(9/8)

%_________Machine Geometry_____________
N_p=24;          % Number of poles
N_t=27;          % Number of teeth
N_c=55;          % Number of coils


r_s=.155/2;      % Stator radius        [m]
l_s=35e-3;       % Stator Axial length   =
h_sy=11e-3;      % Stator Yoke length    =
h_s=17.5e-3;     % Slot/tooth height     =
h_so=2e-3;       % Dovetail height       =  (=10% of the slot height)

b_t=7e-3;        % Tooth width           =
b_tt=12e-3;    % Dovetail width        =  (=+ 2x60% of the tooth width)
l_g=2e-3;        % mechanical air-gap    =
%------------Magnets--------------------
l_m=1.6e-3;      % Magnet length         =
%b_m=20e-3;       % Magnet width  (wrong) =
b_m=15e-3;       % Magnet width (correct)=
B_rm=1.2;        % Remanent flux density [T]
%---------------------------------------
p=N_p/2;                          % pole pairs
tau_p=pi*(r_s+l_g)/p;             % pole pitch
tau_s=2*pi*r_s/N_t;               % slot pitch
tau_s1=2*pi*(r_s-h_so)/N_t;       %
b_s=tau_s1-b_t;                   % slot width
b_so=tau_s-b_tt;                  % slot openning width
b_si=2*pi*(r_s-h_s)/N_t-b_t;      % slot inner width
A_slot=(b_si+b_s)*(h_s-h_so)/2;   % Slot Area

b_p_tau_p=b_m/tau_p;              % pole width by pole pitch ratio
%b_p_tau_p=.8;
```

```
%% _________Machine Parameters_____________

P=3000;              %Desired output power [W]
cofi=.9;             %Power factor

rpm=3156;            %Rotational speed     [rpm]

om_m=rpm/60*2*pi;    % Angualr frequency   [rad/s]
om_e=om_m*p;         % Electrical angular frequency [rad/s]

%H_c=B_rm/mu_0/mu_rm;%Coercive Force       [A/m]


%% Determination of N_s
% R_s=0.43;                          % Phase resistance
% D_Cus=.70e-3;                      % Conductor diameter
% A_Cus=pi*(D_Cus/2)^2;              % Conductor cross section
% l_Cus=R_s*3*A_Cus/rho_Cu;          % Concuctor length
% %l_turn=2*(l_s+pi*1.5*b_t/2);     % conductor length per turn
% %l_turn=2*(l_s+pi*tau_s/2);       % conductor length per turn  (tau_s)
% l_turn=2*(l_s+pi*b_t/2);           % conductor length per turn  (b_t)
% N_s=l_Cus/l_turn;                  % Number of turns per phase
% N_c=N_s*3/N_t;                     % Number of turns per tooth

%% Determination of R_s

N_s=(N_t/3)*N_c/3;                   % Number of turns per phase
l_turn=2*(l_s+pi*1.5*b_t/2);           % conductor length per turn ;
%l_tooth=N_c*l_turn;                % conductor length per tooth
l_Cus=N_s*l_turn;                   % Conductor length per phase
D_Cus=.70e-3;                       % Conductor diameter
A_Cus=pi*(D_Cus/2)^2;               % Conductor cross section
R_s=rho_Cu*l_Cus/(3*A_Cus);         % Phase resistance

%%
gamma=4/pi*(b_so/2/(l_g+l_m/mu_rm)*atan(b_so/2/(l_g+l_m/mu_rm))-
log(sqrt(1+(b_so/2/(l_g+l_m/mu_rm))^2)));
k_Carter=tau_s/(tau_s-gamma*(l_g+l_m/mu_rm));
g_eff=1*(l_g+l_m/mu_rm)*k_Carter;
%______air-gap Flux Density_______
B_g=l_m/g_eff/mu_rm*B_rm;
B_g1=B_g*4/pi*sin(pi/2*b_m/tau_p);
%_____Flux Calculation_______
PHI_pmmax=B_g1*2/pi*tau_p*l_s*k_w*k_fring;
%PHI_pmmax=B_g1*b_m*l_s*k_w*k_fring;
%%PHI_pmmax1=B_rm*l_m/(l_m+mu_rm*l_g)*b_t*l_s;
%_______EMF Calculation________
 emf=N_s*om_e*PHI_pmmax/sqrt(2);
% emf1=N_s*l_s*2*B_g1*om_m*r_s/sqrt(2)*k_w;
%emf=2*N_s*B_g1/sqrt(2)*l_s*r_s*om_m*k_w*k_fring; %*0.875
%____Current___
I_s=P/emf/3/cofi;
%______ Reluctances Calculation____
R_mg=g_eff/mu_0/tau_s/l_s;
R_msigmas=2*b_s/mu_0/(h_s-h_so-b_so/3)/l_s;
R_msigmaso=b_so/mu_0/(h_so+b_so/1.5)/l_s;
R_msigma=1/(1/R_msigmas+1/R_msigmaso);
%_______INDUCTANCE_______
L_s=3/2*N_c^2*(N_t/3)*(6*R_mg+2*R_msigma)/(3*R_mg*R_msigma); %Inductance
X_l=om_e*L_s;                                                %Phase reactance

%F_iideal=3/2*pi/tau_p*N_s*PHI_pmmax;
```

```
%% _______LOSSES CALCULATION________
    %----Copper losses----

P_Cus=3*I_s^2*R_s;  %COPPER LOSSES

V_Cus=3*l_Cus*A_Cus;         % Cu volume
M_Cus=V_Cus*8900;            % Cu Mass

J=I_s/3*A_Cus;                 % Current density

P_gen=3*emf*I_s*cofi;

    %----Iron losses----
B_tmax=PHI_pmmax/l_s/b_t;                          %tooth flux density

V_Fest=N_t*(h_s*b_t+h_so*(b_tt-b_t))*l_s;          %Teeth Volume
M_Fest=V_Fest*rho_mFe;                             %Teeth Mass

P_Festnom=1.6*M_Fest*(B_tmax/1.7)^2*(P_Fe0h*om_e/(2*pi*50)+P_Fe0e*(om_e/(2*pi*50))^2);

B_ymax=B_g1*tau_p*2/pi/2/(h_sy);                   %Yoke flux density

V_Fesy=l_s*pi*((r_s-h_s)^2-(r_s-h_s-h_sy)^2);      %Yoke Volume
M_Fesy=V_Fesy*rho_mFe;                             %Yoke Mass

P_Fesynom=1.6*M_Fesy*(B_ymax/1.7)^2*(P_Fe0h*om_e/(2*pi*50)+P_Fe0e*(om_e/(2*pi*50))^2);

P_Fes=P_Festnom+P_Fesynom;  %IRON LOSSES

V_Fes=V_Fest+V_Fesy;
M_Fes=M_Fest+M_Fesy;

%% Total Losses
P_loss=P_Cus+P_Fes;
Eff=(P_gen-P_loss)/P_gen*100;

%%
V_pm=l_m*.05*N_p*b_m;
M_pm=V_pm*7700;

%% ~~~~~~~~~~~~~~~~~~Thermal~~~~~~~~~~~~~~~~~~~
%___ Constants ___
rho_ThCu=0.385;   % Specific heat capacity of Copper Cu [j/g/K]
rho_ThFe=0.450;   % Specific heat capacity of Iron Fe   [j/g/K]
rho_ThvCu=3.45;   % Volumetric heat capacity of Copper Cu [j/cm^3/K]
rho_ThvFe=3.537;  % Volumetric heat capacity of Iron Fe   [j/cm^3/K]
%-----------------
C_thFes1=M_Fes*1e3*rho_ThFe;
C_ThCus1=M_Cus*1e3*rho_ThCu;

C_Ths1=C_thFes1+C_ThCus1;   %Thermal capacitance of stator [j/K]         (M)

C_thFes=V_Fes*1e6*rho_ThvFe;
C_ThCus=V_Cus*1e6*rho_ThvCu;

C_Ths=C_thFes+C_ThCus;      %Thermal capacitance of stator [j/K]         (V)

%%
```

Appendix_3

EXPERIMENTS RESULTS

EFFICIENCY GRAPHS (NON VALIDATED)

- G3k_9-8c

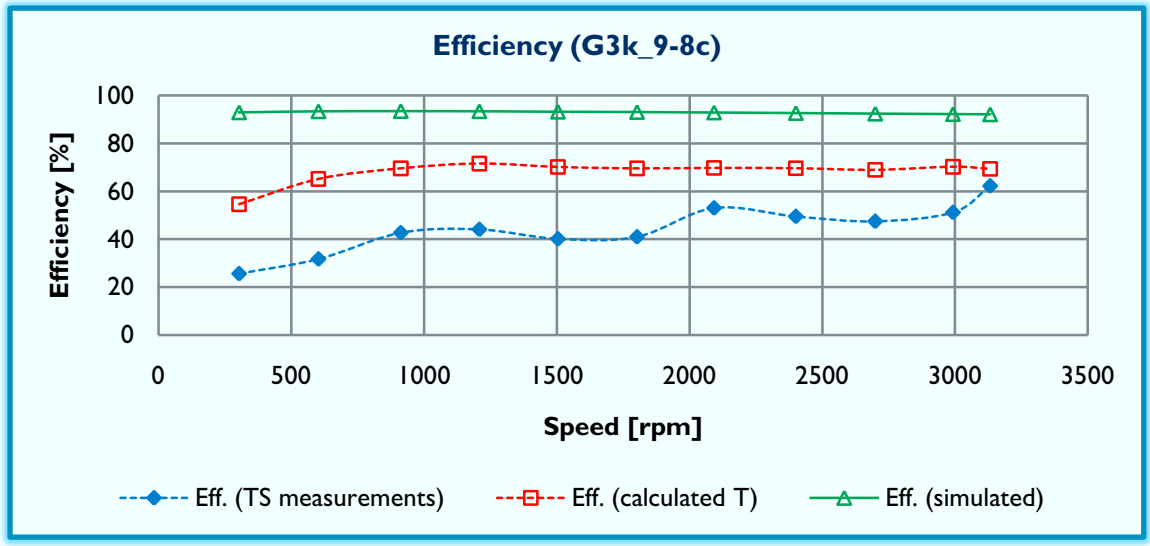

Measured and simulated efficiency versus speed for G3k_9-8c

- G9k_scs

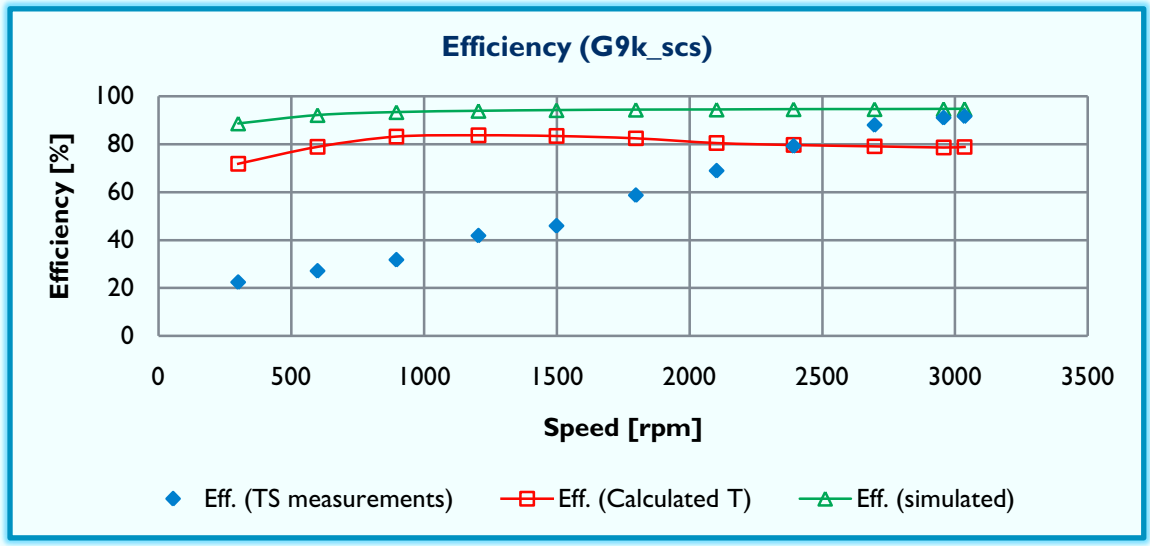

Measured and simulated efficiency versus speed for G9k_scs

G3k_9-8 vs. G3k_9-8c

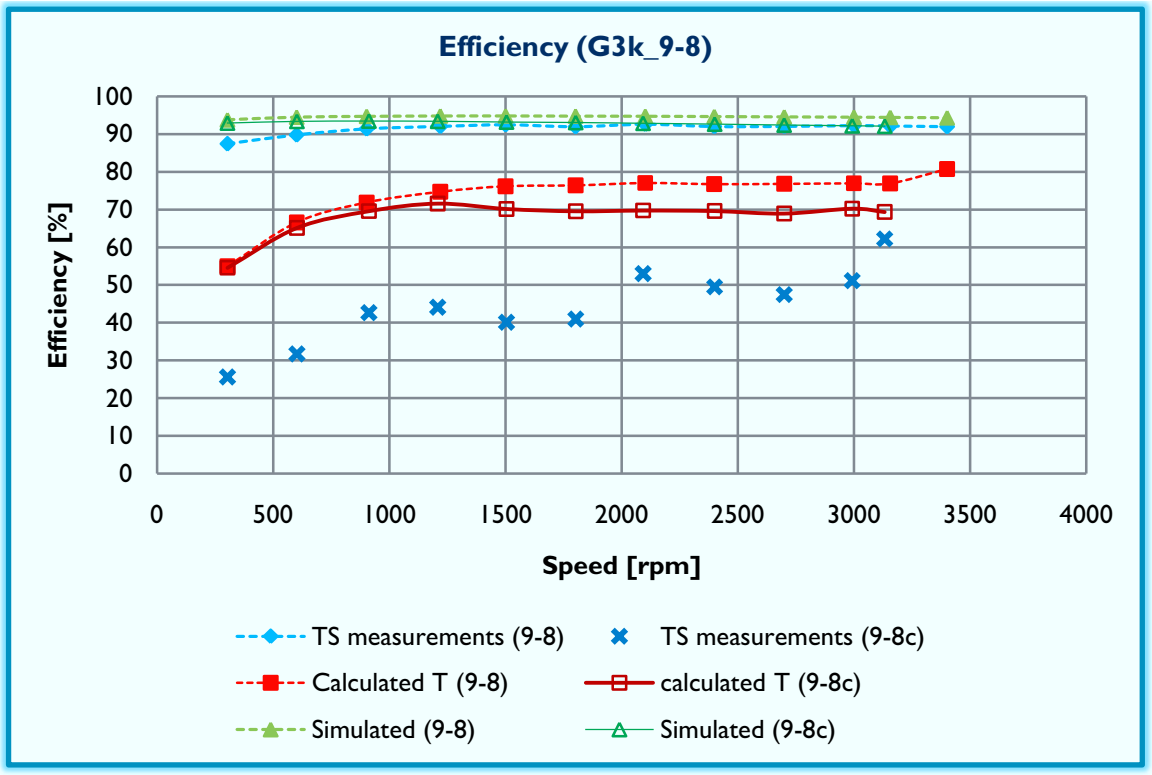

Efficiency versus speed for G3k_9-8 & 3k_9-8c

G3k_3-2 vs. G3k_9-8

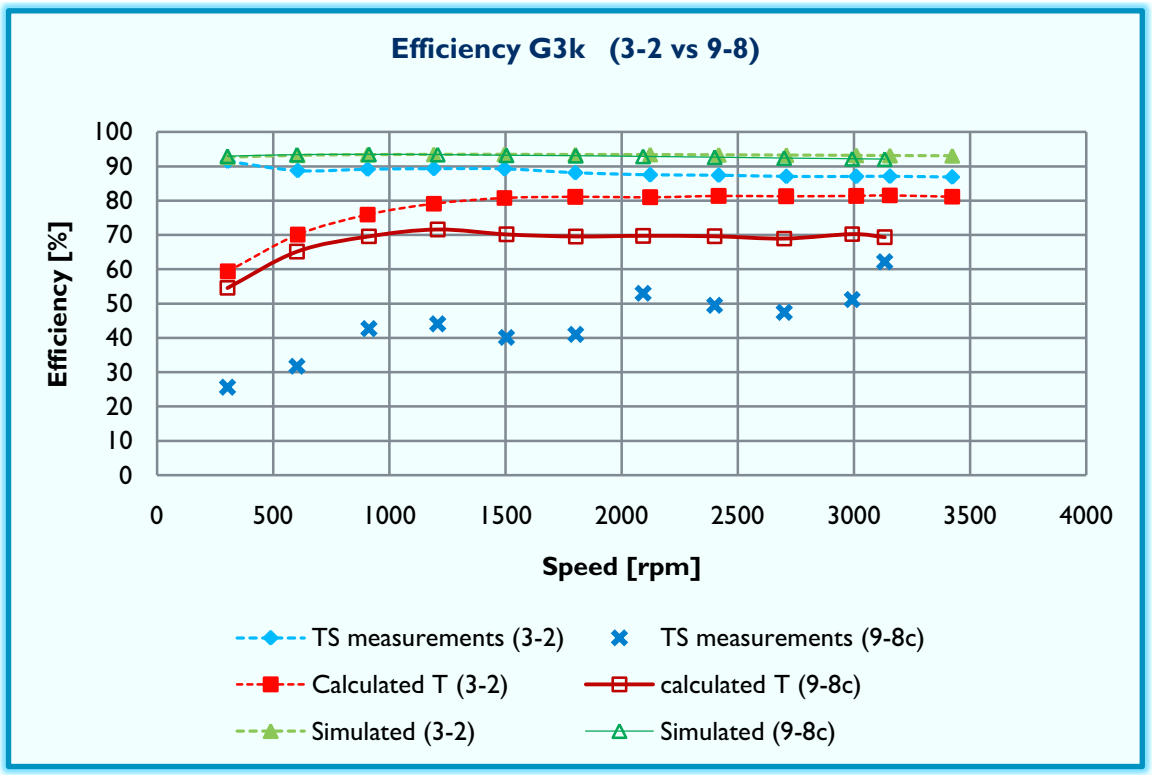

Efficiency versus speed for G3k_3-2 & G3k_9-8c

G9k_os vs. G9k_scs

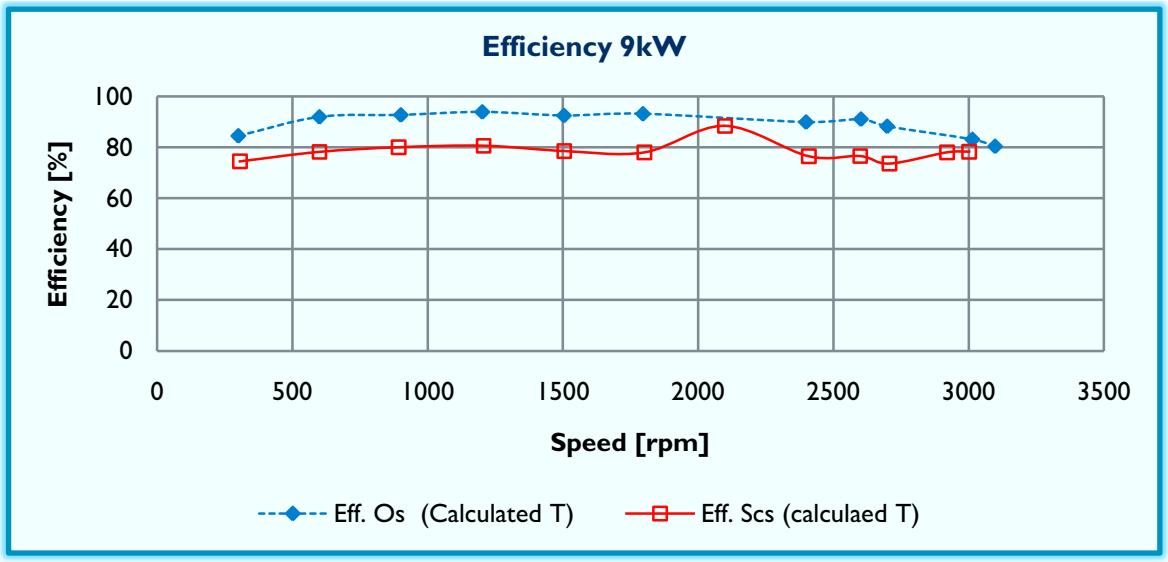

Measured efficiency versus speed for G9k_os & G9k_scs

G3K 3-2 (NOLOAD TEST WITH STATOR)

Speed [rpm]	Torque [Nm]	Voltage [V]	Dc_Current [A]	Dc_Torque [N.m]	T=1.3 X Idc [N.m]	Om_m [rad/s]	P_NL [W]	P_NL (Tcalc) [W]	P_mech [W]	P_mech(clc) [W]	P_Fe [W]	P_Fe(clc) [W]	Measured Voltage_ph [V]	Simulated emf(Brm=1T) [V]	Simulated emf(Brm=1.2) [V]	Simulated P_Fe [W]
0	0.108	0.014	-1.508E-05	0.000E+00	-1.960E-05	0	0	0.000			0.000	0.000	0.008			
300	0.117	16.010	-8.191E-05	0.000E+00	-1.065E-04	31.4159265	3.68848424	-0.003	3.2840069	26.8804384	0.404	-26.884	9.243	8.967	10.761	1.173
603	0.155	32.140	-9.300E-06	0.000E+00	-1.209E-05	63.1460123	9.80413197	-0.001	3.43544592	53.0798958	6.369	-53.081	18.556	18.025	21.630	3.486
902	0.185	48.070	-2.562E-05	0.000E+00	-3.331E-05	94.4572191	17.4398631	-0.003	2.98919274	80.4343095	14.451	-80.437	27.753	26.963	32.356	6.88
1199	0.210	63.950	-2.231E-05	0.000E+00	-2.900E-05	125.558986	26.3050597	-0.004	4.73695419	109.750042	21.568	-109.754	36.922	35.842	43.010	11.345
1501	0.235	80.000	3.100E-06	0.000E+00	4.030E-06	157.184352	36.9668518	0.001	13.9168455	141.346186	23.050	-141.346	46.188	44.869	53.843	17.001
1806	0.261	96.400	1.198E-05	0.000E+00	1.557E-05	189.123878	49.4007266	0.003	-0.0030112	175.711291	49.404	-175.708	55.657	53.987	64.784	23.857
2101	0.291	112.000	-3.326E-05	0.000E+00	-4.324E-05	220.016206	64.0892246	-0.010	-1.7519366	212.066316	65.841	-212.076	64.663	62.805	75.366	31.581
2399	0.310	127.900	-4.091E-05	0.000E+00	-5.318E-05	251.222693	77.9500805	-0.013	-2.4513302	247.379989	80.401	-247.393	73.843	71.713	86.056	40.474
2700	0.337	143.600	-3.100E-07	0.000E+00	-4.030E-07	282.743339	95.2526117	0.000	-2.1887229	290.523313	97.441	-290.523	82.907	80.711	96.853	50.571
3000	0.353	159.500	1.725E-05	0.000E+00	2.243E-05	314.159265	110.857411	0.007	-0.9022608	322.870679	111.760	-322.864	92.087	89.679	107.610	61.747
3151	0.364	167.500	-2.262E-05	0.000E+00	-2.941E-05	329.971948	120.117247	-0.010	1.09879104	337.47331	119.018	-337.483	96.706	94.192	113.030	67.793
3400	0.385	180.500	5.160E-06	0.000E+00	6.708E-06	356.047167	137.073175	0.002	-2.3099133	375.77646	139.383	-375.774	104.212	101.640	121.960	78.377

G3K 3-2 (LOAD TEST)

Speed [rpm]	Torque [Nm]	Voltage [V]	Current [A]	Power [W]	Impedance [Ohm]	Resistance [Ohm]	P_in [W]	P_out [W]	Efficiency [%]	Dc_Current [A]	T=1.3 X Idc [N.m]	Om_m [rad/s]	P_in [W]	P_in (Tcalc) [W]	Eff (Tcalc) [%]	Simulated Eff (sim) [%]	Simulated P_Fe _sim [W]	Simulated P_Cu _sim [W]	Simulated P_loss _sim [W]
304	1.343	15.790	1.430	-19.470	11.070	9.520	42.750	39.109	91.484	1.592	2.069	31.835	42.750	65.876	59.37	92.67	1.19	1.90	3.09
605	2.566	30.410	2.740	-72.580	11.050	9.560	162.556	144.320	88.782	2.500	3.250	63.355	162.556	205.934	70.08	93.23	3.50	6.98	10.48
906	3.764	45.070	4.080	-159.600	11.020	9.560	357.120	318.499	89.185	3.401	4.422	94.876	357.120	419.508	75.92	93.43	6.93	15.48	22.41
1191	4.845	58.590	5.320	-270.800	11.000	9.550	604.245	539.878	89.348	4.209	5.472	124.721	604.245	682.487	79.10	93.50	11.21	26.32	37.53
1495	5.921	72.400	6.600	-416.100	10.900	9.500	926.964	827.643	89.285	5.034	6.544	156.556	926.964	1024.494	80.79	93.52	16.87	40.51	57.38
1800	6.971	85.200	7.850	-585.000	10.800	9.400	1314.000	1158.430	88.161	5.828	7.576	188.496	1314.000	1428.071	81.12	93.46	23.71	57.31	81.02
2122	7.989	98.400	9.120	-783.000	10.780	9.390	1775.336	1554.356	87.553	6.644	8.638	222.215	1775.336	1919.407	80.98	93.45	31.58	77.35	108.93
2417	8.767	109.600	10.220	-976.600	10.740	9.360	2218.934	1940.091	87.433	7.246	9.420	253.108	2218.934	2384.255	81.37	93.38	40.44	97.14	137.58
2708	9.444	120.100	11.210	-1176.000	10.680	9.340	2678.190	2331.896	87.070	7.783	10.118	283.581	2678.190	2869.211	81.27	93.30	50.53	116.87	167.40
3009	10.004	130.000	12.190	-1387.000	10.670	9.310	3152.357	2744.781	87.071	8.232	10.702	315.102	3152.357	3372.246	81.39	93.21	61.70	138.19	199.89
3154	10.234	134.600	12.630	-1486.000	10.660	9.320	3380.036	2944.483	87.114	8.411	10.934	330.286	3380.036	3611.349	81.53	93.16	67.95	148.35	216.30
3422	10.652	142.700	13.420	-1678.000	10.640	9.320	3817.014	3316.936	86.899	8.776	11.408	358.351	3817.015	4088.181	81.13	93.10	78.37	167.49	245.86

G3K 9-8 (NOLOAD TEST WITH STATOR)

Speed [rpm]	Torque [Nm]	Voltage [V]	Dc_Current [A]	Dc_Torque [N.m]	T=1.3X Idc [N.m]	Om_m [rad/s]	P_NL [W]	P_NL (Tcalc) [W]	P_mech [W]	P_mech(clc) [W]	P_Fe [W]	P_Fe(clc) [W]	Measured Voltage_ph [V]	Simulated emf(Brm=1T) [V]	Simulated emf(Brm=1.2) [V]	Simulated P_Fe [W]
308	0.170	19.530	0.671	0.168	8.727E-01	32.2536846	5.47102802	28.148	-0.6009841	23.9203925	6.072	4.227	11.276	11.076	13.292	1.5105
600	0.204	38.160	0.703	0.176	9.137E-01	62.8318531	12.7876958	57.411	-0.7607011	50.1069053	13.548	7.304	22.032	21.578	25.893	4.482
900	0.239	56.920	0.744	0.186	9.667E-01	94.2477796	22.487737	91.108	-0.4118841	76.7122225	22.900	14.395	32.863	32.367	38.840	9.096
1198	0.275	75.800	0.779	0.195	1.013E+00	125.454267	34.5537307	127.118	0.10026199	104.262022	34.453	22.856	43.763	43.084	51.700	15.247
1502	0.315	94.900	0.822	0.206	1.069E+00	157.289072	49.5087488	168.083	1.08453214	132.001214	48.424	36.082	54.791	54.017	64.820	23.129
1805	0.358	114.300	0.883	0.221	1.148E+00	189.019158	67.6860404	216.910	1.92545386	163.376304	65.761	53.534	65.991	64.913	77.896	32.601
2100	0.384	132.700	0.924	0.231	1.201E+00	219.911486	84.4359826	264.053	3.34883366	196.883946	81.087	67.169	76.614	75.523	90.627	43.374
2399	0.416	151.500	0.973	0.243	1.265E+00	251.222693	104.553257	317.904	4.23243453	230.9804	100.321	86.924	87.469	86.276	103.531	55.855
2702	0.454	170.300	1.029	0.257	1.337E+00	282.952778	128.506541	378.417	9.40304254	274.270946	119.103	104.146	98.323	97.173	116.607	70.105
3003	0.482	189.100	1.079	0.270	1.403E+00	314.473425	151.694841	441.136	10.2107225	314.439342	141.484	126.697	109.177	107.998	129.597	85.859
3151	0.498	198.400	1.114	0.278	1.448E+00	329.971948	164.369257	477.813	11.0783231	333.994867	153.291	143.818	114.546	113.320	135.984	94.189
3399	0.526	213.700	1.165	0.291	1.515E+00	355.942448	187.267835	539.098	12.8616953	378.389576	174.406	160.709	123.380	122.239	146.687	109.01

G3K 9-8 (LOAD TEST)

Speed [rpm]	Torque [Nm]	Voltage [V]	Current [A]	Power [W]	Impedance [Ohm]	Resistance [Ohm]	P_in [W]	P_out [W]	Efficiency [%]	Dc Current [A]	T=1.3 X Idc [N.m]	Om_m [rad/s]	P_in [W]	P_in (Tcalc) [W]	Eff (Tcalc) [%]	Simulated Eff (sim) [%]	Simulated P_Fe [W]	Simulated P_Cu [W]	Simulated P_loss [W]
303	1.393	18.440	1.210	-19.330	15.250	13.170	44.195	38.646	87.444	1.705	2.217	31.730	44.195	70.336	54.94	93.77	1.47	1.10	2.57
601	2.643	36.390	2.370	-75.100	15.360	13.310	166.365	149.380	89.790	2.741	3.563	62.937	166.365	224.270	66.61	94.49	4.49	4.21	8.70
902	3.864	54.100	3.560	-167.900	15.200	13.200	365.017	333.586	91.389	3.779	4.913	94.457	365.017	464.037	71.89	94.71	9.13	9.51	18.64
1219	5.105	72.600	4.770	-303.100	15.100	13.200	651.699	599.813	92.038	4.837	6.288	127.653	651.699	802.661	74.73	94.82	15.73	17.06	32.79
1500	6.104	88.100	5.810	-449.300	15.100	13.300	958.744	886.569	92.472	5.699	7.408	157.080	958.743	1163.661	76.19	94.82	23.07	25.32	48.39
1801	7.053	103.400	6.830	-621.500	15.100	13.300	1330.202	1223.212	91.957	6.528	8.486	188.600	1330.202	1600.471	76.43	94.77	32.46	34.99	67.45
2101	7.921	118.700	7.850	-819.400	15.100	13.300	1742.725	1613.916	92.609	7.323	9.520	220.016	1742.725	2094.629	77.05	94.74	43.41	46.22	89.63
2398	8.656	132.400	8.720	-1017.000	15.170	13.360	2173.646	1999.701	91.998	7.981	10.375	251.118	2173.646	2605.447	76.75	94.66	55.81	57.03	112.84
2699	9.313	145.700	9.600	-1234.000	15.190	13.390	2632.325	2422.654	92.035	8.582	11.157	282.639	2632.325	3153.355	76.83	94.57	69.95	69.12	139.07
2999	9.886	158.400	10.440	-1461.000	15.170	13.410	3104.771	2864.285	92.254	9.115	11.850	314.055	3104.771	3721.403	76.97	94.48	85.63	81.75	167.38
3155	10.151	164.600	10.840	-1577.000	15.170	13.410	3353.792	3090.436	92.148	9.353	12.159	330.391	3353.791	4017.359	76.93	94.42	94.41	88.13	182.54
3400	10.517	173.800	11.440	-1758.000	15.160	13.440	3744.441	3443.788	91.971	9.212	11.975	356.047	3744.441	4263.793	80.77	94.32	109.07	98.16	207.23

G3K 9-8C (NOLOAD TEST WITH STATOR)

Speed [rpm]	Torque [Nm]	Voltage [V]	Dc_Current [A]	Dc_Torque [N.m]	T=1.3 X Idc [N.m]	Om_m [rad/s]	P_NL [W]	P_NL (Tcalc) [W]	P_mech [W]	P_mech(clc) [W]	P_Fe [W]	P_Fe(clc) [W]	Measured Voltage_ph [V]	Simulated emf(Brm=1T) [V]	Simulated emf(Brm=1.2) [V]	Simulated P_Fe [W]
304	0.204	16.340	0.677	0.813	8.803E-01	31.8348056	6.49968678	28.023	2.33246179	23.8022182	4.167	4.221	9.434	9.916	11.899	1.217
602	0.210	32.010	0.701	0.841	9.113E-01	63.0412926	13.2227724	57.449	5.4080815	50.5185982	7.815	6.930	18.481	19.636	23.563	3.708
904	0.190	47.990	0.724	0.869	9.413E-01	94.6666586	18.0041406	89.106	12.7928073	74.4595851	5.211	14.646	27.707	29.487	35.385	7.542
1202	0.230	63.700	0.744	0.893	9.669E-01	125.873146	28.9082406	121.708	16.0585463	97.2462043	12.850	24.462	36.777	39.207	47.049	12.619
1503	0.226	79.300	0.778	0.933	1.011E+00	157.393792	35.5594915	159.136	13.3863046	123.180573	22.173	35.955	45.784	49.026	58.831	19.05
1803	0.250	95.300	0.822	0.986	1.068E+00	188.809718	47.1848514	201.641	22.7279132	133.183851	24.457	68.457	55.021	58.811	70.574	26.764
2099	0.274	111.300	0.841	0.420	1.093E+00	219.806766	60.1604085	240.259	27.5736286	178.083786	32.587	62.175	64.259	68.467	82.160	35.65
2401	0.261	126.700	0.889	0.444	1.156E+00	251.432132	65.7394201	290.574	24.5523712	205.408153	41.187	85.166	73.150	78.317	93.981	46.022
2701	0.321	142.900	0.947	0.473	1.231E+00	282.848059	90.858405	348.069	24.7350952	240.800508	66.123	107.268	82.503	88.103	105.724	57.631
3000	-0.620	158.500	0.988	0.494	1.285E+00	314.159265	-194.74717	403.563	-20.152311	282.891757	-174.595	120.671	91.510	97.856	117.428	70.497
3156	0.354	166.400	1.009	0.505	1.312E+00	330.495547	117.120781	433.643	-4.6132459	301.722442	121.734	131.921	96.071	102.945	123.534	77.722
3403	0.341	179.800	1.024	0.512	1.331E+00	356.361327	121.38996	474.355	40.8276712	340.043958	80.562	134.311	103.808	111.002	133.202	89.882

G3K 9-8C (LOAD TEST)

Speed [rpm]	Torque [Nm]	Voltage [V]	Current [A]	Power [W]	Impedance [Ohm]	Resistance [Ohm]	P_in [W]	P_out [W]	Efficiency [%]	Dc Current [A]	T=1.3 X Idc [N.m]	Om_m [rad/s]	P_in [W]	P_in (Tcalc) [W]	Eff (Tcalc) [%]	Simulated Eff (sim) [%]	Simulated P_Fe [W]	Simulated P_Cu [W]	Simulated P_loss [W]
303	5.118	14.930	1.610	-21.030	9.250	8.070	162.400	41.634	25.637	1.849	2.404	31.730	162.400	76.288	54.57	92.96	1.21	1.94	3.15
602	8.044	29.030	3.200	-81.300	9.040	7.900	507.125	160.901	31.728	3.014	3.918	63.041	507.125	246.985	65.15	93.40	3.69	7.68	11.37
912	8.809	43.090	4.810	-181.000	8.950	7.810	841.264	358.990	42.673	4.156	5.402	95.504	841.264	515.930	69.58	93.49	7.66	17.35	25.01
1208	10.805	55.300	6.290	-303.700	8.700	7.600	1366.818	602.471	44.078	5.117	6.652	126.501	1366.818	841.531	71.59	93.42	12.73	29.67	42.40
1504	13.598	65.200	7.610	-436.200	8.500	7.500	2141.628	859.395	40.128	5.982	7.777	157.499	2141.629	1224.834	70.16	93.22	19.07	43.43	62.50
1802	14.973	75.300	8.880	-585.300	8.470	7.410	2825.490	1158.160	40.990	6.787	8.823	188.705	2825.489	1664.997	69.56	93.10	26.73	59.14	85.87
2092	12.128	82.800	9.820	-712.700	8.430	7.370	2656.828	1408.324	53.008	7.090	9.216	219.074	2656.828	2019.085	69.75	92.89	35.42	72.32	107.74
2400	13.515	90.100	10.770	-850.800	8.360	7.330	3396.735	1680.742	49.481	7.390	9.607	251.327	3396.735	2414.453	69.61	92.67	45.98	86.99	132.97
2699	14.323	96.100	11.540	-973.000	8.320	7.300	4048.248	1920.834	47.449	7.582	9.857	282.639	4048.247	2785.936	68.95	92.43	57.54	99.88	157.42
2992	13.640	102.300	12.340	-1109.000	8.280	7.270	4273.818	2186.510	51.161	7.641	9.934	313.322	4273.818	3112.445	70.25	92.22	70.13	114.21	184.34
3132	11.321	105.000	12.700	-1171.000	8.270	7.250	3713.198	2309.690	62.202	7.811	10.154	327.982	3713.199	3330.232	69.36	92.12	76.58	120.97	197.55

G9K SCS (NOLOAD TEST WITH STATOR)

Speed [rpm]	Torque [Nm]	Voltage [V]	Dc_Current [A]	Dc_Torque [N.m]	T=1.3 X Idc [N.m]	Om_m [rad/s]	P_NL [W]	P_NL (Tcalc) [W]	P_mech [W]	P_mech(clc) [W]	P_Fe [W]	P_Fe(clc) [W]	Measured Voltage_ph [V]	Simulated emf(Brm=1T) [V]	Simulated emf(Brm=1.2) [V]	Simulated P_Fe [W]
300	0.591	17.230	0.998	1.298	1.298E+00	31.4159265	18.5683551	40.768	3.7694154	25.8051897	14.799	14.963	9.948	10.121	12.145	16.733
599	0.742	35.130	1.141	1.483	1.483E+00	62.7271333	46.5186742	93.004	11.9459379	55.4252278	34.573	37.579	20.282	20.209	24.250	39.526
900	0.830	51.790	1.227	1.595	1.595E+00	94.2477796	78.1862992	150.325	14.9090347	91.3619601	63.277	58.963	29.901	30.364	36.436	68.639
1200	0.940	69.000	1.313	1.706	1.706E+00	125.663706	118.166572	214.420	24.3840052	125.87317	93.783	88.547	39.837	40.485	48.582	103.81
1500	1.080	86.400	1.411	1.835	1.835E+00	157.079633	169.712448	288.202	26.5419026	168.85963	143.171	119.343	49.883	50.606	60.727	145.13
1809	1.075	106.200	1.500	1.949	1.949E+00	189.438037	203.625241	369.288	9.08421971	216.530926	194.541	152.757	61.315	61.031	73.237	194.12
2104	1.274	122.300	1.587	2.063	2.063E+00	220.330365	280.780204	454.513	40.1677302	261.901744	240.612	192.611	70.610	70.983	85.180	246.97
2407	1.380	141.000	1.690	2.197	2.197E+00	252.060451	347.832835	553.718	67.2836909	306.143391	280.549	247.575	81.406	81.206	97.447	307.44
2700	1.448	159.100	1.763	2.292	2.292E+00	282.743339	409.284555	648.063	73.1075794	343.974158	336.177	304.089	91.856	91.091	109.310	371.88
2996	1.494	175.500	1.868	2.428	2.428E+00	313.740386	468.84579	761.785					101.325	101.080	121.290	442.93
3156	1.562	183.300	1.907	2.480	2.480E+00	330.495547	516.120685	819.500					105.828	106.480	127.770	483.83
3400	1.643	197.100	1.980	2.574	2.574E+00	356.047167	585.038903	916.583					113.796	114.710	137.650	594.57

G9K SCS (LOAD TEST)

Speed [rpm]	Torque [Nm]	Voltage [V]	Current [A]	Power [W]	Impedance [Ohm]	Resistance [Ohm]	P_in [W]	P_out [W]	Efficiency [%]	Dc Current [A]	T=1.3 X Idc [N.m]	Om_m [rad/s]	P_in [W]	P_in (Tcalc) [W]	Eff (Tcalc) [%]	Simulated Eff (sim) [%]	Simulated P_Fe [W]	Simulated P_Cu [W]	Simulated P_loss [W]
300	14.101	17.310	3.310	48.700	5.218	4.424	442.988	99.240	22.402	3.382	4.396	31.416	442.988	138.107	71.86	88.62	10.11	2.63	12.74
599	23.650	35.070	6.620	198.300	5.291	4.513	1483.488	402.119	27.106	6.249	8.124	62.727	1483.488	509.567	78.91	92.12	23.90	10.52	34.42
896	30.817	53.000	10.000	452.000	5.290	4.510	2891.539	917.987	31.747	9.046	11.760	93.829	2891.539	1103.446	83.19	93.36	41.24	24.00	65.24
1205	30.664	70.400	13.270	794.000	5.300	4.510	3869.344	1618.096	41.818	11.779	15.313	126.187	3869.344	1932.316	83.74	93.88	63.15	42.26	105.41
1499	34.170	86.900	16.360	1205.000	5.310	4.500	5363.848	2462.429	45.908	14.462	18.801	156.975	5363.848	2951.314	83.43	94.19	87.66	64.24	151.90
1798	31.498	103.300	19.450	1698.000	5.310	4.490	5930.583	3480.011	58.679	17.240	22.413	188.286	5930.583	4219.974	82.47	94.38	116.25	90.79	207.04
2102	30.023	118.200	22.240	2215.000	5.310	4.470	6608.684	4553.160	68.897	19.768	25.699	220.121	6608.684	5656.830	80.49	94.44	149.10	118.71	267.81
2392	29.635	134.500	25.230	2842.000	5.330	4.460	7423.290	5877.602	79.178	22.654	29.450	250.490	7423.291	7376.850	79.68	94.58	184.00	152.77	336.77
2697	29.232	149.400	28.060	3510.000	5.320	4.450	8256.061	7261.041	87.948	24.996	32.495	282.429	8256.060	9177.395	79.12	94.61	224.44	188.97	413.41
2957	30.647	163.000	30.590	4159.000	5.320	4.440	9489.921	8636.300	91.005	27.281	35.465	309.656	9489.923	10981.873	78.64	94.67	261.95	224.58	486.53
3036	31.178	167.100	31.360	4368.000	5.320	4.430	9912.343	9076.390	91.567	27.849	36.203	317.929	9912.342	11510.084	78.86	94.73	268.73	236.03	504.76

G9K OS (NOLOAD TEST WITH STATOR)

Speed [rpm]	Torque [Nm]	Voltage [V]	Dc_Current [A]	Dc_Torque [N.m]	T=1.3 X Idc [N.m]	Om_m [rad/s]	P_NL [W]	P_NL (Tcalc) [W]	P_mech [W]	P_mech(clc) [W]	P_Fe [W]	P_Fe(clc) [W]	Measured Voltage_ph [V]	Simulated emf(Brm=1T) [V]	Simulated emf(Brm=1.2) [V]	Simulated P_Fe [W]
306	0.840	21.190	1.170	1.521	1.521E+00	32.0442451	26.9247571	48.739	3.7694154	25.8051897	23.155	22.934	12.234	9.75	11.702	8.465
605	1.066	40.470	1.379	1.793	1.793E+00	63.3554518	67.5083384	113.575	11.9459379	55.4252278	55.562	58.150	23.365	19.28	23.136	19.789
900	1.347	58.210	1.578	2.051	2.051E+00	94.2477796	126.907745	193.314	14.9090347	91.3619601	111.999	101.952	33.608	28.681	34.417	33.919
1205	1.568	77.500	1.777	2.310	2.310E+00	126.187305	197.84163	291.470	24.3840052	125.87317	173.458	165.597	44.745	38.401	46.081	51.615
1502	1.811	95.100	1.938	2.520	2.520E+00	157.289072	284.812446	396.364	26.5419026	168.85963	258.271	227.504	54.906	47.866	57.439	71.865
1801	1.823	112.500	2.131	2.770	2.770E+00	188.600279	343.900161	522.503	9.08421971	216.530926	334.816	305.972	64.952	57.394	68.873	95.258
2101	2.221	130.600	2.309	3.001	3.001E+00	220.016206	488.703736	660.295	40.1677302	261.901744	448.536	398.393	75.402	66.955	80.345	121.76
2404	2.388	147.500	2.464	3.203	3.203E+00	251.746291	601.276381	806.443	67.2836909	306.143391	533.993	500.299	85.159	76.61	91.933	151.61
2702	2.702	166.000	2.684	3.490	3.490E+00	282.952778	764.58368	987.411	73.1075794	343.974158	691.476	643.436	95.840	86.107	103.333	184
3001	2.794	181.500	2.794	3.633	3.633E+00	314.263985	877.97218	1141.652					104.789	95.636	114.76	219.5
3151	2.854	189.900	2.870	3.731	3.731E+00	329.971948	941.581884	1231.115					109.639	100.42	120.5	238.44
3399	2.899	203.900	2.973	3.865	3.865E+00	355.942448	1031.9455	1375.637					117.722	108.32	129.98	271.44

G9K OS (LOAD TEST)

Speed [rpm]	Torque [Nm]	Voltage [V]	Current [A]	Power [W]	Impedance [Ohm]	Resistance [Ohm]	P_in [W]	P_out [W]	Efficiency [%]	Dc Current_ [A]	T=1.3 X Idc [N.m]	Om_m [rad/s]	P_in [W]	P_in (Tcalc) [W]	Eff (Tcalc) [%]	Simulated Eff (sim) [%]	Simulated P_Fe [W]	Simulated P_Cu [W]	Simulated P_loss [W]
300	33.23	17.45	4.11	61.70	4.24	3.65	1,043.98	124.22	11.90	3.60	4.68	31.42	1,043.97	147.03	84.49	90.71	8.26	4.46	12.72
600	31.24	35.26	8.24	253.20	4.28	3.73	1,963.03	503.23	25.64	6.70	8.71	62.83	1,963.03	547.27	91.95	93.07	19.57	17.92	37.49
901	37.07	52.85	12.30	569.40	4.29	3.76	3,497.81	1,125.93	32.19	9.90	12.87	94.35	3,497.81	1,214.32	92.72	93.84	33.97	39.94	73.91
1202	31.33	70.00	16.35	1,006.00	4.28	3.75	3,943.38	1,982.33	50.27	12.90	16.77	125.87	3,943.38	2,110.89	93.91	94.20	51.42	70.57	121.99
1504	29.40	87.00	20.36	1,563.00	4.27	3.76	4,630.94	3,068.02	66.25	16.20	21.06	157.50	4,630.94	3,316.92	92.50	94.42	72.01	109.44	181.45
1796	30.49	103.10	24.11	2,197.00	4.27	3.77	5,733.61	4,305.43	75.09	18.90	24.57	188.08	5,733.61	4,621.04	93.17	94.55	94.84	153.46	248.30
2399	34.45	134.10	31.34	3,740.00	4.28	3.80	8,653.87	7,279.28	84.12	24.79	32.227	251.22	8,653.87	8,096.15	89.91	94.66	151.10	259.30	410.40
2602	35.55	143.10	33.45	4,270.00	4.27	3.81	9,687.00	8,290.80	85.59	25.70	33.41	272.48	9,687.00	9,103.58	91.07	94.65	172.79	295.39	468.18
2699	36.04	146.80	34.30	4,492.00	4.27	3.81	10,187.25	8,721.29	85.61	26.90	34.97	282.64	10,187.25	9,883.87	88.24	94.64	183.65	310.59	494.24
3014	37.33	158.70	37.08	5,267.00	4.28	3.83	11,782.39	10,192.42	86.51	29.90	38.87	315.63	11,782.39	12,268.36	83.08	94.58	221.11	362.98	584.09
3098	37.52	161.40	37.70	5,450.00	4.28	3.83	12,173.15	10,539.15	86.58	31.10	40.43	324.42	12,173.15	13,116.37	80.35	94.56	231.66	375.22	606.88

Appendix_4

MEASUREMENTS AUTOMATION

GRAPHIC USER INTERFACE OF THE MEASUREMENT AUTOMATION

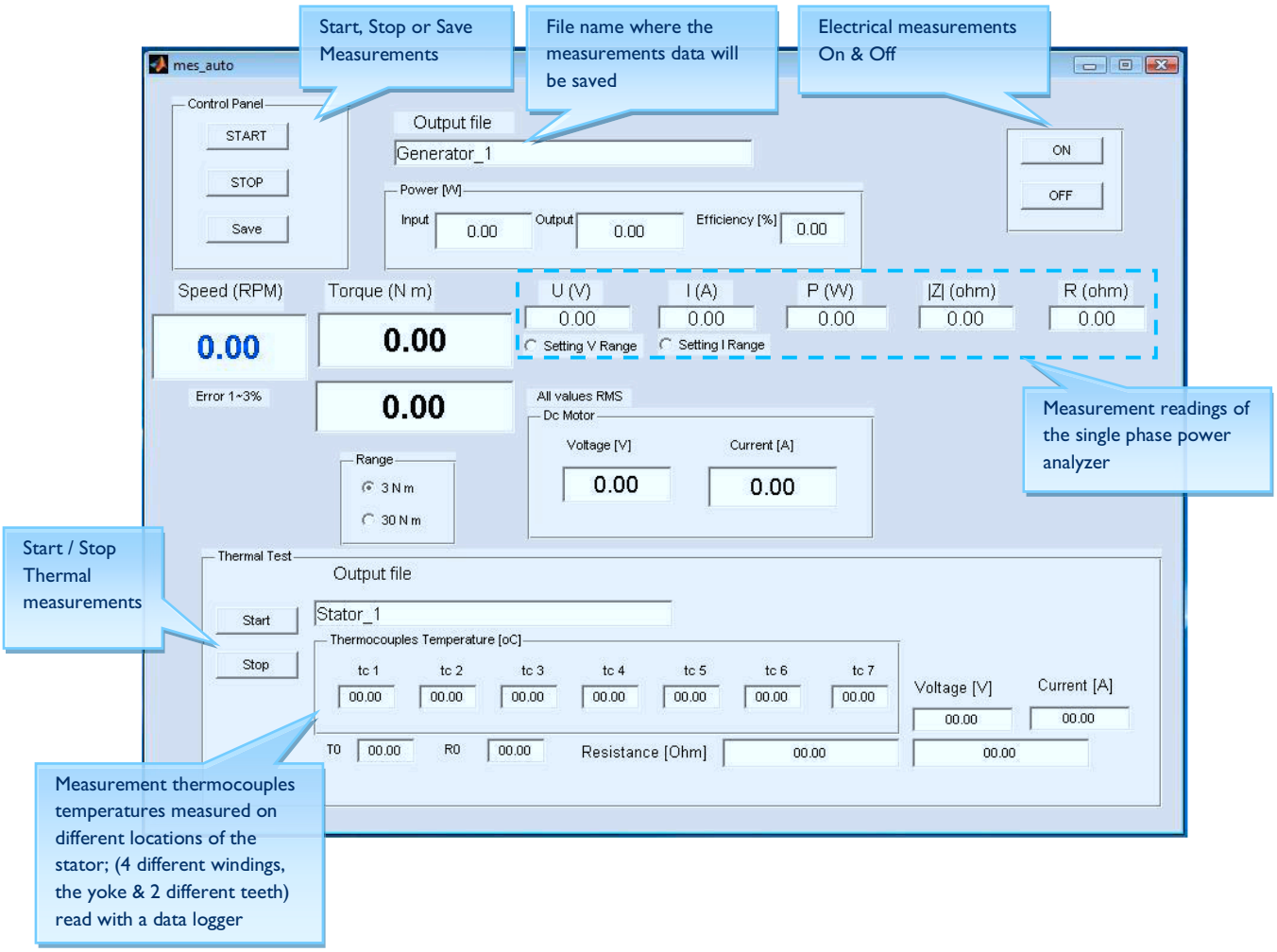

Appendix_5

TECHNICAL DATA & DRAWINGS

WINDING OF THE 3KW NDFEB GENERATORS

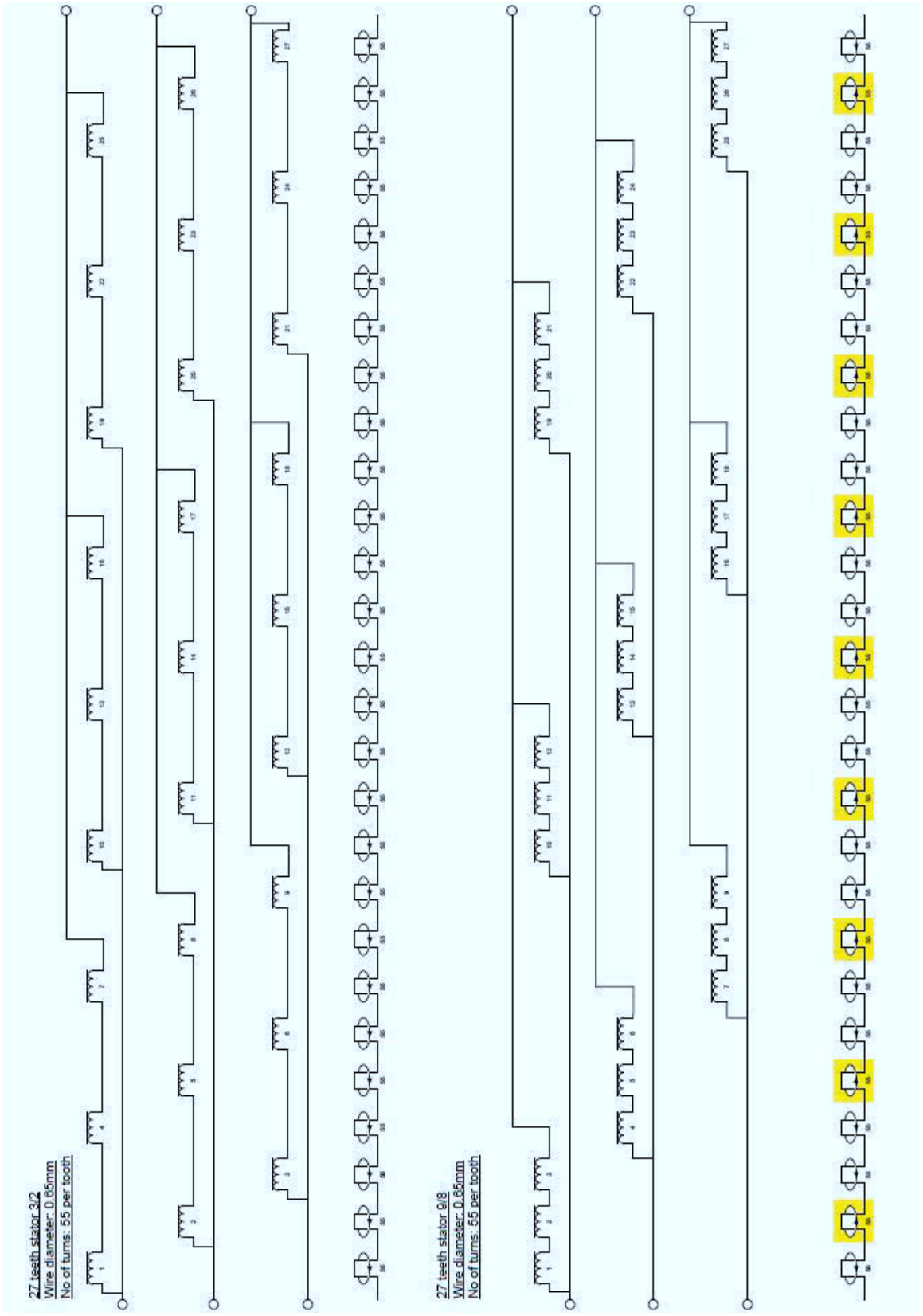

27 tooth stator with open slots

3 inlets, 3 outlets, each 9 stages connected

Wire area: 2 x 2.08mm^2 (AWG 14) parallel
Number of turns: 10 clockwise

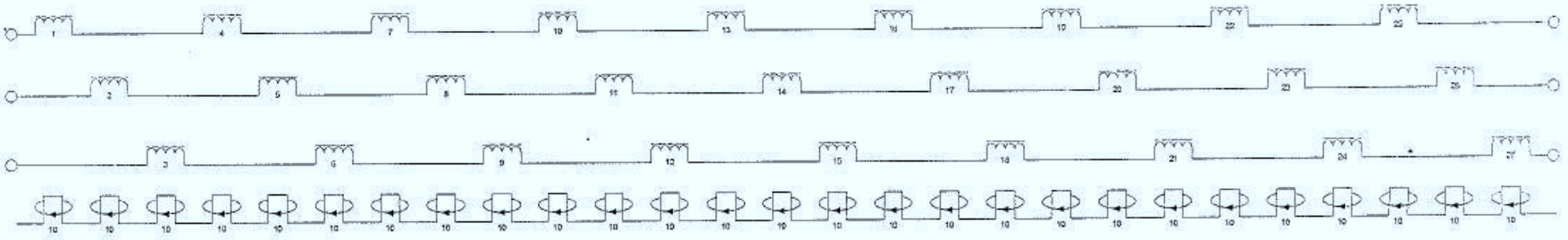

27 tooth stator with semi closed slots

3 inlets, 3 outlets, each 9 stages connected

Wire area: ~~2 x 2.08mm^2 (AWG 14) parallel~~ C_1 2 × 1.767 mm^2 (Φ1.50) parallel
Number of turns: ~~8 and 9 clockwise~~ C_2 9 clockwise

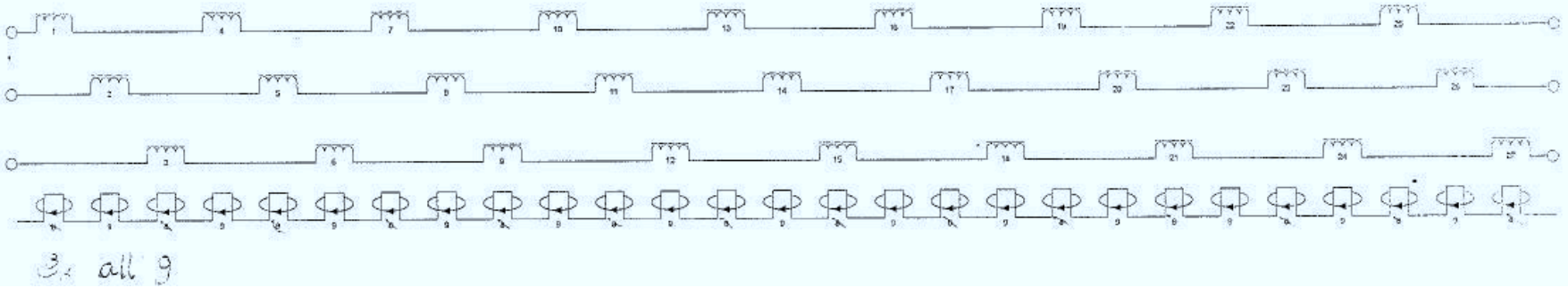

3 × all 9

STATOR DRAWINGS OF THE 9KW GENERATORS

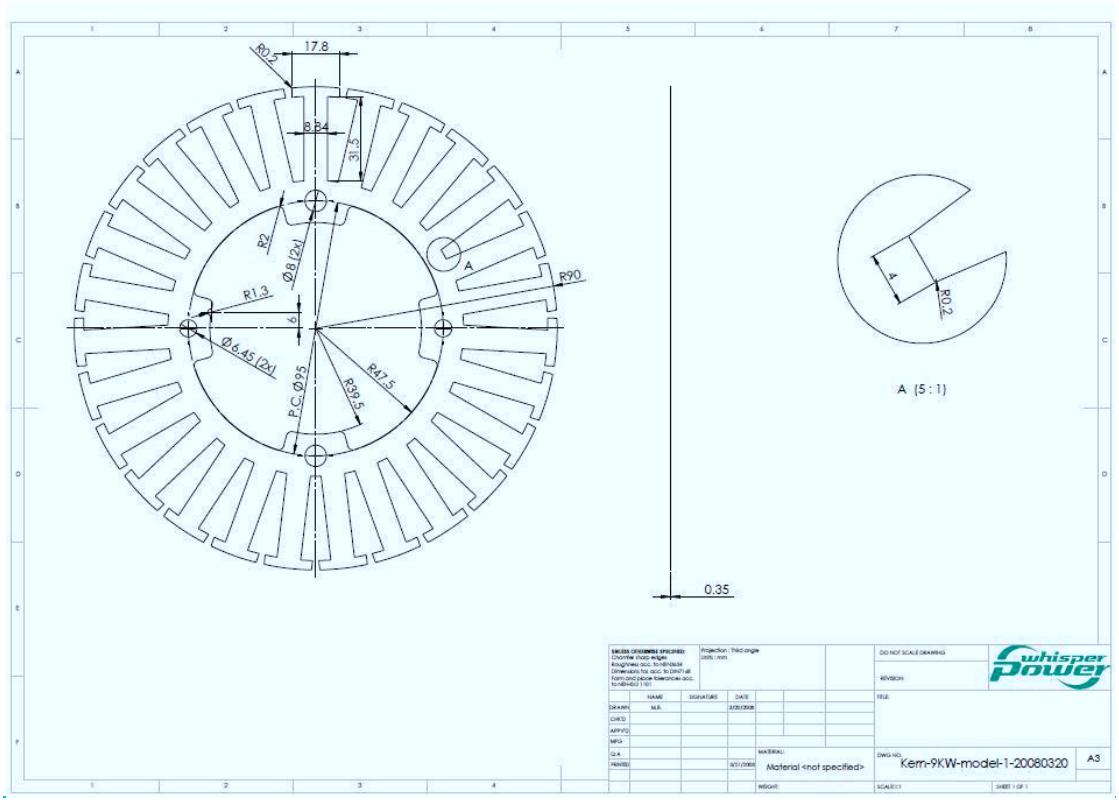

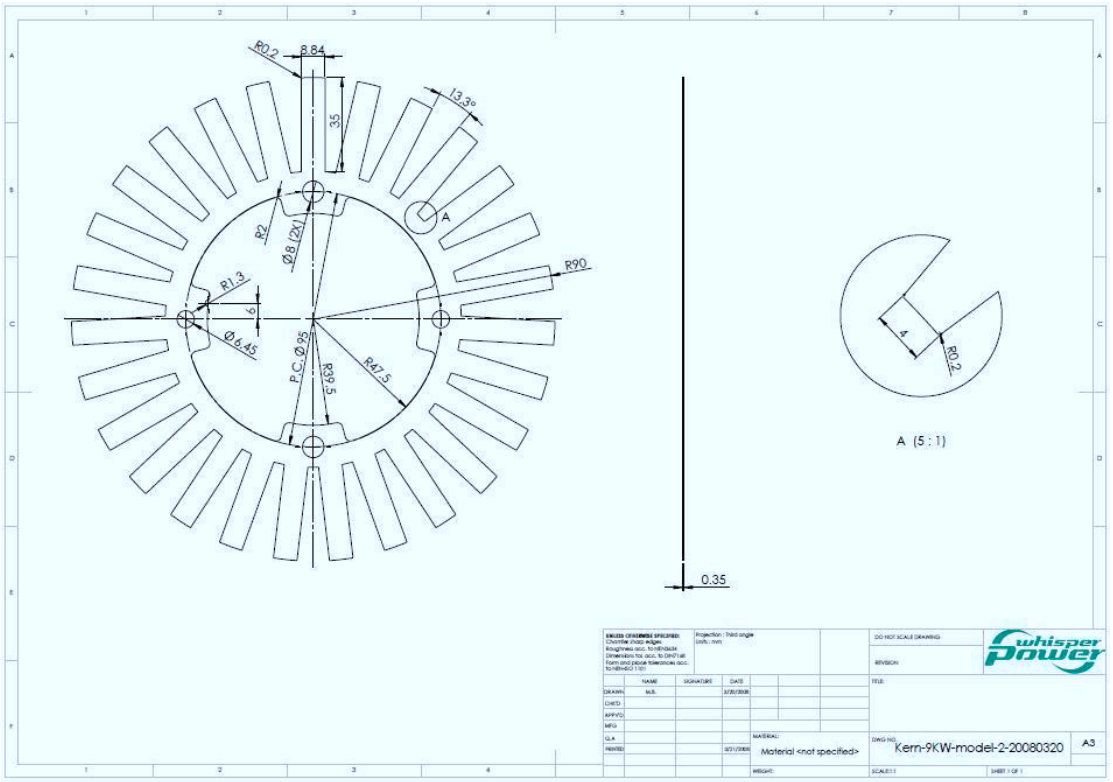

KUBOTA DIESEL ENGINE (PRIME MOVER OF THE GENPOWERBOX ®)

D722

Dimensions mm(in.)

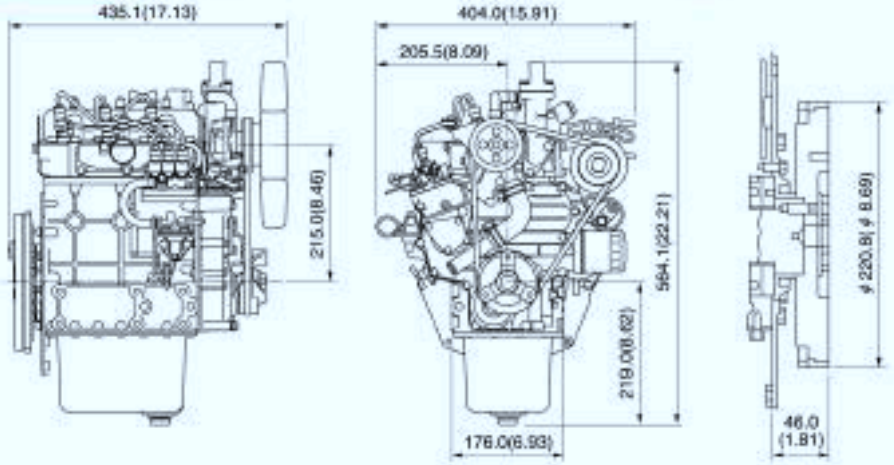

Specifications

				D722
Model				
Cylinders				3
Bore x Stroke			mm (in)	67 x 68 (2.64 x 2.68)
Displacement			L (cu.in.)	0.719 (43.88)
Combustion / Intake system				E-TVCS/NA
Cooling System				Liquid-Cooled
Starter			V-A	12-0.7
Output Industrial Use	Gross Intermittent	3600	kW/HP/PS	14.9/20.0/20.3
		3000		12.4/16.6/16.9
		2800		11.5/15.4/15.7
		2600		10.7/14.3/14.6
		2400		9.9/13.3/13.5
		2200		9.0/12.1/12.3
	Net Intermittent	3600	kW/HP/PS	14.0/18.8/19.1
		3000		11.8/15.9/16.1
		2800		11.0/14.7/15.0
		2600		10.3/13.8/14.0
		2400		9.5/12.7/13.0
		2200		8.7/11.7/11.9
	Net Continuous	3600	kW/HP/PS	12.2/16.3/16.6
		3000		10.3/13.8/14.0
		2800		9.6/12.9/13.0
		2600		8.9/11.9/12.2
		2400		8.3/11.1/11.3
		2200		7.6/10.2/10.3
Output Generator Use	Stand-by	3600	kW/HP/PS	13.4/18.0/18.2
		3000		11.3/15.1/15.4
	Continuous	3600	kW/HP/PS	12.1/16.2/16.5
		3000		10.3/13.8/14.0
Dimensions	Length		mm(in.)	435.1(17.13)
	Width		mm(in.)	404.0(15.91)
	Height		mm(in.)	564.1(22.21)
Dry Weight			kg (lbs)	63.1(139.1)

*Specifications are subject to change without notice.
*Dry weight is according to Kubota's standard specification. When specification varies, the weight will vary accordingly.

Performance Curve

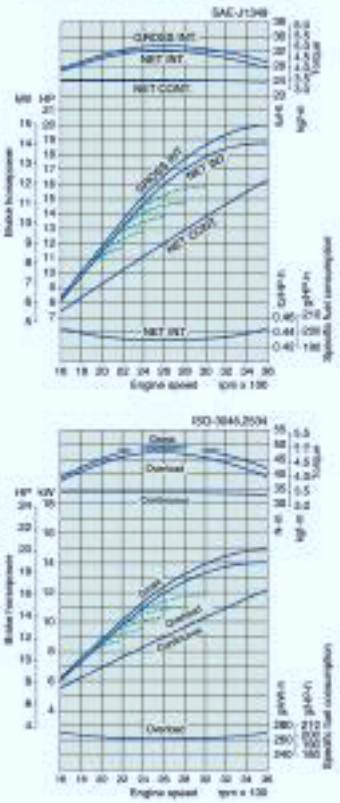

Bibliography

[1]. Mastervolt. *www.mastervolt.com.*

[2]. S.A.Nasar, I.Boldea and L.E.Unnewehr, "*Permanent Magnet,Reluctance, and Self-Synchronous Motors*", CRC Press, 1993.

[3]. N. AlFartusi, "*La Commande Direct du Couple (DTC) de la Machine Synchrone à Aimant Permanent Basée sur les réseaux de Neurones Artificiels*", Eng. thesis, Centre Universitaire Yahia Farès de Médéa,Algeria,2003.

[4]. J.A. Ferreira. Course electromagnetics, TuDelft, 2006.

[5]. A. Parvianen,"*Design of axial-flux permanent-magnet low-speed machines and performance comparison between radial-flux and axial-flux machines*",Lappeenranta University of Technology, Finland, 2005.

[6]. F. Mangussen, "*On design and analysis if synchronous permanent magnet machines for field-weakening operation in hybrid electric vehicles*". PhD thesis, Royal Institut of Technology, Stockholm, Sweden : 2004.

[7]. K. Sitapati and R. Krishnan, " *Performance comparison of radial and axial field permanent magnet brushless machines*", Industry Applications Conference, 2000, Conference Record of the 2000 IEEE, Vol. 1, pp. pp. 228 –234.

[8]. S.A. Nasar and I. Boldea ,"*Linear electric actuators and generators*",Cambridge University Press, Cambridge, UK,1997.

[9]. H. Polinder, M.E.C. Damen and F. Gardner," *Design, modelling and test results of the AWS PM linear generator*", Euro. Trans. Electr. Power, 2005, Vol. 15 , pp. 245-256.

[10]. F. Libert and J. Soulard, " *Design study of a direct-driven surface-mounted permanent magnet motor for low speed application*", Royal Institute of Technology, Stockholm, Sweden.

[11]. J. Viarouge, P. Cros, "*Synthesis of high performance PM motors with concentrated windings*", IEEE Transactions on Energy Conversion. June 2002, Vol. 17, No. 2, pp. 248-253.

[12]. H. Polinder, M.J. Hoeijmakers and M. Scuotto, "*Eddy-Current Losses in the solid back-iron of PM machines for different concentrated fractional pitch windings*", IEEE International Conference on Power Electronic, Machines and Drives. 4-6 April 2006, Vol. 1, pp. 333-339.

[13]. K.J. Binns, P.J. Lawrenson and C.W. Trowbridge,"*The analytical and numerical solution ofelectric and magnetic fields*", John Willey & sons, 1992.

[14]. S.E. Skaar, O. Krovel and R. Nilsse,"*Distribution, Coil-span and winding factors for PM machines with concentrated windings*", ICEM, Crete, Greece , 2006.

[15]. F. Magnussen and C. Sadarangani,"*Winding factor and joule losses of permanent magnet machines with concentrated windings*",Electric Machines and Drives Conference (IEMDC'03), June 2003, Vol. 1, pp. 333-339.

[16]. H. Toda, Z. Xia, J. Wang, K. atallah and D. Howe, "*Rotor eddy-current loss in permanent magnet brushless machines*", IEEE transactions on magnetics, July 2004, Vol. 40, pp. 2104-2106.

[17]. M.J. Hoeijmakers and H. Polinder, "*Eddy-current losses in the segmented surface-mounted magnets of a PM machine*", IEEE. Proc. Electr. Power Appl., May 1999, Vol. 146.

[18]. Z.O. Zhu, K. Ng, N. Schofield and D. Howe," *Improved analytical modelling of rotor eddy current loss in brushless achines equiped with surface-mounted permanent magnts*", IEE Proc. Electr. Power Appl., November 2004, Vol. 151.